

FIBULIN-5 PROMOTES PANCREATIC TUMOR GROWTH THROUGH INHIBITION OF
INTEGRIN-INDUCED ROS: INSIGHTS INTO TUMOR-MATRIX SIGNALING

APPROVED BY THESIS COMMITTEE:

Mentor: Rolf A. Brekken, Ph.D. _____

Chairperson: Lance Terada, M.D. _____

Melanie Cobb, Ph.D. _____

John Abrams, Ph.D. _____

I would like to dedicate this to my mother and father, Margarita and Mike Topalovski, who emigrated from Bitola, Macedonia to provide a beautiful life full of opportunities for my sister and me.

FIBULIN-5 BLOCKS INTEGRIN-INDUCED ROS PRODUCTION IN PANCREATIC
CANCER: INSIGHTS INTO TUMOR-MATRIX SIGNALING

By

MARY TOPALOVSKI

DISSERTATION

Presented to the Faculty of the Graduate School of Biomedical Sciences

The University of Texas Southwestern Medical Center at Dallas

In Partial Fulfillment of the Requirements

For the Degree of

DOCTOR OF PHILOSOPHY

Cancer Biology

The University of Texas Southwestern Medical Center at Dallas

Dallas, Texas

August 2016

Copyright

by

MARY TOPALOVSKI, 2016

All Rights Reserved

FIBULIN-5 BLOCKS INTEGRIN-INDUCED ROS PRODUCTION IN PANCREATIC CANCER: INSIGHTS INTO TUMOR-MATRIX SIGNALING

Mary Topalovski, Ph.D.

The University of Texas Southwestern Medical Center

Supervising Professor: Rolf A. Brekken, Ph.D.

Elevated oxidative stress is an aberration seen in many solid tumors, and exploiting this biochemical difference has the potential to enhance the efficacy of anti-cancer agents. Homeostasis of reactive oxygen species (ROS) is important for normal cell function, but excessive production of ROS can result in cellular toxicity and therefore ROS levels must be balanced finely. Here, we highlight the relationship between the extracellular matrix and ROS production by reporting a novel function of the matricellular protein Fibulin-5 (Fbln5). We found that Fbln5 is abundantly expressed in mouse and human pancreatic cancer compared to normal pancreas. By employing genetically engineered mouse models of pancreatic ductal adenocarcinoma (PDA), we showed that mutation of the integrin-binding domain of Fbln5 led to decreased tumor growth, increased survival, and enhanced chemoresponse to standard PDA therapies. Through mechanistic investigations, we found that improved survival was due to increased levels of oxidative stress in Fbln5 mutant tumors. Furthermore, loss of the Fbln5-integrin interaction augmented fibronectin (FN) signaling, driving integrin-induced ROS production in a 5-lipoxygenase-dependent manner. These data indicate that Fbln5 promotes PDA progression by functioning as a molecular rheostat that modulates cell-ECM interactions to reduce ROS production and thus tip the balance in favor of tumor cell survival and treatment-refractory disease.

The latter part of this thesis is focused on the underlying mechanism that leads to upregulation of Fbln5 in PDA. The deposition of ECM is a defining feature of PDA where ECM signaling can promote cancer cell survival and epithelial plasticity programs. ECM-mediated signaling is governed by expression of the ECM proteins, the presence of cell surface receptors and the expression and activity of matricellular proteins that function as extracellular adaptors to reduce ECM–cell interaction. As stated above, Fbln5 is a matricellular protein that blocks FN-integrin interaction and thus directly limits ECM-driven ROS production and supports PDA progression. Compared to normal pancreatic tissue, Fbln5 is expressed abundantly in the stroma of PDA; however, the mechanisms underlying the stimulation of Fbln5 expression in PDA are undefined. Using *in vitro* and *in vivo* approaches, we report that hypoxia triggers Fbln5 expression in a transforming growth factor β (TGF- β)- and PI3K-dependent manner. Pharmacologic

inhibition of TGF- β receptor (TGF- β R), PI3K, or protein kinase B (AKT) was found to block hypoxia-induced Fbln5 expression in mouse embryonic fibroblasts and 3T3 fibroblasts. Moreover, tumor-associated fibroblasts from mouse PDA were also responsive to TGF- β R and PI3K/Akt inhibition with regard to suppression of Fbln5. In genetically engineered mouse models of PDA, therapy-induced hypoxia elevated Fbln5 expression while pharmacologic inhibition of TGF- β signaling reduced Fbln5 expression. These findings offer insight into the signaling axis that induces Fbln5 expression in PDA and a potential strategy to block its production.

TABLE OF CONTENTS

Chapter 1. Introduction.....	1
The function and composition of the extracellular matrix (ECM).....	1
The role of the ECM in tumor development with emphasis on FN.....	3
Matricellular proteins: extracellular modulators of the ECM.....	5
Fibulin-5 (Fbln5).....	6
Fbln5 in cell adhesion/migration.....	8
Fbln5 in cell proliferation/survival.....	9
Fbln5 in angiogenesis.....	10
Fbln5 in tumor progression.....	12
References.....	16
 Chapter 2. Fbln5 promotes pancreatic tumor growth through inhibition of integrin-induced ROS.....	 23
Introduction.....	23
Results.....	25
Fbln5 expression in pancreatic cancer.....	25
Characterization of KIC and KPC mice.....	28
Ablation of Fbln5-integrin interaction reduces tumor growth and prolongs survival.....	31
Increased oxidative stress in RGE-KIC and RGE-KPC tumors.....	33
Angiogenesis is reduced in RGE-KIC and RGE-KPC tumors.....	35
Induction of the oxidative stress responsive gene Nqo1 by FN-induced ROS <i>in vitro</i> and <i>in vivo</i>	37
Nqo1 induction is dependent on FN- β 1 integrin interaction and 5-lipoxygenase (5-Lox) activity.....	39
ROS induction has an additive therapeutic effect when combined with standard chemotherapy agents and development of Fbln5 targeted agents.....	41
Discussion.....	43
Materials and Methods.....	49
References.....	55
 Chapter 3. Hypoxia and TGF-β cooperate to induce fibulin-5 expression in pancreatic cancer.....	 59
Introduction.....	59
Results.....	61
Fbln5 expression is restricted to the stroma of PDA.....	61
Hypoxia induces Fbln5 expression and requires TGF- β activity.....	63
Fbln5 expression requires PI3K/Akt activity.....	66

Fbln5 expression in tumor-associated fibroblasts also requires TGF- β and PI3K activity.....	68
Inhibition of TGF- β signaling reduces Fbln5 expression in mouse PDA.....	70
Hypoxia drives Fbln5 expression in mouse PDA.....	70
Discussion.....	72
Materials and Methods.....	75
References.....	79
 Chapter 4.	
Discussion	82
References.....	89
 Acknowledgements	91

PRIOR PUBLICATIONS

Topalovski, M., Brekken, RA (2015). The contribution of fibronectin signaling to pancreatic cancer: new insights. *Cancer Letters*. DOI: 10.1016/j.canlet.2015.12.027.

Wang* M, **Topalovski* M**, Toombs JE, Wright C, Moore Z, Castrillon H, Boothman DA, Yanagisawa H and Brekken RA (2015). Reduction of fibronectin-driven ROS by fibulin-5 supports angiogenesis and growth of pancreatic cancer. *Cancer Research*. DOI: 10.1158/0008-5472.CAN-15-0744

***equal contribution**

Ostapoff KT, Cenik BK, Wang M, Ye R, Xu X, Nugent D, Hagopian MM, **Topalovski M**, Rivera LB, Carroll KD and Brekken RA. (2014). Neutralizing the activity of murine TGF- β receptor 2 promotes a differentiated tumor cell phenotype and inhibits pancreatic cancer metastasis. *Cancer Research*. DOI: 10.1158/0008-5472.CAN-13-1807

LIST OF FIGURES

Chapter 1. Introduction:

Figure 1.1.....	7
-----------------	---

Chapter 2. Fbln5 promotes pancreatic tumor growth through inhibition of integrin-induced ROS

Figure 2.1.....	27
Figure 2.2.....	30
Figure 2.3.....	32
Figure 2.4.....	34
Figure 2.5.....	36
Figure 2.6.....	38
Figure 2.7.....	40
Figure 2.8.....	42
Figure 2.9.....	48

Chapter 3. Hypoxia and TGF- β cooperate to induce fibulin-5 expression in pancreatic cancer

Figure 3.1.....	62
Figure 3.2.....	65
Figure 3.3.....	67
Figure 3.4.....	69
Figure 3.5.....	71
Figure 3.6.....	74

LIST OF ABBREVIATIONS

- Reactive oxygen species (**ROS**)
- Fibulin-5 (**Fbln5**)
- *Fbln5*^{-/-} (**mice with global loss of Fbln5**)
- *Fbln5*^{RGE/RGE} (**mice harboring a point mutation in the RGD-integrin binding domain of Fbln5**)
- Fibronectins (**FN**)
- Pancreatic ductal adenocarcinoma (**PDA**)
- Extracellular matrix (**ECM**)
- Transforming growth factor β (**TGF- β**)
- Focal adhesion kinase (**FAK**)
- Epidermal growth factor (**EGF**)
- Basic fibroblast growth factor (**FGF**)
- Connective tissue growth factor (**CTGF**)
- Interleukin-1 β (**IL-1 β**)
- Platelet-derived growth factor (**PDGF**)
- Tumor microenvironment (**TME**)
- Vascular endothelial growth factor (**VEGF**)
- Thrombospondin-1 & 2 (**TSP-1 & 2**)
- Tenascin-C (**TNC**)
- Secreted protein acidic and rich in cysteine (**SPARC**)
- Osteopontin (**OPN**)
- Calcium-binding EGF-like repeats (**cbEGF**)
- Extracellular superoxide dismutase (**ecSOD**)
- Lysyl-oxidase-like 1 (**LOXL1**)
- Smooth muscle cells (**SMCs**)
- Mitogen-activated protein kinase (**MAPK**)
- Vascular smooth muscle cells (**VSMCs**)
- Immunohistochemistry (**IHC**)

- Mouse embryonic fibroblasts (**MEFs**)
- Electron transport chain (**ETC**)
- NADPH oxidase (**NOX**)
- 5-lipoxygenase (**5-LOX**)
- Nitric oxide synthase (**NOS**)
- Genetically engineered mouse models (**GEMMs**)
- Pancreatic intraepithelial neoplasias (**PanINs**)
- Dihydroethidium (**DHE**)
- N-acetylcysteine (**NAC**)
- 2'-7'-dichlorodihydrofluorescein diacetate (**DCF-DA**)
- Microvessel density (**MVD**)
- NADP(H):quinone oxidoreductase 1 (**Nqo1**)
- Diphenyleneiodonium chloride (**DPI**)
- Nordihydroguaiaretic acid (**NDGA**)
- Gemcitabine (**Gem**)
- Abraxane (**Abx**)
- Tissue microarray (**TMA**)
- TGF- β receptor 1 (**TGF- β R1**)
- Endothelial monocyte activating polypeptide II (**EMAP II**)
- Chromatin-immunoprecipitation (**ChIP**)

Chapter 1. Introduction

The function and composition of the extracellular matrix (ECM)

The extracellular matrix (ECM) is a dynamic collection of secreted molecules, which occupies the space between cells and provides the structural framework necessary to maintain integrity of tissues. Some major examples of these structural proteins are collagen, fibronectin, laminin, and elastin. Collagens are the most abundant protein in the ECM and for that matter, the human body. There are multiple types of collagen found within the ECM and they exist as fibrillar proteins providing stiffness to support surrounding cells [1]. Fibronectins (FN) are glycoproteins that bind to other ECM proteins and help connect cells to the ECM and promote cell movement [2]. Laminins are glycoproteins found in the basal laminae of all cell types where they form web-like networks that provide tensile strength to tissue [3]. Finally, elastins are proteins that provide flexibility to tissue, allowing tissue to retain shape after stretching or contraction [4]. Various cell types secrete ECM molecules, however, fibroblasts are the major cell type that synthesize and secrete ECM.

The most common and well-studied function of the ECM is in cell-adhesion and cell-to-cell communication. ECM proteins are anchored to the cell through cell surface receptors, the most intensively studied of which are integrins. Integrins are heterodimeric transmembrane receptors consisting of α and β subunits. In mammals, there are at least 18 α subunits and 8 β subunits, generating 24 unique integrins [5]. The various functions and ligands of integrins depend on the specific integrin type. For example, $\alpha 5 \beta 1$ (a major FN receptor) is important during angiogenesis [6], whereas

$\alpha 1\beta 1$ and $\alpha 2\beta 1$ (major collagen receptors) are critical for leukocyte adhesion and inflammation [7, 8].

In addition to providing a structural framework for tissues, the ECM also regulates a myriad of important signaling pathways. As integrins bind to their respective ligands, they form clusters at the membrane referred to as focal adhesions. Focal adhesion complexes are essential to induce downstream signaling, as the cytoplasmic tails of integrins do not harbor any detectable enzymatic activity [5]. Integrin clustering results in the reorganization of the actin cytoskeleton and the activation of a number of signaling complexes. Integrins are unique in that they relay signals from inside the cell to the outside (inside-out signaling) and vice versa (outside-in signaling) [9]. Integrin contact with the ECM results in outside-in signaling, whereas protein complexes from inside the cell bind to integrin tails, which is thought to prime integrins for ECM interaction.

Integrin clustering and focal adhesion assembly activates a number of protein tyrosine kinases such as focal adhesion kinase (FAK) [10]. FAK was one of the first phosphorylation targets discovered downstream of integrin activation [11]. An immediate downstream target of FAK activity is the major protein kinase Src, which promotes survival, proliferation, and migration [12]. FAK functions as a central signaling scaffold that is critical for the activation of downstream signaling pathways, namely the Rho-family GTPases, which support cytoskeletal changes and promote cell movement. Furthermore, activation of integrins also promotes growth factor receptor activation. For

example, optimum cell stimulation with epidermal growth factor (EGF) requires integrin-mediated cell adhesion in some cultured models [13]. Therefore, integrins regulate a range of important biological processes from cell migration to cell growth and proliferation.

The role of the ECM in tumor development with emphasis on FN

The ECM is also critical in the formation and maintenance of solid tumors. Most solid tumors display an increased deposition of ECM proteins compared to their normal tissue counterparts. ECM affects tumorigenic processes and functions including tumor cell proliferation, survival, apoptosis, migration, adhesion, angiogenesis, and chemoresistance [14-20]. Desmoplasia, the robust deposition of ECM, is induced in tumors by growth factors such as transforming growth factor β (TGF- β), basic fibroblast growth factor (FGF) connective tissue growth factor (CTGF), interleukin-1 β (IL-1 β), and platelet-derived growth factor (PDGF) [21-24] and environmental conditions including hypoxia [14]. The ECM is a major facet of the tumor microenvironment (TME), which is a collective term referring to the immediate environment surrounding tumor cells. In addition to ECM proteins, the TME contains multiple types of non-cancer cells such as immune cells, fibroblasts, and endothelial cells that contribute to tumor progression [25-27].

Under normal conditions, cells remain anchored to their surrounding ECM; detachment from this supportive matrix results in a form of cell death termed anoikis [28]. However, tumor cells have evolved to circumvent this anchorage dependence leading to the

presence of circulating tumor cells (CTCs) that can metastasize to a distant organ [29]. When metastatic tumor cells reach their new site, they must create a microenvironment conducive for survival and growth. Recent work in a mouse model of pancreatic ductal adenocarcinoma (PDA) shows that FN is critical in supporting engraftment of metastatic cancer cells in target organs (e.g., liver and lung) [30].

The expression of FN is elevated in many solid tumors, especially PDA [31-33]. In this context, FN contributes to cancer cell survival, invasion and metastasis, chemoresistance, and angiogenesis [34]. For instance, the human PDA cell lines Panc-1 and Capan-1 showed increased resistance to cytotoxic agents including gemcitabine, cisplatin, and doxorubicin when cells were grown on FN-coated plates [20]. The pro-survival effect of FN has been attributed to activation of the PI3K/AKT/mTOR pathway [17, 35]. Moreover, it was reported that FN stimulates reactive oxygen species (ROS) in PDA cells, which led to increased survival that could be reversed by antioxidant treatment [36]. ROS, in moderate amounts, serve as signaling molecules that stimulate proliferation and promote survival through the Ras-Raf-MEK-ERK and NF- κ B pathways, respectively [37].

FN is also an important contributor to angiogenesis, the formation of new blood vessels from pre-existing vessels. In addition to growth factors such as vascular endothelial growth factor (VEGF), ligation of the ECM via integrin receptors is essential for angiogenesis. The use of knockout mice revealed that integrins β 1, α v, α 4, and α 5 are required for angiogenesis [38]. Integrin α 5 knockout mice die at embryonic day E10.5

due to severe vascular defects [39], and deletion of FN results in vascular abnormalities and death at day E9.5 [40]. Tumors require angiogenesis to persist and thrive. Although still under active investigation, FN has been shown to be important in tumor angiogenesis as well. Early studies revealed that targeting the FN- $\alpha 5\beta 1$ interaction via antibody antagonists blocked angiogenesis in the chick chorioallantoic membrane assay [6]. Moreover, $\alpha 5\beta 1$ targeting antibodies, such as volociximab, inhibit tumor growth in various animal models of cancer, but these promising pre-clinical results have yet to be recapitulated in patients [31, 41-46].

At the molecular level, FN may stimulate angiogenesis by various mechanisms. Integrin adhesion to the ECM, and to FN specifically, triggers endothelial cell migration and microvessel elongation [47]. Furthermore, the alternatively spliced extra domain A of FN can stimulate VEGF-C expression in a PI3K/Akt dependent manner in colorectal carcinoma [48]. Along these lines, FN can stimulate ROS production [36, 49, 50], mainly in the form of hydrogen peroxide, which is known to induce VEGF expression when present in moderate amounts [51].

Matricellular proteins: extracellular modulators of the ECM

Integrin activation by abundant ECM proteins such as FN and collagen is controlled by regulatory proteins found within the ECM referred to as matricellular proteins. Matricellular proteins as a class do not function as structural components of the ECM, instead they mediate ECM-receptor interactions [52, 53]. Some major examples of matricellular proteins are thrombospondin-1 & 2 (TSP-1 & 2), tenascin-C (TNC) secreted

protein acidic and rich in cysteine (SPARC), osteopontin (OPN), and the fibulin family of proteins. Matricellular proteins can regulate ECM function by directly binding to cell surface receptors or structural and soluble proteins within the ECM. For example, SPARC binds directly to collagen and blocks collagen mediated signaling via the discoidin domain receptors [14, 54]. In this context, the absence of SPARC enhanced collagen-mediated tumor progression. Moreover, TSP-1 blocks FN-induced focal adhesions in endothelial cells [55]. Similarly, TNC interferes with FN-integrin interaction and reduces FN-mediated adhesion of fibroblasts [56, 57].

Matricellular proteins are typically expressed abundantly during development and reactivated during wound healing and other tissue remodeling events [52]. Phenotypes of mice lacking a particular matricellular protein are usually mild, reinforcing the fact that these proteins do not contribute to the structural integrity of tissues [58, 59]. However, deficiencies in response to wound healing and tissue repair are often seen [60]. Abnormal expression of matricellular proteins is seen in certain pathologies, such as cancer. The matricellular protein Fibulin-5 is aberrantly expressed in many cancers [49, 61-64]. Fibulin-5 has important contributions to normal physiology and development as well as cancer.

Fibulin-5 (Fbln5)

Fibulin-5 (Fbln5) is a 66 kDa matricellular glycoprotein. It is a member of the fibulin family of ECM proteins, which are characterized by six calcium-binding EGF-like repeats (cbEGF) at the N-terminus (for protein stability and interactions) and a globular

C-terminal fibulin module [65]. Similar to other ECM proteins, Fbln5 is a TGF- β - and hypoxia-inducible gene [66, 67]. Fbln5 is distinct amongst the fibulins in that it contains an RGD-integrin binding domain (Fig. 1).

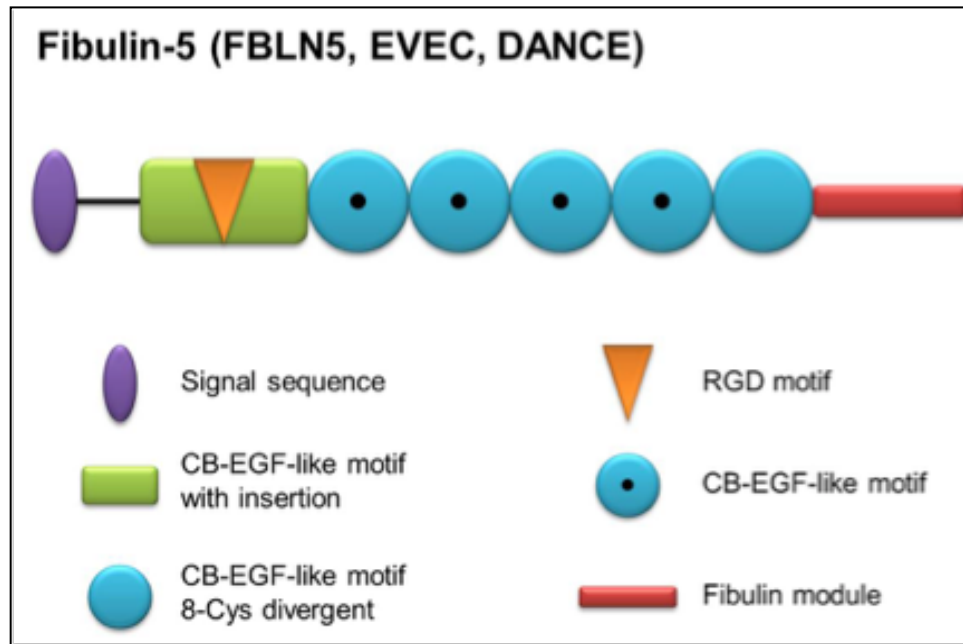


Figure 1. Domain structure of Fbln5 (by Miao Wang)

Fbln5 was discovered as a gene highly expressed in large vessels during development; however, it is down-regulated in most adult tissues except where active tissue remodeling is occurring [59, 68, 69]. Fbln5 is induced by models of vascular injury including balloon withdrawal injury and in atherosclerotic plaques, highlighting its contribution to vascular function and maintenance [68, 69]. The generation of Fbln5 knockout mice revealed a major function of Fbln5 in elastic fiber formation [59, 70]. *Fbln5*^{-/-} mice exhibit general connective tissue defects such as loose skin, tortuous vessels, emphysematous lung, and genital prolapse. This provided the first animal

model for congenital elastic fiber disorders [71]. These seminal studies laid the foundation for future discoveries regarding Fbln5.

Fbln5 in cell adhesion/migration

As mentioned above, Fbln5 contains an RGD-integrin binding domain and has been reported (although not shown conclusively) to ligate RGD-binding integrins including $\alpha 4\beta 1$, $\alpha 5\beta 1$, $\alpha v\beta 3$, $\alpha v\beta 5$, and $\alpha 9\beta 1$ [59, 72]. Fbln5 supports adhesion of endothelial cells and smooth muscle cells (SMCs) in an RGD-dependent manner [68, 69, 72]. Furthermore, Fbln5 interacts with multiple extracellular proteins including extracellular superoxide dismutase (ecSOD) where it tethers ecSOD to vascular tissues and helps regulate ROS production [73]. Fbln5 also binds to tropoelastin and lysyl-oxidase-like 1 (LOXL1), which is thought to be critical for normal elastogenesis to occur [74].

Fbln5 regulates cell migration in a context-dependent manner. For example, Fbln5 failed to induce migration in SMCs compared to FN [72]. SMCs plated onto Fbln5-coated dishes appeared rounded and less spread compared to cells plated on FN. Immunofluorescence staining showed that focal adhesion and actin stress fiber formation were significantly reduced in the presence of Fbln5 compared to FN. Finally, cells plated on either Fbln5 or FN were analyzed for migratory capacity by imposing a wound in the adherent cultures. Closure of the wound was monitored between the two conditions, which revealed reduced migration in cells plated on Fbln5 [72]. Treatment with an activating $\beta 1$ integrin antibody reversed the negative effects of Fbln5 on migration and stress fiber formation. These results suggest passive ligation of Fbln5 by

integrins in SMCs.

Fbln5 also antagonized endothelial cell migration [75]. In this context, ectopic expression of Fbln5 in endothelial cells dampened migration as tested by the ability of these cells to move through a matrigel matrix and also by measuring trans-well migration (Boyden-chamber assay). Moreover, treating endothelial cells with recombinant Fbln5 blocked angiogenic sprouting *in vitro* [75]. In contrast, Fbln5 induced migration of fibrosarcoma cells [76]. Using a slightly modified version of the Boyden-chamber assay where FN was coated on the bottom of the porous membrane, Fbln5-expressing fibrosarcoma cells displayed enhanced migration towards FN. Together; these findings highlight cell-type specific effects of Fbln5 signaling that likely reflect the variable integrin expression profile between cell types and whether these specific integrins are subject to inhibition by Fbln5.

Fbln5 in proliferation/survival

Similar to the context-specific effects on cell motility, Fbln5 can positively and negatively regulate proliferation depending on cell type. For instance, overexpression of Fbln5 in 3T3 fibroblasts revealed increased activation of ERK1/2 and p38 mitogen-activated protein kinase (MAPK) [76]. This group also showed that Fbln5 synergized with TGF- β to stimulate proliferation and DNA synthesis in 3T3 cells. Conversely, Fbln5 was shown to induce an anti-proliferative response in epithelial cells through decreased expression of cyclin A, thus abrogating progression of the cell cycle.

Endothelial cells stimulated with Fbln5 did not show activation of ERK1/2 and p38-MAPK but Fbln5 did reduce VEGF expression, which resulted in reduced endothelial cell proliferation [75]. Likewise, Fbln5 failed to induce proliferation in SMCs compared to cells plated on FN due to a reduction in β 1 integrin signaling [72]. In addition, recent studies performed in ovarian cancer cells also revealed changes in proliferation upon Fbln5 overexpression [77]. Expression of Fbln5 in SKOV3 ovarian carcinoma cells led to G2/M arrest but did not adversely affect colony-forming ability. Conversely, knockdown of Fbln5 in human gastric cancer cells blocked cell proliferation as tested by BrdU incorporation [63]. Together, these data support an anti-proliferative effect of Fbln5 in endothelial cells and a pro-proliferative effect in fibroblasts. Yet, it is unclear whether Fbln5 promotes or blocks proliferation in epithelial cells. Since Fbln5 blocks FN-mediated integrin signaling, it is germane to evaluate the effect of integrin-activating or -inhibiting antibodies on proliferation in contexts where Fbln5 has been manipulated.

Fbln5 in angiogenesis

Fbln5 was identified by two separate groups who were interested in proteins that regulate cardiovascular development and disease [68, 69]. Each group identified Fbln5 as being expressed in the embryonic arterial vasculature, however, downregulated in most adult vascular beds. They also found that expression of Fbln5 was reactivated in diseased adult vasculature, namely atherosclerotic and balloon-injured arteries. Fbln5 knockout mice were created shortly after these original findings, which revealed the important function of Fbln5 in elastogenesis such that Fbln5-deficient animals had tortuous vessels in addition to loose skin and emphysematous lung as a result of

incomplete elastic fiber formation [59, 70]. Elasticity is a major characteristic of blood vessels and critical for proper vessel function. These observations led to the investigation of Fbln5 as a regulator of angiogenesis in several model systems.

Sullivan et al. [78] revealed that polyvinyl alcohol sponges implanted into *Fbln5*^{-/-} mice had significantly increased vascular invasion as seen by CD31 (PECAM-1) staining. Interestingly, fibroblast migration into these sponges remained unchanged in the absence of Fbln5. This group then examined a possible mechanism by which Fbln5 was antagonizing vascularization and found that the pro-angiogenic factors, Ang-1, Ang-2, Ang-3, and VEGF, were increased in sponges removed from *Fbln5*^{-/-} mice as seen by quantitative PCR. Moreover, vascular smooth muscle cells (VSMCs) isolated from WT and Fbln5-deficient mice also showed an increase of these pro-angiogenic factors in the absence of Fbln5. The authors of this paper did not examine the function of integrins in this phenotype. Therefore, based on these studies alone it is difficult to determine whether Fbln5 directly antagonizes vascular function or if this is an integrin-dependent phenomenon. Given the evidence that Fbln5 binds to but does not support activation of $\alpha 4\beta 1$ and $\alpha 5\beta 1$ integrins in SMCs [72], it is probable that enhanced integrin activation in the absence of Fbln5 results in increased endothelial cell migration and proliferation in this context [79, 80].

The function of Fbln5 in tumor angiogenesis has also produced mixed results. Forced expression of Fbln5 by fibrosarcoma cells resulted in tumors that were significantly less vascularized compared to tumors derived from control cells [81]. These results suggest

that Fbln5 antagonizes tumor angiogenesis, which again, is likely a consequence of reduced FN-integrin signaling by Fbln5. In stark contrast, our lab has reported that subcutaneous and orthotopic pancreatic tumor growth (Pan02) in *Fbln5*^{-/-} mice results in reduced tumor blood vessel density [82]. In this study, we found that loss of Fbln5 in tumors results in overwhelming ROS production mediated by FN-integrin signaling. The discrepancy between these two findings is likely attributed to the complete lack of host Fbln5 in our model as well as the lack of Fbln5 expression in Pan02 cells [49, 82]. In the fibrosarcoma model, it is difficult to distinguish between the function of host- or tumor-derived Fbln5 with regard to regulation of angiogenesis. Moreover, the loss of Fbln5 function in tumors produces a much different effect on angiogenesis compared to non-tumor tissue (e.g. the polyvinyl alcohol sponge model mentioned above), which we propose is due to the high amount of FN in tumors vs. normal tissue. A major biological outcome of FN-integrin signaling is ROS production [50], therefore, Fbln5 functions as a molecular rheostat to control this outcome.

Fbln5 in tumor progression

As described above, the cellular effects of Fbln5 are context-dependent and thus the effect of Fbln5 on tumor progression may also be tumor-specific. Initial studies on Fbln5 and tumor growth relied on forced expression of Fbln5 in cancer cell lines that were then implanted into immunodeficient mice. Lee et al. [62] revealed increased Fbln5 expression from human breast tumors, and that Fbln5 expression in 4T1 breast cancer cells enhanced tumor growth in mice. Yue et al. [83] reported that Fbln5-expressing H460 lung cancer cells displayed decreased metastasis to the lungs after iv injection.

This study did not examine primary lung tumor growth in the context of Fbln5, however, lung cancer patient samples showed a downregulation of Fbln5 compared to matched normal lung specimens as seen by RT-PCR and immunohistochemistry (IHC) analysis of a tissue microarray.

Our lab was the first to report on tumor studies performed in Fbln5 mutant mice. As mentioned previously, Schluterman et al. [82] showed that subcutaneous and orthotopic Pan02 tumors implanted into *Fbln5*^{-/-} mice had a significant reduction in tumor growth and blood vessel density [82]. To identify a mechanism for this reduction in angiogenesis and tumor growth, we examined ROS levels in tumors from *WT* and *Fbln5*^{-/-} mice. The rationale behind this was that Fbln5 had been shown to regulate ROS production in vascular tissue through binding ecSOD, and the deletion of Fbln5 resulted in increased ROS production in mouse aortas [73]. Consistent with this, we also found elevated levels of ROS production in tumors grown in *Fbln5*^{-/-} mice compared to tumors grown in *WT* mice. Moreover, mice containing a point mutation in the RGD-integrin binding domain of Fbln5 (RGD → RGE) recapitulated the phenotype seen in *Fbln5*^{-/-} mice with regard to tumor growth, angiogenesis, and ROS production, highlighting the importance of Fbln5-integrin interaction in this phenotype. Using mouse embryonic fibroblasts (MEFs) *in vitro*, we found that increased ROS production was a consequence of increased integrin signaling by FN in the absence of functional Fbln5. Furthermore, antioxidant treatment restored tumor growth and microvessel density in *Fbln5*^{RGE/RGE} mice, confirming that reduced tumor growth was a direct consequence of elevated ROS production driven by loss of Fbln5-integrin binding. This data is in line

with other evidence that shows Fbln5 competes with FN to negatively regulate $\beta 1$ integrin function [72].

Elevated oxidative stress is seen in many solid tumors compared to normal tissues, and exploiting this biochemical difference has the potential to enhance the efficacy of anticancer agents [84]. For instance, ROS accumulation after gemcitabine treatment in PDA cells contributes significantly to the cytotoxic activity of this nucleoside analog [85]. Furthermore, elevated hydrogen peroxide levels was shown to be a mechanism by which paclitaxel killed lung cancer cells [86]. Homeostasis of ROS is important for normal cell function and signaling, but excessive ROS can result in cellular toxicity, and therefore ROS levels must be tightly controlled. ROS can be produced by a number of enzymes including but not limited to, the electron transport chain (ETC), NADPH oxidase (NOX), 5-lipoxygenase (5-LOX), and nitric oxide synthase (NOS) [87].

ECM proteins can stimulate the activation of these enzymes and thus indirectly induce ROS production. Chiarugi et al. [50] showed that integrin activation by FN induces ROS production in a 5-LOX and NOX dependent manner in 3T3 fibroblasts [50]. Another group showed that PDA cells are responsive to FN in terms of increased ROS production by 5-LOX and NOX [36]. Given that FN can stimulate ROS production via integrin activation and that the loss or mutation of Fbln5 results in higher ROS production, we propose Fbln5 blocks integrin-induced ROS production. In PDA, where ECM is abundant [16, 88], oxidative stress levels are much higher compared to normal

pancreas [89]. Thus, Fbln5 is a novel target to investigate as a potential strategy to manipulate ROS levels in the TME.

While we found that genetically ablating Fbln5 can reduce subcutaneous and orthotopic pancreatic tumor growth, there are some limitations to this model with regard to recapitulating human disease. The major shortcoming with implant models is that they do not always represent the histology, genetics, and overall progression of the disease. Genetically engineered mouse models (GEMMs) can help address some of these limitations. Therefore, the goal of my project was to study the effect of Fbln5 in a GEMM of PDA. I sought to understand the effect of endogenous Fbln5 on drug-response and tumor progression in this model with emphasis on ROS production and vascular function. Moreover, I examined the mechanism by which ROS is produced in the context of mutant Fbln5. Lastly, I determined the molecular mechanism by which Fbln5 expression is controlled in PDA.

References:

1. Vogel, W.F., *Collagen-receptor signaling in health and disease*. Eur J Dermatol, 2001. **11** (6): p. 506-14.
2. Pankov, R., *Fibronectin at a glance*, in *Journal of Cell Science*. 2002. p. 3861-3863.
3. Beck, K., I. Hunter, and J. Engel, *Structure and function of laminin: anatomy of a multidomain glycoprotein*. FASEB J, 1990. **4**(2): p. 148-60.
4. Mithieux, S.M. and A.S. Weiss, *Elastin*. Adv Protein Chem, 2005. **70**: p. 437-61.
5. Harburger, D.S. and D.A. Calderwood, *Integrin signalling at a glance*. J Cell Sci, 2009. **122**(Pt 2): p. 159-63.
6. Kim, S., et al., *Regulation of angiogenesis in vivo by ligation of integrin $\alpha 5 \beta 1$ with the central cell-binding domain of fibronectin*. Am J Pathol, 2000. **156**(4): p. 1345-62.
7. de Fougères, A.R., et al., *Regulation of inflammation by collagen-binding integrins $\alpha 1 \beta 1$ and $\alpha 2 \beta 1$ in models of hypersensitivity and arthritis*. J Clin Invest, 2000. **105**(6): p. 721-9.
8. Kriegstein, C.F., et al., *Collagen-binding integrin $\alpha 1 \beta 1$ regulates intestinal inflammation in experimental colitis*. J Clin Invest, 2002. **110**(12): p. 1773-82.
9. Giancotti, F.G., *Integrin Signaling*, in *Science*. 1999. p. 1028-1033.
10. Lipfert, L., et al., *Integrin-dependent phosphorylation and activation of the protein tyrosine kinase pp125FAK in platelets*. J Cell Biol, 1992. **119**(4): p. 905-12.
11. Masur, S.K., et al., *Integrin-dependent tyrosine phosphorylation in corneal fibroblasts*. Invest Ophthalmol Vis Sci, 1995. **36**(9): p. 1837-46.
12. Schlaepfer, D.D., et al., *Integrin-mediated signal transduction linked to Ras pathway by GRB2 binding to focal adhesion kinase*. Nature, 1994. **372**(6508): p. 786-91.
13. Eliceiri, B.P., *Integrin and growth factor receptor crosstalk*. Circ Res, 2001. **89**(12): p. 1104-10.
14. Aguilera, K.Y., et al., *Collagen signaling enhances tumor progression after anti-VEGF therapy in a murine model of pancreatic ductal adenocarcinoma*. Cancer Res, 2014. **74**(4): p. 1032-44.
15. Akiyama, S.K., K. Olden, and K.M. Yamada, *Fibronectin and integrins in invasion and metastasis*. Cancer Metastasis Rev, 1995. **14**(3): p. 173-89.

16. Bachem, M.G., et al., *Pancreatic carcinoma cells induce fibrosis by stimulating proliferation and matrix synthesis of stellate cells*. Gastroenterology, 2005. **128**(4): p. 907-21.
17. Han, S., F.R. Khuri, and J. Roman, *Fibronectin stimulates non-small cell lung carcinoma cell growth through activation of Akt/mammalian target of rapamycin/S6 kinase and inactivation of LKB1/AMP-activated protein kinase signal pathways*. Cancer Res, 2006. **66**(1): p. 315-23.
18. Itano, N., L. Zhuo, and K. Kimata, *Impact of the hyaluronan-rich tumor microenvironment on cancer initiation and progression*. Cancer Sci, 2008. **99**(9): p. 1720-5.
19. Lu, P., V.M. Weaver, and Z. Werb, *The extracellular matrix: A dynamic niche in cancer progression*, in *The Journal of Cell Biology*. 2012. p. 395-406.
20. Miyamoto, H., et al., *Tumor-stroma interaction of human pancreatic cancer: acquired resistance to anticancer drugs and proliferation regulation is dependent on extracellular matrix proteins*. Pancreas, 2004. **28**(1): p. 38-44.
21. Hcevar, B.A., T.L. Brown, and P.H. Howe, *TGF-beta induces fibronectin synthesis through a c-Jun N-terminal kinase-dependent, Smad4-independent pathway*. EMBO J, 1999. **18**(5): p. 1345-56.
22. Leask, A. and D.J. Abraham, *TGF-beta signaling and the fibrotic response*. FASEB J, 2004. **18**(7): p. 816-27.
23. Bonner, J.C., *Regulation of PDGF and its receptors in fibrotic diseases*. Cytokine Growth Factor Rev, 2004. **15**(4): p. 255-73.
24. Zhao, J.C., et al., *Cooperation between Polycomb and androgen receptor during oncogenic transformation*. Genome Res, 2012. **22**(2): p. 322-31.
25. Weis, S.M. and D.A. Cheresh, *Tumor angiogenesis: molecular pathways and therapeutic targets*. Nat Med, 2011. **17**(11): p. 1359-70.
26. Mao, Y., et al., *Stromal cells in tumor microenvironment and breast cancer*. Cancer Metastasis Rev, 2013. **32**(1-2): p. 303-15.
27. Gajewski, T.F., H. Schreiber, and Y.X. Fu, *Innate and adaptive immune cells in the tumor microenvironment*. Nat Immunol, 2013. **14**(10): p. 1014-22.
28. Frisch, S.M. and R.A. Screaton, *Anoikis mechanisms*. Curr Opin Cell Biol, 2001. **13**(5): p. 555-62.
29. Guadamillas, M.C., A. Cerezo, and M.A. Del Pozo, *Overcoming anoikis--pathways to anchorage-independent growth in cancer*. J Cell Sci, 2011. **124**(Pt 19): p. 3189-97.
30. Costa-Silva, B., et al., *Pancreatic cancer exosomes initiate pre-metastatic niche formation in the liver*, in *Nature Cell Biology*. 2015. p. 816-826.

31. Ramakrishnan, V., et al., *Preclinical evaluation of an anti-alpha5beta1 integrin antibody as a novel anti-angiogenic agent*. J Exp Ther Oncol, 2006. 5(4): p. 273-86.
32. Ramaswamy, S., et al., *A molecular signature of metastasis in primary solid tumors*. Nat Genet, 2003. 33(1): p. 49-54.
33. Stenman, S. and A. Vaheri, *Fibronectin in human solid tumors*. Int J Cancer, 1981. 27(4): p. 427-35.
34. Topalovski, M. and R.A. Brekken, *Matrix control of pancreatic cancer: New insights into fibronectin signaling*. Cancer Lett, 2015.
35. Chen, H.C. and J.L. Guan, *Association of focal adhesion kinase with its potential substrate phosphatidylinositol 3-kinase*. Proc Natl Acad Sci U S A, 1994. 91(21): p. 10148-52.
36. Edderkaoui, M., et al., *Extracellular matrix stimulates reactive oxygen species production and increases pancreatic cancer cell survival through 5-lipoxygenase and NADPH oxidase*. Am J Physiol Gastrointest Liver Physiol, 2005. 289(6): p. G1137-47.
37. Reuter, S., et al., *Oxidative stress, inflammation, and cancer: How are they linked?*, in *Free Radical Biology and Medicine*. 2010, Elsevier Inc. p. 1603-1616.
38. Schaffner, F., A. Ray, and M. Dontenwill, *Integrin $\alpha 5 \beta 1$, the Fibronectin Receptor, as a Pertinent Therapeutic Target in Solid Tumors*, in *Cancers*. 2013. p. 27-47.
39. Yang, J.T., H. Rayburn, and R.O. Hynes, *Embryonic mesodermal defects in alpha 5 integrin-deficient mice*. Development, 1993. 119(4): p. 1093-105.
40. George, E.L., et al., *Defects in mesoderm, neural tube and vascular development in mouse embryos lacking fibronectin*. Development, 1993. 119(4): p. 1079-91.
41. Besse, B., et al., *Phase Ib safety and pharmacokinetic study of volociximab, an anti- $\alpha 5 \beta 1$ integrin antibody, in combination with carboplatin and paclitaxel in advanced non-small-cell lung cancer*, in *Annals of Oncology*. 2012. p. 90-96.
42. Bhaskar, V., et al., *Volociximab, a chimeric integrin alpha5beta1 antibody, inhibits the growth of VX2 tumors in rabbits*. Invest New Drugs, 2008. 26(1): p. 7-12.
43. Bhaskar, V., et al., *A function blocking anti-mouse integrin alpha5beta1 antibody inhibits angiogenesis and impedes tumor growth in vivo*. J Transl Med, 2007. 5: p. 61.

44. Cranmer LD, B.A., Ribas A *Phase II study of volociximab (M200), an $\alpha 5\beta 1$ anti-integrin antibody in metastatic melanoma*. J Clin Oncol, 2005. **24** (Abstr 8011).
45. Kuwada, S.K., *Drug evaluation: Volociximab, an angiogenesis-inhibiting chimeric monoclonal antibody*. Curr Opin Mol Ther, 2007. **9**(1): p. 92-8.
46. Ricart, A.D., *Volociximab, a chimeric monoclonal antibody that specifically binds $\alpha 5\beta 1$ integrin: a phase I, pharmacokinetic, and biological correlative study*. Clin. Cancer Res., 2008. **14**: p. 7924-7929.
47. Nicosia, R.F., E. Bonanno, and M. Smith, *Fibronectin promotes the elongation of microvessels during angiogenesis in vitro*. J Cell Physiol, 1993. **154**(3): p. 654-61.
48. Xiang, L., et al., *The extra domain A of fibronectin increases VEGF-C expression in colorectal carcinoma involving the PI3K/AKT signaling pathway*. PLoS One, 2012. **7**(4): p. e35378.
49. Wang, M., et al., *Fibulin-5 Blocks Microenvironmental ROS in Pancreatic Cancer*. Cancer Res, 2015. **75**(23): p. 5058-69.
50. Chiarugi, P., et al., *Reactive oxygen species as essential mediators of cell adhesion: the oxidative inhibition of a FAK tyrosine phosphatase is required for cell adhesion*. J Cell Biol, 2003. **161**(5): p. 933-44.
51. Zhu, J.W., et al., *Upregulation of vascular endothelial growth factor by hydrogen peroxide in human colon cancer*. World J Gastroenterol, 2002. **8**(1): p. 153-7.
52. Bornstein, P. and E.H. Sage, *Matricellular proteins: extracellular modulators of cell function*. Curr Opin Cell Biol, 2002. **14**(5): p. 608-16.
53. Wong, G.S. and A.K. Rustgi, *Matricellular proteins: priming the tumour microenvironment for cancer development and metastasis*. Br J Cancer, 2013. **108**(4): p. 755-61.
54. Arnold, S.A., et al., *Lack of host SPARC enhances vascular function and tumor spread in an orthotopic murine model of pancreatic carcinoma*. Dis Model Mech, 2010. **3**(1-2): p. 57-72.
55. Murphy-Ullrich, J.E., et al., *Heparin-binding peptides from thrombospondins 1 and 2 contain focal adhesion-labilizing activity*. J Biol Chem, 1993. **268**(35): p. 26784-9.
56. Chiquet-Ehrismann, R., et al., *Tenascin interferes with fibronectin action*. Cell, 1988. **53**(3): p. 383-90.
57. Huang, W., et al., *Interference of tenascin-C with syndecan-4 binding to fibronectin blocks cell adhesion and stimulates tumor cell proliferation*. Cancer Res, 2001. **61**(23): p. 8586-94.

58. Chapman, S.L., et al., *Fibulin-2 and Fibulin-5 Cooperatively Function to Form the Internal Elastic Lamina and Protect From Vascular Injury*, in *Arteriosclerosis, Thrombosis, and Vascular Biology*. 2009. p. 68-74.
59. Nakamura, T., et al., *Fibulin-5/DANCE is essential for elastogenesis in vivo*. *Nature*, 2002. **415**(6868): p. 171-5.
60. Kyriakides, T.R. and P. Bornstein, *Matricellular proteins as modulators of wound healing and the foreign body response*. *Thromb Haemost*, 2003. **90**(6): p. 986-92.
61. Hwang, C.F., et al., *Oncogenic fibulin-5 promotes nasopharyngeal carcinoma cell metastasis through the FLJ10540/AKT pathway and correlates with poor prognosis*. *PLoS One*, 2013. **8**(12): p. e84218.
62. Lee, Y.H., et al., *Fibulin-5 initiates epithelial-mesenchymal transition (EMT) and enhances EMT induced by TGF- in mammary epithelial cells via a MMP-dependent mechanism*, in *Carcinogenesis*. 2008. p. 2243-2251.
63. Shi, X.-Y., et al., *Effect of Fibulin-5 on cell proliferation and invasion in human gastric cancer patients*, in *Asian Pacific Journal of Tropical Medicine*. 2014, Hainan Medical College. p. 787-791.
64. Tang, J.-C., *Effect of fibulin-5 on adhesion, migration and invasion of hepatocellular carcinoma cells viaan integrin-dependent mechanism*, in *WJG*. 2015. p. 11127.
65. Yanagisawa, H., M.K. Schluterman, and R.A. Brekken, *Fibulin-5, an integrin-binding matricellular protein: its function in development and disease*, in *J. Cell Commun. Signal*. 2009. p. 337-347.
66. Kuang, P.P., et al., *Fibulin-5 gene expression in human lung fibroblasts is regulated by TGF-beta and phosphatidylinositol 3-kinase activity*, in *AJP: Cell Physiology*. 2006. p. C1412-C1421.
67. Guadall, A., et al., *Fibulin-5 Is Up-regulated by Hypoxia in Endothelial Cells through a Hypoxia-inducible Factor-1 (HIF-1)-dependent Mechanism*, in *Journal of Biological Chemistry*. 2011. p. 7093-7103.
68. Kowal, R.C., et al., *EVEC, a Novel Epidermal Growth Factor Like Repeat-Containing Protein Upregulated in Embryonic and Diseased Adult Vasculature*, in *Circulation Research*. 1999. p. 1166-1176.
69. Tomoyuki Nakamura, P.R.-L., Volkhard Lindner,fDaisuke Yabe, and Y.F. Masafumi Taniwaki, Kazuhiro Kobuke, Kei Tashiro, Zhijian Lu,Nancy L. Andon, Robert Schaub, Akira Matsumori, Shigetake Sasayama, Kenneth R. Chien, and Tasuku Honjoa, *DANCE, a Novel Secreted RGD Protein Expressed in Developing, Atherosclerotic, and Balloon-injured Arteries*. *The Journal of Biological Chemistry*, 1999. **274**(32): p. 22467-22483.
70. Yanagisawa, H., et al., *Fibulin-5 is an elastin-binding protein essential for elastic fibre development in vivo*. *Nature*, 2002. **415**(6868): p. 168-71.

71. Loeys, B., et al., *Homozygosity for a missense mutation in fibulin-5 (FBLN5) results in a severe form of cutis laxa*. Hum Mol Genet, 2002. 11(18): p. 2113-8.
72. Lomas, A.C., et al., *Fibulin-5 binds human smooth-muscle cells through alpha5beta1 and alpha4beta1 integrins, but does not support receptor activation*. Biochem J, 2007. 405(3): p. 417-28.
73. Nguyen, A.D., et al., *Fibulin-5 is a novel binding protein for extracellular superoxide dismutase*. Circ Res, 2004. 95(11): p. 1067-74.
74. Liu, X., et al., *Elastic fiber homeostasis requires lysyl oxidase-like 1 protein*. Nat Genet, 2004. 36(2): p. 178-82.
75. Albig, A.R. and W.P. Schiemann, *Fibulin-5 antagonizes vascular endothelial growth factor (VEGF) signaling and angiogenic sprouting by endothelial cells*. DNA Cell Biol, 2004. 23(6): p. 367-79.
76. Schiemann, W.P., *Context-specific Effects of Fibulin-5 (DANCE/EVEC) on Cell Proliferation, Motility, and Invasion. FIBULIN-5 IS INDUCED BY TRANSFORMING GROWTH FACTOR-beta AND AFFECTS PROTEIN KINASE CASCADES*, in *Journal of Biological Chemistry*. 2002. p. 27367-27377.
77. Heo, J.H., et al., *Fibulin-5 is a tumour suppressor inhibiting cell migration and invasion in ovarian cancer*. J Clin Pathol, 2015.
78. Sullivan, K.M., et al., *Fibulin-5 functions as an endogenous angiogenesis inhibitor*, in *Lab Invest*. 2007. p. 818-827.
79. Lamalice, L., F. Le Boeuf, and J. Huot, *Endothelial cell migration during angiogenesis*. Circ Res, 2007. 100(6): p. 782-94.
80. Clark, R.A., et al., *Blood vessel fibronectin increases in conjunction with endothelial cell proliferation and capillary ingrowth during wound healing*. J Invest Dermatol, 1982. 79(5): p. 269-76.
81. Albig, A.R., *Fibulins 3 and 5 Antagonize Tumor Angiogenesis In vivo*, in *Cancer Research*. 2006. p. 2621-2629.
82. Schluterman, M.K., et al., *Loss of fibulin-5 binding to $\alpha 1$ integrins inhibits tumor growth by increasing the level of ROS*, in *Disease Models & Mechanisms*. 2010. p. 333-342.
83. Yue, W., et al., *Fibulin-5 Suppresses Lung Cancer Invasion by Inhibiting Matrix Metalloproteinase-7 Expression*, in *Cancer Research*. 2009. p. 6339-6346.
84. Trachootham, D., J. Alexandre, and P. Huang, *Targeting cancer cells by ROS-mediated mechanisms: a radical therapeutic approach?* Nat Rev Drug Discov, 2009. 8(7): p. 579-91.
85. Ju, H.Q., et al., *Mechanisms of Overcoming Intrinsic Resistance to Gemcitabine in Pancreatic Ductal Adenocarcinoma through the Redox Modulation*. Mol Cancer Ther, 2015. 14(3): p. 788-98.

86. Alexandre, J., et al., *Accumulation of hydrogen peroxide is an early and crucial step for paclitaxel-induced cancer cell death both in vitro and in vivo*. Int J Cancer, 2006. **119**(1): p. 41-8.
87. Holmstrom, K.M. and T. Finkel, *Cellular mechanisms and physiological consequences of redox-dependent signalling*. Nat Rev Mol Cell Biol, 2014. **15**(6): p. 411-21.
88. Mahadevan, D. and D.D. Von Hoff, *Tumor-stroma interactions in pancreatic ductal adenocarcinoma*, in *Molecular Cancer Therapeutics*. 2007. p. 1186-1197.
89. Blum, R. and Y. Kloog, *Metabolism addiction in pancreatic cancer*. Cell Death Dis, 2014. **5**: p. e1065.

Chapter 2. Fbln5 promotes pancreatic tumor growth through inhibition of integrin-induced ROS.

Introduction:

PDA is a lethal cancer with a 5-year survival rate of 6% and a median survival of ~6 months, making it the 4th leading cause of cancer-related deaths in the United States [1]. However, a recent and alarming report has projected that PDA will become the 2nd leading cause of cancer-related deaths in the United States by 2030 [2]. The poor prognosis of this disease can be attributed to late-stage detection, resistance to standard therapies, and metastatic spread. Thus, understanding the biological features that contribute to tumor progression is critical in order to discover novel therapeutic strategies.

A dense fibrotic response by the host is a major feature of PDA. This increased deposition of ECM can often occupy more than half of the tumor mass. The desmoplastic reaction of PDA results in recruitment of fibroblasts, endothelial cells, and immune cells, which are surrounded by tumor cells and embedded in an acellular ECM network [3]. GEMMs of PDA serve as excellent tools to study ECM-tumor interactions because they mimic the histopathology of human PDA [4, 5] (Figs. 1 & 2).

ECM signaling depends on the specific ECM-receptor interaction and the expression and activity of matricellular proteins that function as extracellular adaptors to regulate these interactions [6-9]. For instance, Fbln5 binds to but does not support integrin

activation and competes with FN for integrin binding [9, 10]. As a result, tissues that lack functional Fbln5 experience an increase in integrin signaling, which have context-specific effects depending on the tissue or disease state. As previously stated, genetic deletion of Fbln5 in mice stimulates angiogenesis in normal pancreas; however, reduces angiogenesis in tumors from syngeneic models of PDA [11]. In this context, subcutaneous and orthotopic Pan02 tumors exhibited a reduction in overall tumor growth in *Fbln5*^{-/-} mice. The discrepancy in vascular function between normal and tumor-bearing pancreas of *Fbln5*^{-/-} mice may be attributed to the levels of FN present. Normal pancreas displays little FN compared to PDA (Fig. 1H). Thus, we postulated that the increased expression of FN in PDA combined with the loss of functional Fbln5 is leading to enhanced FN signaling through integrins.

A potentially harmful byproduct of integrin signaling is ROS [12]. At basal levels, ROS functions as a signaling molecule by modifying redox-sensitive proteins and reversibly altering their activity; however, excess production of ROS can lead to genomic instability and cell death, thus ROS production must be tightly regulated [13]. Interestingly, driving ROS production is therapeutically effective in various models of cancer [14]. Elevated ROS is seen in many solid tumors, and studies have revealed that oxidative tumors, such as PDA, have heightened sensitivity to further ROS insults [15, 16].

Given the high expression of FN in the stroma of PDA and increasing evidence supporting enhanced ROS production as an anti-cancer strategy [17], we evaluated the consequence of ablating the integrin binding ability of Fbln5 in robust GEMMs of PDA.

Blocking Fbln5-integrin interaction dampened tumor growth and progression in mice through an increase in ROS production by 5-lipoxygenase (5-LOX). A consequence of elevated ROS production in this context resulted in an anti-angiogenic effect. Additionally, we found that Fbln5 was expressed abundantly in the stroma of human PDA tumors. The majority of these findings were published in *Cancer Research* [9], and the remainder of this chapter will summarize the results of that manuscript.

Results:

Fbln5 expression in pancreatic cancer

The expression of Fbln5 is prominent during development, particularly in blood vessels and elastin-rich tissues, however, is diminished in most adult organs, but can be reactivated in injured vessels [18]. We examined Fbln5 expression in multiple mouse and human cell lines and tumor lysates. The mouse endothelial cell line bEnd.3 and fibroblasts, including mouse embryo fibroblasts (MEFs) and fibroblasts isolated from mouse PDA (NG2⁺ cells), expressed Fbln5 (Fig. 1A), as did human PDA lysate (Fig. 1B). In contrast, pancreatic cancer cell lines including three human lines (MiaPaCa-2, Panc1 and AsPC-1) (Fig. 1B) and 2 mouse lines (Pan 02 and MPLR B9) (Fig. 1A) did not express detectable levels of Fbln5 protein.

Fbln5 immunohistochemistry (IHC) in syngenic pancreatic Pan02 tumors grown subcutaneously in *Fbln5*^{+/+} (WT) or *Fbln5*^{-/-} (KO) mice revealed that Fbln5 is produced by stromal cells (Fig. 1E). Co-staining of Fbln5 with the endothelial cell marker Meca32

shows that Fbln5 can be produced by endothelial cells within the tumor (Fig. 1E). IHC analysis of Fbln5 expression in multiple mouse models of PDA revealed Fbln5 reactivity mainly in the stroma (Fig. 1C-D and data not shown). We also examined FBLN5 in human PDA by IHC and found the protein was expressed in all human PDAs examined (n=25). The staining pattern was confined largely to the stromal compartment; however, not all regions of stroma were positive for FBLN5 protein (Fig. 1F). The nature of the heterogeneous stromal staining pattern is unclear but suggests that FBLN5 expression is controlled tightly.

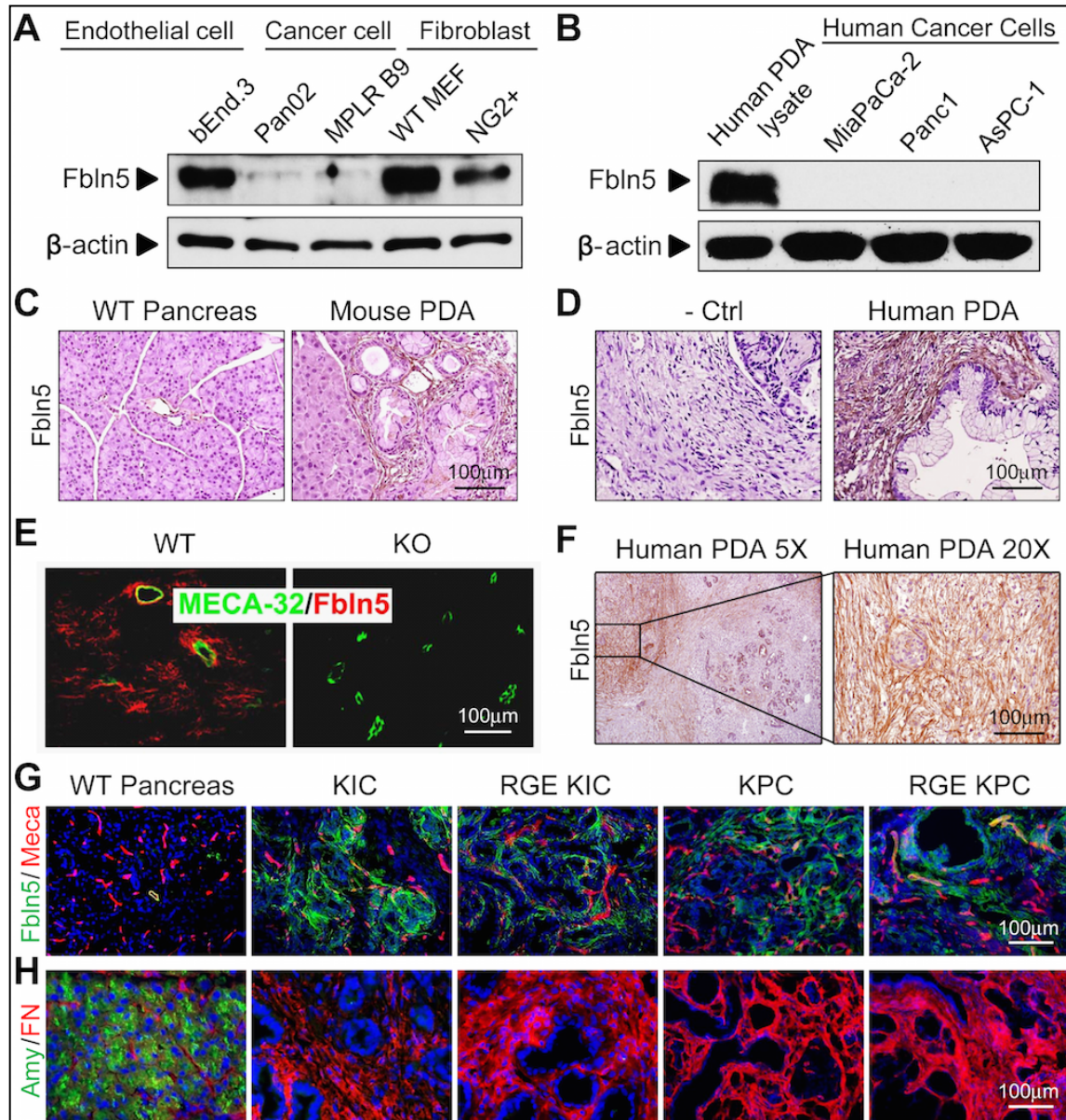


Figure 1 (legend on top of next page)

Figure 1. Expression pattern of Fbln5 in mouse and human PDA. (A-B) Protein lysates from mouse endothelial cells, cancer cells and fibroblasts (A) and human PDA tissue and cancer cell lines (B) were probed for indicated targets by Western blot. (C-D) Immunohistochemical (IHC) staining for Fbln5 on mouse (C) and human (D) PDA sections. (E) Immunofluorescence (IF) staining of Fbln5 (Red) and MECA-32 (Green) on subcutaneously grown pancreatic tumor (Pan02) in Fbln5 *WT* and *KO* mice. (F) Representative images of FBLN5 expression in human PDA, showing heterogeneous expression in the stroma. (G-H) Immunofluorescence (IF) staining of *WT* pancreas, *KIC* and *RGE KIC* tumors, *KPC* and *RGE KPC* tumors for Fbln5 (green) and endothelial cell marker Meca32 (Meca) (red) in panel (G), acinar cell marker amylase (Amy) (green) and FN (red) in panel (H). Nucleuses were counterstained with DAPI (blue). Scale bars are presented as indicated.

Characterization of *KIC* and *KPC* mice

To evaluate the contribution of Fbln5 to PDA development and progression we utilized *KIC* and *KPC* mice, two well established conditional GEMMs of PDA based on the $p48^{Cre}$ (also known as *Ptf1a*) driver, which is expressed in pancreatic bud progenitor cells [19-21]. *KIC* animals express an active form of *Kras* and have biallelic inactivation of the *Cdkn2a* locus ($LSL-Kras^{G12D/+}; Cdkn2a^{Lox/Lox}; p48^{Cre}$) [20]. *KPC* animals express the same activating G12D mutation in *Kras* and also harbor a R172H point mutation in *p53*, the Li-Fraumeni human ortholog ($LSL-Kras^{G12D/+}; LSL-Trp53^{R172H/+}; p48^{Cre}$) [21]. Histological examination of *KIC* and *KPC* pancreatic tissue by a pathologist revealed that each model developed early pancreatic intraepithelial neoplasias (PanINs) and highly infiltrative adenocarcinomas ranging from well-differentiated areas with clear malignant gland formation to areas that were more poorly differentiated (Fig. 2A). Similar to human PDA, Masson's trichrome staining showed extensive collagen deposition in the area of PanINs and PDA in *KIC* and *KPC* tumors (Fig. 2B).

KIC mice appeared normal with no obvious phenotype up to 1.5 months of age but later became moribund, usually accompanied by weight loss (Fig 2D). Moreover, some mice developed jaundice or ascites. Autopsies revealed the presence of large solid tumors with limited gross metastases. Liver micrometastasis was seen in the majority of *KIC* mice in the survival study necropsies (Fig. 2C,E). *KPC* mice appeared healthy up to 3 month old and were sacrificed between 3 to 9 months, commonly presenting with body weight loss, jaundice or ascites. Gross liver metastasis was seen in 30-40% of animals (Fig. 2D,E)

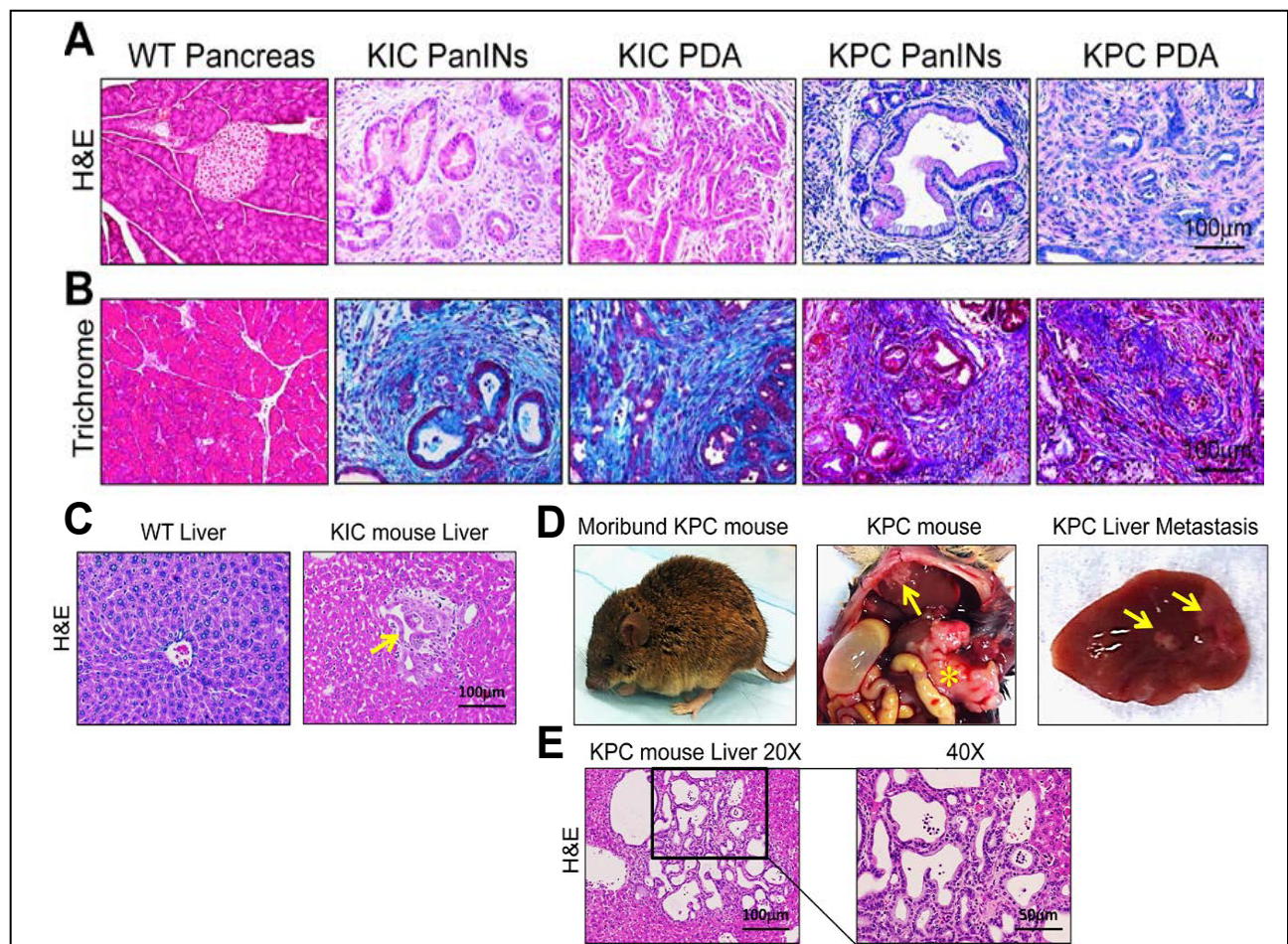


Figure 2 (legend on top of next page)

Figure 2. Characterization of KIC and KPC mice. (A-B) Representative H&E (A) and Masson's trichrome staining (B) of wildtype (WT) pancreas, KIC and KPC tumors. (C) Representative H&E staining of a KIC mouse liver after sacrificed for survival study. The liver micrometastasis originating from the primary pancreatic tumor was indicated by a yellow arrow. (D) Representative images of a KPC mouse before and after sacrificed for survival study. Primary pancreatic tumor region was indicated by yellow asterisk. Liver metastases were indicated by yellow arrows. (E) Representative H&E staining of a KPC mouse liver from the survival study shows liver metastasis. Scale bars are presented as indicated.

Ablation of Fbln5-integrin interaction reduces tumor growth and prolongs survival

Mutation of the Fbln5 integrin binding sequence from RGD to RGE renders the protein incapable of binding to integrins [18]. *Fbln5*^{RGE/RGE} (*RGE*) mice are viable, fertile and phenotypically normal compared to *WT* animals [22]. To study the contribution of Fbln5 to PDA development, we crossed *RGE* mice with *KIC* or *KPC* animals to generate genetically matched *KIC* and *RGE-KIC*, *KPC* and *RGE-KPC* mice. There was no difference in Fbln5 expression levels between *KIC* and *RGE-KIC* or *KPC* and *RGE-KPC* tumors (Fig. 1G). However, tumors had significantly increased Fbln5 expression compared to normal pancreas (Fig. 1C,G). Pancreatic and mouse body weights were determined in *KIC* and *RGE-KIC* mice at 1, 1.5 and 2 months (Fig. 3A-B). There is no significant difference for tumor/body weight at 1 and 1.5 months (Fig. 3A). *RGE-KIC* mice exhibited significantly lower tumor/body weight at 2 months than *KIC* mice, with tumor weights ranging from 0.24 to 0.86 gram for *RGE-KIC* mice and 0.72 to 1.11 gram for *KIC* mice (Fig. 3A). This is consistent with significantly reduced proliferating cells in *RGE-KIC* tumors (Fig. 3C-D). Similar results were observed in the *KPC* model, which were analyzed at 3 and 5 months of age (Fig. 3B and 3E-F).

Survival analysis revealed that *RGE-KIC* mice lived significantly longer than *KIC* mice (Fig. 3G) with a median survival of 74 days for *RGE-KIC* mice and 61.5 days for *KIC* mice. *KIC* and *RGE-KIC* mice appeared normal with no obvious phenotype up to 1.5 months of age but later became moribund, usually accompanied by weight loss. Moreover, some mice developed jaundice or ascites. Autopsies revealed the presence of large solid tumors with limited gross metastases. Liver micrometastasis was seen in the majority of *KIC* and *RGE-KIC* mice in the survival study necropsies (Fig. 2E). Similarly, *RGE-KPC* show significantly prolonged survival compared to *KPC* mice (175 days vs 143.5 days) (Fig. 3H). *KPC* and *RGE-KPC* mice appeared healthy up to 3 month old and were sacrificed between 3 to 9 months, commonly presenting with body weight loss, jaundice or ascites. Gross liver metastasis was seen in 30-40% of animals (Fig. 2C-E).

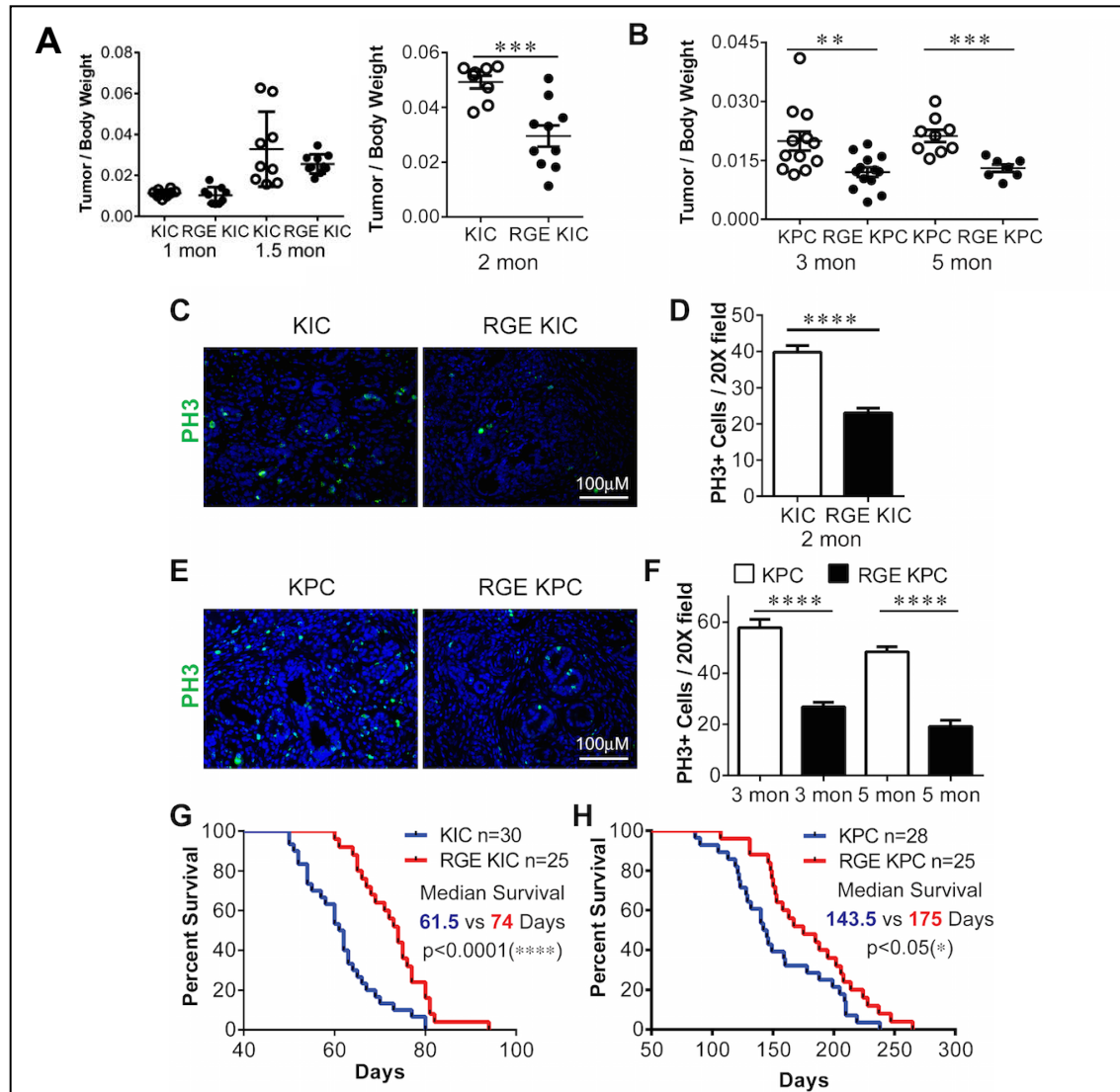


Figure 3. *RGE KIC* and *RGE KPC* mice show reduced tumor growth and prolonged survival compared to *KIC* and *KPC* mice. (A-B) Whole tumors were isolated and weighed and normalized against body weight at 1, 1.5, and 2 months for *KIC* and *RGE KIC* mice (A) or 3 and 5 months for *KPC* and *RGE KPC* mice (B). $n \geq 7$ tumors per group. (C, E) IF staining on tumor sections for phospho-Histone H3 (PH3) (green). $n \geq 4$ tumors per group. (D, F) Quantification of PH3 positive (+) cells per 20X field from 4-5 tumors per group with 8-10 pictures per tumor. Results are shown as mean \pm s.e.m. (G-H) Kaplan-Meier survival curve of *KIC* and *RGE KIC* mice (G), *KPC* and *RGE KPC* mice (H). Scale bars are presented as indicated. For statistical analysis, unpaired t test was used for panel (A), (B), (D) and (F). Log-rank test was used for panel (G) and (H). *, $p < 0.05$, **, $p < 0.01$, ***, $p < 0.001$, ****, $p < 0.0001$.

Increased oxidative stress in *RGE-KIC* and *RGE-KPC* tumors

We reported previously that the growth of subcutaneous Pan02 tumors in *Fbln5*^{-/-} mice was significantly reduced compared to *WT* animals due to increased ROS [23]. Dihydroethidium (DHE) staining of tumors from the GEMMs showed that the *Fbln5 RGE* mutation significantly induced ROS levels in *KIC* and *KPC* tumors (Fig. 4A-B). Accordingly, the level of γ H2AX, a commonly used marker for oxidative stress-induced DNA damage [24], was higher in *RGE-KIC* tumors than *KIC* tumors (Fig. 4C). However, in the context of normal pancreatic tissue, the *Fbln5 RGE* mutation did not alter ROS levels (Fig. 4E-F). This is consistent with the level of FN expression, which was elevated in PDA compared to normal pancreatic tissue (Fig. 1H). To determine whether ROS induction contributed to the prolonged survival in *RGE* animals, *KIC* and *RGE-KIC* mice were treated with the antioxidant N-acetylcysteine (NAC) and survival was examined (Fig. 4D). Prolonged NAC treatment decreased survival of *RGE-KIC* mice but did not affect the survival of *KIC* mice (Fig. 4D). ROS production was also examined in NAC-treated *KIC* and *RGE-KIC* tumors, which revealed no difference between the two groups (Fig. 4G-H). Collectively, ROS induction driven by the *Fbln5 RGE* mutation resulted in reduced tumor growth and prolonged survival.

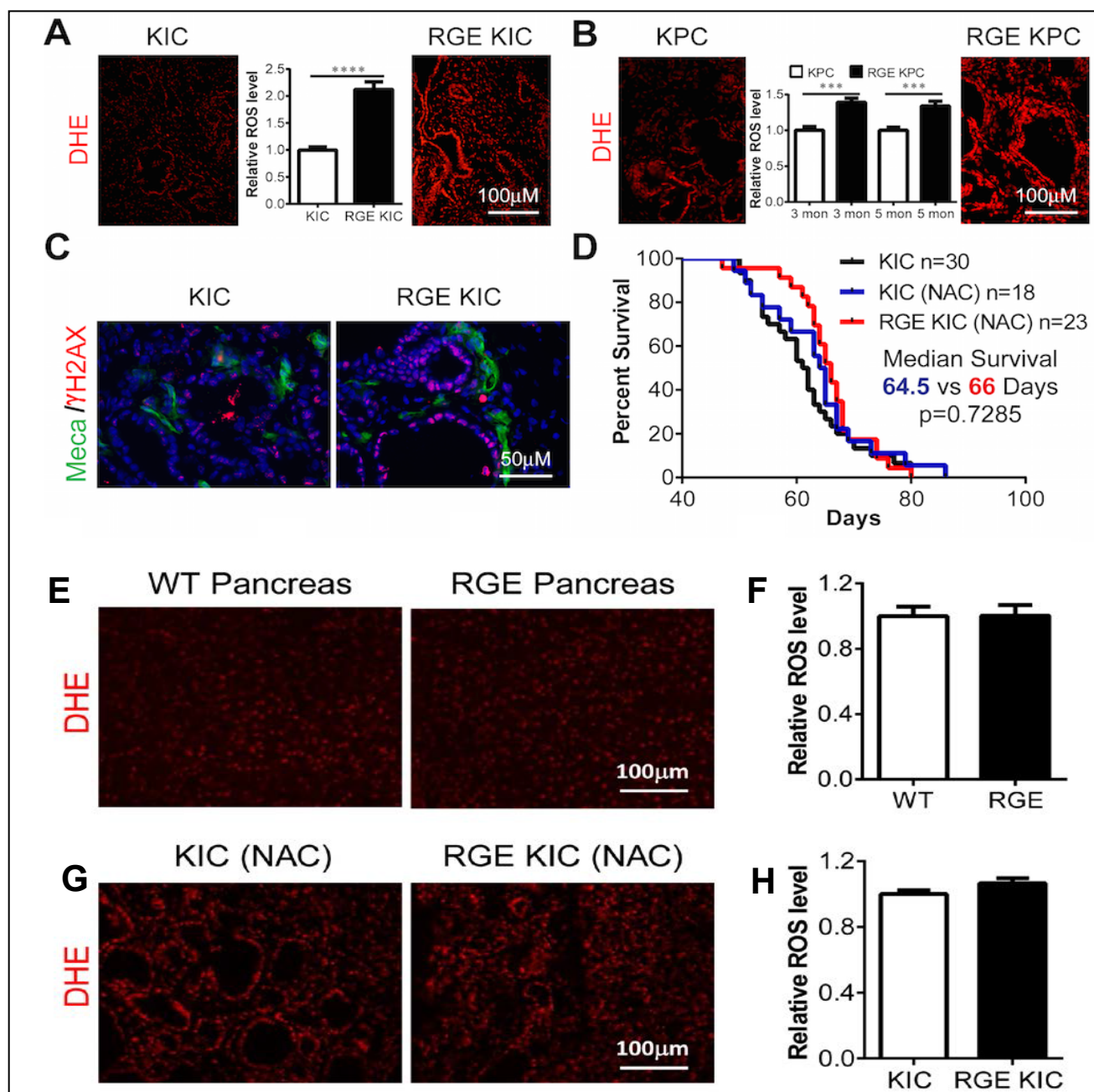


Figure 4 (legend on top of next page)

Figure 4. Increased oxidative stress in *RGE KIC* and *RGE KPC* tumors compared to *KIC* and *KPC* tumors. (A-B) Dihydroethidium (DHE) (red) staining on freshly cut frozen sections of *KIC* and *RGE KIC* (A), *KPC* and *RGE KPC* (B) tumors for *in situ* detection of ROS. Relative ROS level was quantified by fluorescence intensity using the software NIS-Elements and shown inside images. Quantification was from 3 tumors per group with 6-10 images per tumor. (C) IF staining on *KIC* and *RGE KIC* tumor sections for Meca32 (Meca) (green) and g-H2AX (red). n=3 tumors per group. (D) Kaplan-Meier survival curve of *KIC* and *RGE KIC* mice treated with the antioxidant N-acetyl-Cysteine (NAC) by drinking water starting at 4 weeks old. (E-H) *In situ* detection of ROS in normal pancreas from WT and RGE mice (E-F) and post NAC treatment in *KIC* and *RGE KIC* tumors (G-H). *, p<0.05, **, p<0.01, ***, p<0.001, ****, p<0.0001.

Angiogenesis is reduced in *RGE-KIC* and *RGE-KPC* tumors

Prior studies indicate that Fbln5 can modulate angiogenesis [25] and we reported that loss of Fbln5 resulted in decreased angiogenesis in pancreatic tumors [23]. Therefore, we examined microvessel density (MVD) in *KIC* and *RGE-KIC*, *KPC* and *RGE-KPC* tumors by immunostaining with the endothelial cell marker endomucin. MVD was significantly reduced in *RGE-KIC* compared to *KIC* in tumor regions (Fig. 5A-B). Immunostaining and quantification of MVD from 3 and 5 month old *KPC* and *RGE-KPC* tumors also revealed significantly reduced MVD in *RGE-KPC* tumors (Fig. 5C-D). We found that the number of proliferating endothelial cells co-stained with phospho-histone H3 and endomucin was decreased in tumors in *RGE* animals compared to tumors in *WT* mice, supporting the reduction of MVD in *RGE-KIC* and *RGE-KPC* tumors (Fig. 5E-I). Additionally, pancreas tissue from non-tumor bearing *WT* and *RGE* mice were analyzed for MVD (Fig. 5J-M). Again, no significant difference between the two groups was observed. Thus, the reduction of MVD correlated with tumor specific induction of ROS in *RGE* animals. These data suggest that the absence of functional Fbln5 impairs

endothelial cell survival specifically in the TME.

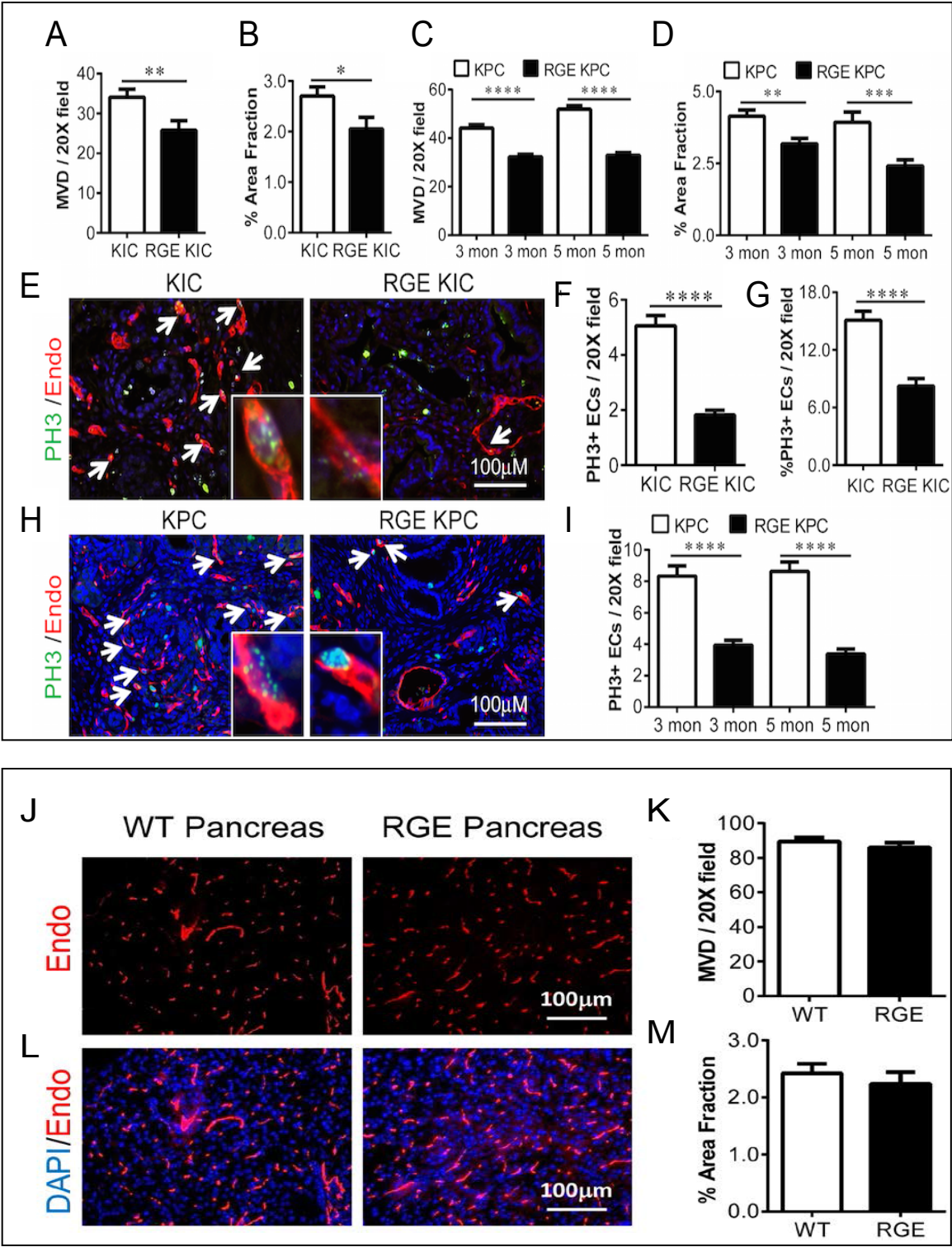


Figure 5 (legend on top of next page)

Figure 5. Reduced microvessel density (MVD) and endothelial cell (EC) proliferation in *RGE KIC* and *RGE KPC* tumors compared to *KIC* and *KPC* tumors. (A-D) MVD was counted per 20X field from 4-5 *KIC* and *RGE KIC* (A), *KPC* and *RGE KPC* (C) tumors with 8-10 pictures per tumor. (B, D) Quantification of MVD for *KIC* and *RGE KIC* (B), *KPC* and *RGE KPC* (D) tumors using the software NIS-Elements. Endomucin (Endo) stained areas are counted as % area fraction. (E-I) IF staining on 2 month old *KIC* and *RGE KIC* (E) and 3 month old *KPC* and *RGE KPC* (H) tumor sections for PH3 (green) and Endo (red). Arrows indicate double labeled ECs, one of which was enlarged and shown in an insert box for each image. (F-G) Quantification of PH3 and Endo co-stained cells (PH3+ ECs) per 20X field in *KIC* and *RGE KIC* (F-G) and *KPC* and *RGE KPC* (I) tumors at indicated ages. (J-M) MVD of WT and RGE non-tumor bearing pancreas. Scale bars are presented as indicated. All the results shown are mean \pm s.e.m. For statistical analysis, unpaired t test was used for panel (A-D), (F-G) and (K-M). *, p<0.05, **, p<0.01, ***, p<0.001, ****, p<0.0001.

Induction of the oxidative stress responsive gene *Nqo1* by FN-induced ROS *in vitro* and *in vivo*

Our data suggested that Fbln5 controls ROS production through FN- β 1 integrin interaction. To elucidate the underlying molecular mechanism of ROS generation, we isolated *WT*, *KO* and *RGE* primary MEFs. Fbln5 expression levels were equivalent between *WT* and *RGE* MEFs (Fig. S6). We found that ROS was elevated in *KO* and *RGE* MEFs but not in *WT* MEFs when cells were plated on FN (Fig. 6A). Next, we performed qPCR arrays to screen for oxidative stress and antioxidant response pathway related genes using RNA harvested from *WT* and *RGE* MEFs. From these arrays, NADP(H):quinone oxidoreductase 1 (*Nqo1*) was a reproducible and reliable target that was increased in *RGE* MEFs after plating on FN. *Nqo1* is an antioxidant enzyme that is responsible for the reduction of quinones to hydroquinones utilizing NAD(P)H as an electron donor [26]. Reducing quinone levels lowers the occurrence of ROS generation as a result of redox cycling [26]. Induction of *Nqo1* can be mediated by

the Keap1/Nrf2/ARE pathway [27]. The induction of Nqo1 in *RGE* MEFs when plated on FN was confirmed by quantitative real-time PCR (Fig. 6B), enzymatic activity (Fig. 6C) and Western blot (Fig. 6D). Concordantly, the induction of Nqo1 expression was reversed by antioxidant treatment (with NAC) in a dose-dependent manner (Fig. 6E), showing that the elevation of Nqo1 is a consequence of increased ROS status in *RGE* MEFs. In addition, Nqo1 induction was elevated in tumors from *RGE* animals (Fig. 6F-G).

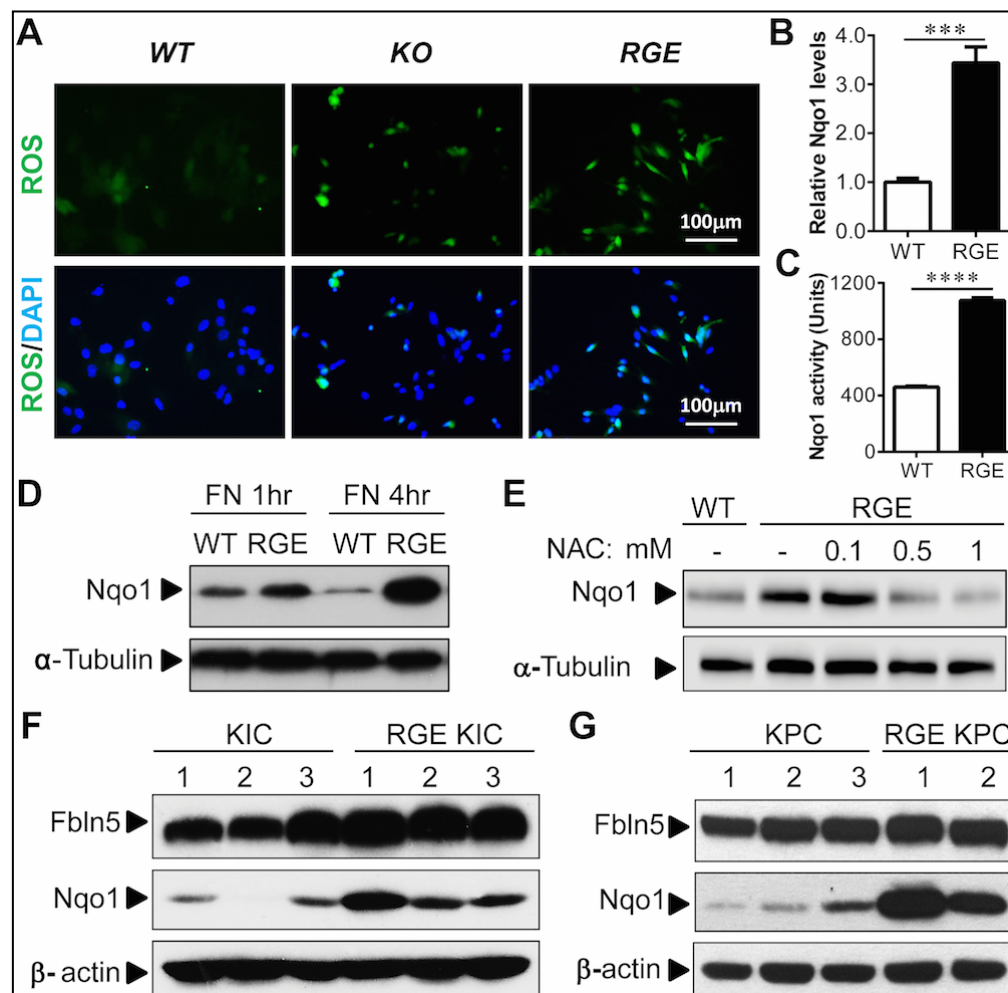


Figure 6 (legend on top of next page)

Figure 6. *Fbln5* RGE mutation induces ROS production and oxidative stress responsive protein Nqo1 *in vitro* and *in vivo*. (A) MEFs harvested from *Fbln5* WT, KO and RGE mice were grown on FN for 16hr and stained with DCF-DA (green) to detect ROS. Nucleus was counterstained in blue with DAPI. (B) Real time PCR result with RNA isolated from WT or RGE MEFs plated on FN for 24hr. (C) Enzymatic activity of Nqo1 was measured and normalized against protein concentration with samples isolated from WT or RGE MEFs plated on FN for 4hr. (D) Western blot using lysates harvested from WT or RGE MEFs plated on FN for 1 or 4hr. (E) Western blot using lysates harvested from WT or RGE MEFs plated on FN for 4hrs and treated with increasing concentration of antioxidant N-acetyl cysteine (NAC). (F, G) Western blot using lysates harvested from several randomly selected KIC and RGE KIC tumors (F) or KPC and RGE KPC tumors (G). α -tubulin or b-actin was used as loading control. Scale bars are presented as indicated. All the results in (B) and (C) are mean \pm s.e.m. For statistical analysis, unpaired t test was used for panel (B) and (C). ***, $p < 0.001$, ****, $p < 0.0001$.

Nqo1 induction is dependent on FN- β 1 integrin interaction and 5-lipoxygenase (5-Lox) activity

It has been reported that integrin activation by FN can induce ROS production [12]. Accordingly, when the endothelial cell line bEnd.3 was treated with a α 5 β 1 integrin-activating antibody, Nqo1 levels were induced (Fig. 7A). The induction of Nqo1 was specific to activation by FN and was not present when cells were plated on plastic or collagen (Fig. 7B). Induction was partially blocked by β 1 integrin blockade (Fig. 7B). Given this data, we conclude that the induction of Nqo1 is responsive to ROS production induced by FN mediated β 1 integrin ligation.

To determine the cellular source of ROS production in the absence of *Fbln5*-integrin interaction, we used inhibitors for various ROS sources including the mitochondrial respiratory chain inhibitor Rotenone, NADPH oxidase (NOX) inhibitor Diphenyleneiodonium chloride (DPI) and 5-lipoxygenase (5-Lox) inhibitor, nordihydroguaiaretic acid (NDGA). Treatment with Rotenone or DPI did not suppress

the induction of Nqo1, suggesting mitochondria and NOX are not the intracellular source of ROS production (Fig. 7C). In addition, there was no induction of NOX enzymatic activity in *RGE* MEFs compared to WT MEFs by FN (Fig. 7F). In contrast, inhibition of 5-Lox by NDGA reduced Nqo1 levels, indicating 5-Lox as the potential source of ROS (Fig. 7D). The quantification results were shown in Fig. 7E. This is consistent with a previous discovery that 5-Lox contributes to a strong burst of ROS production by FN-integrin engagement [28].

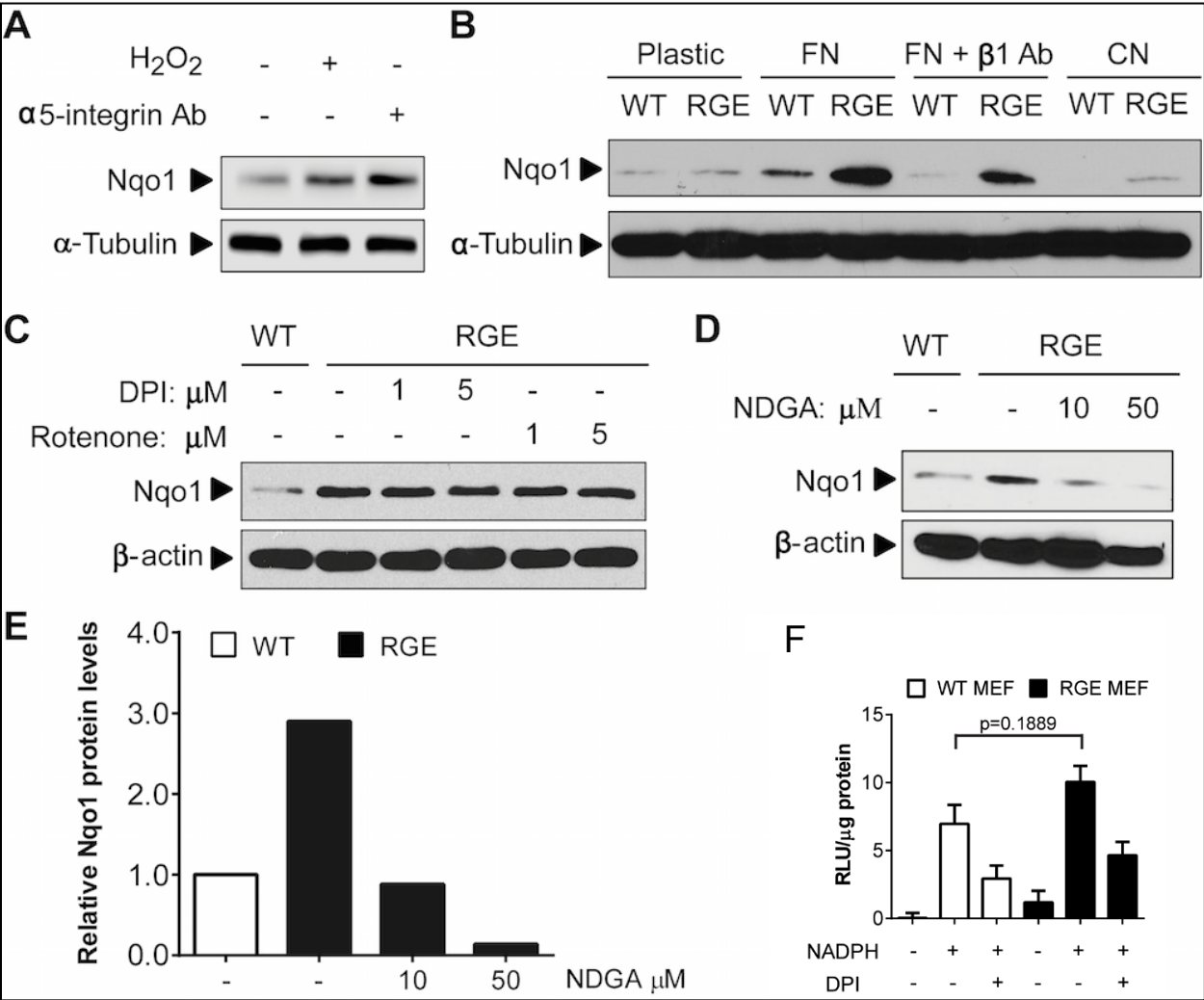


Figure 7 (legend on top of next page)

Figure 7. 5-LOX activation through FN-integrin interaction is responsible for ROS induction in *RGE* MEFs. (A) bEnd.3 cells were plated on FN for 4 hr and treated with 100 mM H₂O₂ or 10 mg/ml α 5 integrin activating antibody at time of plating and probed for Nqo1 by Western blot. (B) *WT* or *RGE* MEFs were plated on plastic, FN, FN + β 1 integrin blocking antibody (10 mg/ml) or Collagen (CN) for 4 hr. Lysates were then harvested and subjected to Western blot. (C) *RGE* MEFs were plated on FN and treated with the NADPH Oxidase (NOX) inhibitor DPI or the mitochondrial electron transport chain inhibitor Rotenone at the time of plating. Lysates were harvested after 4 hrs for Western blot. (D) *RGE* MEFs were plated on FN and treated with a 5-lipoxygenase (5-LOX) inhibitor (NDGA) at the time of plating and harvested 4 hrs later for Western blot. (E) Quantification results of relative Nqo1 protein levels from panel (D) using the software Image Studio Digits. (F) NADPH oxidase enzymatic assay in *WT* vs. *RGE* MEFs. α -tubulin or β -actin was used as loading control for all Western blots.

ROS induction has an additive therapeutic effect when combined with standard chemotherapy agents and development of *Fbln5* targeted agents

To determine if increased integrin-induced ROS improved response to chemotherapy we compared the efficacy of standard chemotherapy agents Gemcitabine (Gem) and Abraxane (Abx) in *KIC* and *RGE-KIC* mice. Due to poor diagnosis for pancreatic cancer, most patients received therapy in later stages. To mimic patient condition, all therapy started at 1.5 month old when both *KIC* and *RGE-KIC* mice have established solid tumors. We found that low-dose Gemcitabine (GemL) and Abx were more effective in the context of mutant *Fbln5* (Fig. 8A-B). Survival studies were also performed with cohorts of *KIC* and *RGE-KIC* mice treated with GemL, high-dose Gemcitabine (GemH) and Abx. *RGE-KIC* mice consistently survived significantly longer in all three treatment groups than similarly treated *KIC* mice (Fig. 8C-E). These data suggest that increasing integrin-induced ROS augments the activity of standard chemotherapy.

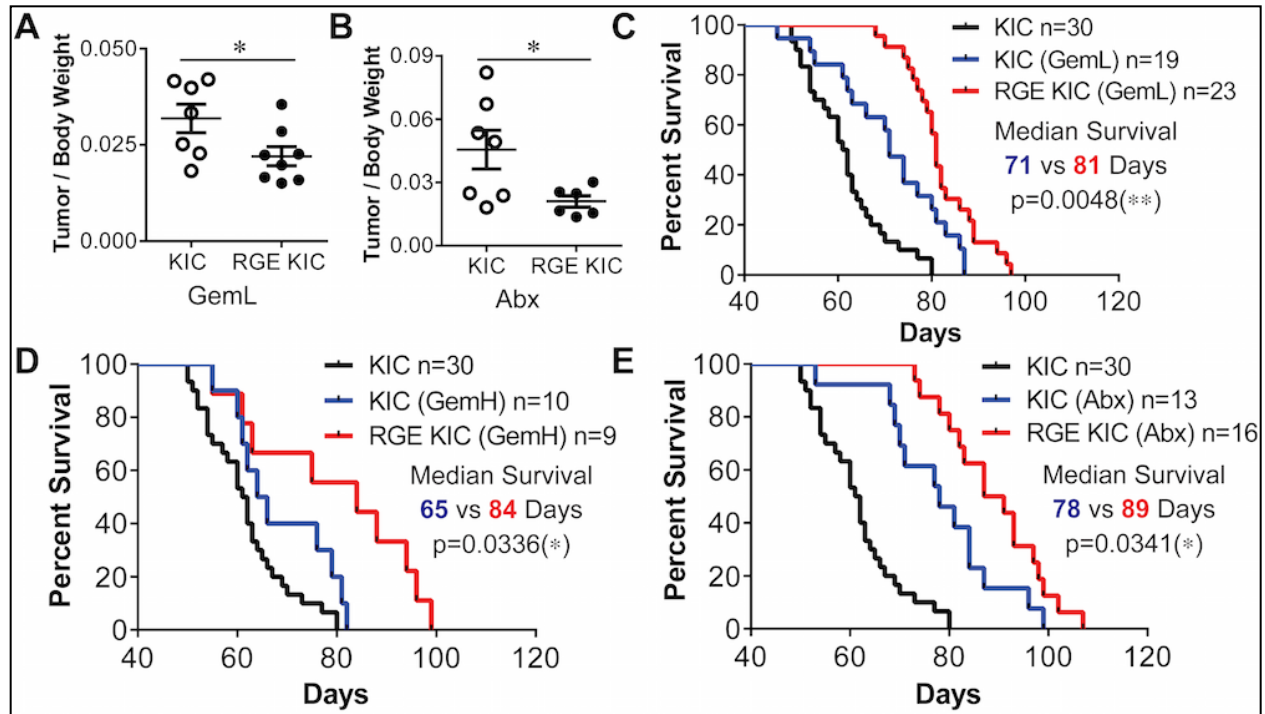


Figure 8. RGE KIC mice have increased survival compared to KIC mice when given chemotherapy. (A, B) KIC and RGE KIC mice were treated with 12.5 mg/kg Gemcitabine (Gem) 3X/wk (GemL) (A) or 5 mg/kg Abraxane (Abx) 2X/wk (B) for 3 wks starting at 7 week old. Mice were then sacrificed and tissues were isolated for analysis. Tumor size is presented as the mean ratio of tumor / body weight \pm s.e.m. $n \geq 6$ tumors per group. (C-E) Kaplan-Meier survival curve of KIC control, KIC and RGE KIC mice treated with GemL (C), GemH (D) or Abx (E). All therapies were given to mice from 7 week old until moribund. For GemL, 12.5 mg/kg Gem was given to mice 3X/wk by intraperitoneal (i.p.) injection. For GemH, 50 mg/kg Gem was given to mice 1X/wk by i.p. injection. For Abx, 5 mg/kg was given to mice 2X/wk by i.p. injection. For statistical analysis, unpaired t test was used for panel (A-B). Log-rank test was used for panel (C-E). *, $p < 0.05$, **, $p < 0.01$.

Discussion

We demonstrated that Fbln5 expression is induced in a significant percentage of pancreatic cancers and that it promotes tumor progression by competing with FN for integrin ligation. Global loss of Fbln5-integrin interaction resulted in decreased tumor growth and prolonged survival of tumor-bearing mice with no apparent adverse effects in normal tissues. The decrease in tumor burden was dependent on increased FN-mediated integrin activation, which increased ROS production through 5-Lox activity and resulted in reduced angiogenesis in the TME. These findings are summarized in Figure 9.

The ECM provides a structural framework in which tumors develop and progress. ECM signaling contributes to cell survival, proliferation and migration, thus regulation of cellular events initiated by the ECM is critical for tumor progression. To date, pharmacologic modification of the ECM in PDA has not resulted in improvement of chemoresponse or overall survival in patients [29-31]. However, preclinical studies focused on inhibiting pathways that stimulate ECM deposition (e.g., TGF β) have shown promise in promoting tumor control [32]. Here, we have highlighted that increased integrin activation can result in decreased tumor growth by elevating integrin-induced ROS production. The extent of cell-ECM interaction is regulated in part by matricellular proteins, including Fbln5. Yet, the contribution of Fbln5 to cancer has been limited largely to expression studies [33-36], which have not defined a clear function for Fbln5 in tumorigenesis. We found that FBLN5 protein was expressed in all of the human PDA samples (n=25) we evaluated. Expression was largely restricted to the stromal

compartment, yet the pattern of expression was not uniform as there were some areas of stroma that were negative or only weakly reactive. This heterogeneity suggests that evaluation of FBLN5 and potentially other matricellular proteins in human tissue microarrays could be challenging. Additional studies on the expression of Fbln5 protein in clinically annotated tumor samples are needed to elucidate if Fbln5 expression has predictive value.

To extend our studies, we sought to understand how Fbln5-integrin interaction functions in the context of the microenvironment of PDA. We employed two distinct but related GEMMs of PDA that recapitulate common mutations observed in the human disease [37-39]. The expression of Fbln5 in each model is similar to the expression level and pattern of Fbln5 expression in human PDA. Furthermore, FN and $\alpha 5\beta 1$ integrin are expressed abundantly in animal models of PDA as well as human PDA [40, 41]. To study Fbln5-integrin interaction we took advantage of the fact that 1) Fbln5 binds but does not activate $\alpha 5\beta 1$ [10, 18], suggesting that it can function to reduce binding of other ligands of the integrin; and 2) knockin mice carrying a point mutation in the integrin binding domain of Fbln5 (*RGE* mice) are viable and fertile [22]. The described essential function of Fbln5 is in elastic fiber assembly as shown by Fbln5-deficient animals [42, 43] and biochemical analysis [44, 45]. However, *RGE* mice have intact elastic fibers [22], indicating that Fbln5-integrin binding is not required for elastic fiber assembly. These data strongly suggest that the phenotype in the *RGE* animals is not due to changes in elastic fiber assembly but a result of an increase in integrin activation by ligands other than Fbln5. Given the dramatic increase in FN expression as well as

other stromal components in PDA we postulated that the TME would provide a biologically meaningful stress to ascertain the functional consequences of increased integrin ligation in *RGE* animals.

ROS production as a result of integrin ligation is a well-established [12, 28], although underappreciated signalling pathway. Previously, we discovered that the loss of Fbln5-integrin interaction results in increased integrin-induced ROS production [23]. Cellular redox homeostasis is tightly regulated by the balance between ROS scavenging and eliminating systems [14]. Cancer cells often generate higher levels of ROS due to metabolic abnormality, activation of oncogenes or loss of functional p53 [14]. For example, increased levels of ROS, particularly H₂O₂ are highly mutagenic and contribute to elevated mutation levels and heterogeneity. Thus an imbalance in ROS scavenging and eliminating systems is likely to result in acute consequences in the TME. For example, increasing ROS levels might result in inhibition of cell proliferation and ultimately cell death [46]. However, cancer cells have developed adaptive mechanisms to manage increased ROS levels [14]. One adaptive mechanism is the induction of the antioxidant response transcription factor Nrf2 to increase the expression of the ROS detoxification enzyme Nqo1 [47, 48]. We found that the loss of Fbln5-integrin interaction induces Nqo1 and that this response is ROS-dependent. Nqo1 levels as a result further validated the elevation of oxidative stress in tumors grown in *RGE* mice and also provided a tractable biochemical endpoint to evaluate the signaling cascade induced by FN in the absence of integrin binding Fbln5. Furthermore, using Nqo1 levels as an endpoint, we discovered that ablation of Fbln5-integrin interaction

increased 5-Lox activity in a FN-dependent manner. Pharmacologic inhibition of 5-Lox rescued the FN-driven phenotype *in vitro* implicating that 5-Lox is downstream of integrin activation. This is consistent with previous reports showing that integrin activation by FN can stimulate ROS production primarily through 5-Lox [12, 28]. FN has also been reported to stimulate intracellular ROS in pancreatic cancer cells through NOX and the mitochondria [49], although we did not find evidence of this in our system.

We found that stromal and tumor cells express the integrin profile required for FN-induced ROS production. However, changes in endothelial cells were the most apparent phenotype in tumors from *RGE* mice. Endothelial cells are sensitive to elevated ROS [50] and this was evident by the consistent reduction in microvessel density and reduction in proliferating endothelial cells in tumors grown in *RGE* animals. Fibroblasts from *RGE* mice produce elevated levels of ROS in culture in a FN and integrin-dependent manner. Yet, surprisingly, we found no significant changes in the presence or activation of fibroblasts in tumors from *RGE* mice (data not shown). Global analysis of ROS using DHE indicates that many cell types, including tumor cells, display elevated ROS levels in tumors from *RGE* mice. However, *in vitro* studies suggest that Fbln5 does not affect ECM-mediated ROS induction in tumor cells (data not shown). It is plausible that long-lived ROS molecules (e.g., H₂O₂) travel from stromal cells and increase oxidative stress in tumor cells resulting in decreased proliferation and reduced tumor growth. It is also feasible that endothelial cells in the TME succumb to elevated ROS induced by mutant Fbln5 and the decreased tumor growth is akin to an anti-angiogenic effect. In contrast, Fbln5 null mice display an exaggerated vascular

response after subcutaneous implantation of polyvinyl alcohol sponges [24]. However, the mechanism of how Fbln5 directly affects endothelial cell function and the contribution of integrins in this phenotype is poorly understood. In our model, non-tumor bearing pancreata of *WT* and *RGE* mice show similar microvessel density (Fig. S5). However, in the context of the TME the basal level of ROS is increased compared to normal pancreas, therefore inducing further ROS by mutation of Fbln5 may explain the negative effect on endothelial cell function. If so, this suggests that the mutation in Fbln5 functions as an endogenous inhibitor of angiogenesis selectively in the TME. These hypotheses are currently being evaluated.

Our studies show that Fbln5 functions as a rheostat to dampen integrin-mediated ROS production. This function of reducing cell-ECM interaction is similar to what has been observed for other matricellular proteins. For example, SPARC reduces the binding of fibrillar collagens to discoidin domain receptors thereby reducing collagen induced cell signaling and attachment [51]. It remains unclear how integrin-mediated signaling activates 5-Lox in the context of mutant Fbln5, although previous studies would suggest that this is dependent on activation of the GTPase Rac [12, 28]. Overall, this chapter illustrates how the matricellular protein Fbln5 functions to reduce FN-integrin interaction and suggests that Fbln5 is a novel therapeutic target for pancreatic cancer. The following chapter will focus on the mechanism of Fbln5 expression in PDA and strategies to block its production in the TME.

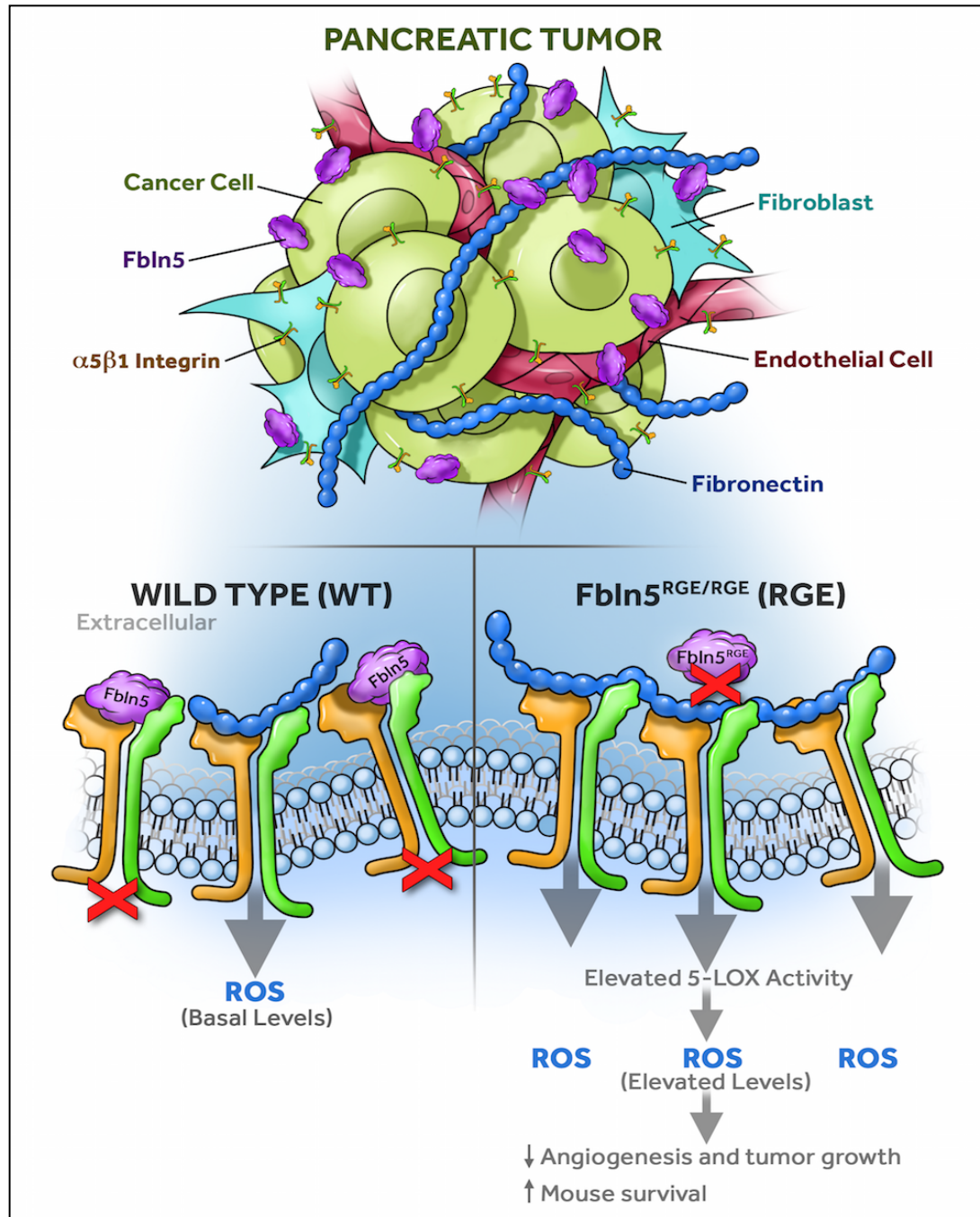


Figure 9. Fbln5 controls ROS production in the TME. Fbln5 is mainly secreted into the TME by tumor-associated fibroblasts (TAFs) and ECs. Fbln5 competes with FN for integrin binding. In the absence of Fbln5-integrin interaction (*RGE*), more FN will bind to integrin receptors and increase ROS production, resulting in increased 5-LOX activity and reduced angiogenesis and tumor growth.

Materials and Methods

Mouse models

Fbln5^{RGE/RGE} (RGE), *Fbln5*^{-/-} (KO), *LSL-Kras*^{G12D/+}; *Cdkn2a*^{Lox/Lox} (KI) and *Cdkn2a*^{Lox/Lox}; *p48*^{Cre} (IC) mice were generated as previously described [22, 51-53]. RGE mice were used to breed with KI and IC mice to generate genetically matched *LSL-Kras*^{G12D/+}; *Cdkn2a*^{Lox/Lox}; *p48*^{Cre} (KIC) mice and RGE-KIC mice. *LSL-Trp53*^{R172H/+} mice were obtained from National Cancer Institute (NCI) Mouse Repository [21]. RGE mice were also used to breed with *LSL-Kras*^{G12D/+}; *LSL-Trp53*^{R172H/+} (KP) and *p48*^{Cre} mice to generate genetically matched *LSL-Kras*^{G12D/+}; *LSL-Trp53*^{R172H/+}; *p48*^{Cre} (KPC) mice and RGE-KPC mice. All mice were housed in a pathogen-free facility and all experiments were performed under written protocols approved by the Institutional Animal Care and Use Committee at the University of Texas Southwestern (UTSW) Medical Center at Dallas.

Animal studies

For endpoint studies, KIC and RGE-KIC mice were sacrificed and entire tissues including pancreas/tumor, liver and spleen were harvested and weighed at 1, 1.5 and 2 months old. KPC and RGE-KPC mice were sacrificed at 3 and 5 months, n≥8 mice per time point per group. For all survival studies, mice were carefully monitored and sacrificed when they appeared moribund. For antioxidant treatment, N-acetyl cysteine (NAC) (Sigma Aldrich) was given to mice at 7 mg/ml in the drinking water from 4 weeks old until moribund. For endpoint therapy experiments, KIC and RGE-KIC mice were

treated for 3 weeks starting at 7 weeks (1.5 months) of age with intraperitoneal (i.p.) injection of low dose Gemcitabine (GemL; 12.5 mg/kg 3x/week) or Abraxane (Abx; 5 mg/kg 2x/week). Mice were sacrificed and tissues were isolated for analysis, $n \geq 6$ mice per group. For survival studies with therapy, cohorts of *KIC* and *RGE-KIC* mice were treated similarly with GemL, high dose Gemcitabine (GemH; 50 mg/kg 1x/week i.p.) or Abx until moribund.

Histology, immunohistochemistry (IHC) and immunofluorescence (IF) staining

Tissues were snap frozen and embedded in OCT (Tissue-Tek) for frozen sections or fixed with 4% paraformaldehyde (PFA) overnight and embedded in paraffin for sectioning. Frozen sections were fixed in ice-cold acetone for 5 minutes (min), air dried for 10 min followed by 10 min incubation with PBS to dissolve the OCT. Paraffin sections were deparaffinized and rehydrated with xylene and serial dilutions of ethanol followed by antigen retrieval with 0.01 M citric acid buffer (pH 6.0). Sections were blocked with 20% aquablock and incubated with primary antibodies in blocking solution (5% BSA in TBST) at 4°C overnight. Primary antibodies used for staining were: rabbit polyclonal anti-mouse Fbln5 (1:100) (purified polyclonal IgG by our lab, 1.6 mg/ml) [43], rat anti-Meca32 (1:100) (purified IgG from hybridoma by our lab) [54], goat anti-Amylase (1:2000) (sc-12821, Santa Cruz Biotechnology), rabbit anti-fibronectin (1:100) (DP3060, Acris), rabbit anti-vinculin (1:50) (Sigma, V4139) and rabbit anti- γ H2AX (1:50) (NB100-2280, NOVUS). Primary antibodies used for paraffin sections were: rabbit anti-human Fbln5 (1:75) (HPA000868, Sigma Aldrich), rabbit anti-Phospho-Histone H3 (PH3) (1:100) (06-570, Millipore), rabbit anti-Amylase (1:2000) (3796S, Cell Signaling) and rat

anti-endomucin (1:100) (sc-65495, Santa Cruz Biotechnology). Fluorescein Isothiocyanate (FITC)-conjugated donkey anti-rabbit, rat IgGs, Cyanine 3 (Cy3)-conjugated donkey anti-rat, mouse, rabbit IgGs and Horseradish Peroxidase (HRP)-conjugated donkey anti-rabbit IgGs from Jackson ImmunoResearch were used as secondary antibodies.

Slides with sections of FFPE de-identified human pancreatic cancer tissue were obtained from the UT Southwestern Tissue Resource and the Department of Pathology, UT MD Anderson Cancer Center. Human PDA sections were stained for Fbln5 expression using rabbit anti-Fbln5 (HPA000868, Sigma Aldrich) as indicated above.

Western blot analysis

Western blots were performed as previously described [55]. In brief, protein lysates from cell culture or tumor tissues were extracted in ice-cold RIPA buffer (50 mM Tris-Cl, 150 mM NaCl, 1% NP-40, 0.5% sodium deoxycholate, 0.1% SDS) containing cocktails of protease (Thermo Scientific) and phosphatase inhibitors (Sigma-Aldrich), by centrifugation (13000g, 15 min) at 4°C following 3 freeze-thaw cycles. Proteins were separated by SDS-PAGE and transferred to methanol activated polyvinylidene difluoride (PVDF) membrane (VWR). The primary antibodies used include the following: rabbit anti-mouse Fbln5 (1:1000), rabbit anti-human Fbln5 (1:500) (HPA000868, Sigma Aldrich), anti-Nqo1 (1:1000) (ab34173, Abcam), anti- α -Tubulin (1:1000) (ab4047, Abcam) and anti- β -actin (1:5000) (A2066, Sigma-Aldrich). HRP-conjugated donkey anti-rabbit IgG (1:10000) (Jackson Immunoresearch) as secondary antibodies were used.

Cell culture

Cell lines used include mouse endothelial cell line bEnd.3 [23], mouse pancreatic cancer cell lines Pan02 [23] and mPLR B9 [51], and human pancreatic cell lines MiaPaCa-2, AsPC-1 and Panc1 (all purchased from ATCC). NG2⁺ cells were isolated using anti-NG2 antibody conjugated magnetic beads from a *KIC* tumor [56]. *Fbln5*^{+/+} (WT), *Fbln5*^{-/-} (KO) and *Fbln5*^{RGE/RGE} (RGE) mouse embryonic fibroblasts (MEFs) were isolated from embryonic day E12.5-E14.5 embryos and genotypes were confirmed by PCR. bEnd.3 cells were treated with 100 μ M H₂O₂ or 10 μ g/ml α 5 β 1 integrin activating antibody and lysates were collected for Western blot analysis. MEFs were cultured in reduced serum medium Opti-MEM (Life Technologies) overnight before being plated on plastic, FN (Sigma Aldrich) or collagen I (Fisher Scientific), each at 10 μ g/ml unless otherwise noted. After plating, MEFs were grown in serum free medium (SFM) supplemented with FN, collagen, β 1 integrin blocking antibody (each at 10 μ g/ml) or various chemicals. Inhibitors used for various ROS sources include Rotenone (R8875-1G, Sigma Aldrich), Diphenyleneiodonium chloride (DPI) (D2926, Sigma-Aldrich) and nordihydroguaiaretic acid (NDGA) (479975, Millipore). All cells were maintained in Dulbecco's modified Eagle's medium (DMEM) (Mediatech, Inc.) with 10% fetal bovine serum (FBS) and were grown in 37°C humidified incubator with 5% CO₂. MEFs were used between passages 2-5 for all experiments.

ROS detection

The detailed protocol on ROS detection and quantification has been described previously [23]. In brief, for tissues, 5 μ M dihydroethidium (DHE) (D11347, Life technologies) was applied to freshly sectioned tissues and incubated at 37°C for 30 minutes. 6-10 images were taken randomly from each tissue and at least 3 tissues were included in each group. Fluorescence intensity was quantified by the software NIS-Elements. To visualize ROS in cells, 10 μ M of 2'-7'-dichlorodihydrofluorescein diacetate (DCF-DA) (D-399, Life Technologies) was added to cells grown on fibronectin (FN)-coated chamber slides. 8-10 pictures were taken randomly from each condition and area fraction was quantified and normalized to cell number by DAPI using the software NIS-Elements. Three independent experiments for each condition were evaluated.

qPCR array and Real-time PCR

WT and *RGE* MEFs were cultured in reduced serum medium Opti-MEM overnight before plating on FN. Upon plating, MEFs were grown in serum free medium (SFM) supplemented with FN for 4, 16 and 24 hrs. RNA lysates were isolated using RNeasy plus mini kit (Qiagen). RT² first strand kit (Qiagen) was used for cDNA synthesis. Then cDNA samples were subjected to RT² Profiler™ PCR array to analyze gene expression changes related to mouse oxidative stress and antioxidant defense pathways (Qiagen, PAMM-065A). Experiments were performed and data were analyzed following manufacturer's instructions. All the candidate genes were further checked and confirmed by Real-time PCR. Ribosome protein S6 (RPS6) was used as the internal control. Following primers were used for real-time PCR: Nqo1 (forward): 5'-

AGACCTGGTGATATTTTCAGTTCCCATTG-3';	Nqo1	(reverse):	5'-
CAAGGTCTTCTTATTCTGGAAAGGACCGT-3';	RPS6	(forward):	5'-
AAGCTCCGCACCTTCTAT-3';	RPS6R	(reverse)	:5'-
TGACTGGACTCAGACTTAGAAGTAGAAGC-3'.			

Nqo1 activity assay

Nqo1 enzyme activity was measured in a reaction mixture containing 200 μ M NADH (Sigma Aldrich) as an electron donor and 10 μ M menadione (Sigma Aldrich) as an Nqo1 substrate and intermediate electron acceptor as described [57, 58]. Cytochrome c serves as the terminal electron acceptor. Therefore, the measured rate of cytochrome c reduction correlates with Nqo1 enzymatic activity. To prepare lysates, cells were scraped in PBS and samples were sonicated. Lysate was added to the reaction mixture and the reduction of cytochrome c (Sigma Aldrich) over two minutes was monitored by absorbance at 550 nm. Dicoumarol, a selective inhibitor of Nqo1, was added as a negative control. Enzyme activity units were calculated as nmol of cytochrome c reduced/min/ μ g lysate.

Statistical analysis

For statistical analysis, unpaired *t*-test was used for comparison between genotypes and various groups. Log-rank (Mantel-Cox) test was used for all the mouse survival studies. Overall, *P* value less than 0.05 was considered as statistically significant. *, $p < 0.05$; **, $p < 0.01$; ***, $p < 0.001$; ****, $p < 0.0001$.

References:

1. Vincent, A., et al., *Pancreatic cancer*. Lancet, 2011. **378**(9791): p. 607-20.
2. Smith, B.D., et al., *Future of cancer incidence in the United States: burdens upon an aging, changing nation*. J Clin Oncol, 2009. **27**(17): p. 2758-65.
3. Topalovski, M. and R.A. Brekken, *Matrix control of pancreatic cancer: New insights into fibronectin signaling*. Cancer Lett, 2015.
4. Westphalen, C.B. and K.P. Olive, *Genetically engineered mouse models of pancreatic cancer*. Cancer J, 2012. **18**(6): p. 502-10.
5. Leach, S.D., *Mouse models of pancreatic cancer: the fur is finally flying!* Cancer Cell, 2004. **5**(1): p. 7-11.
6. Kyriakides, T.R. and P. Bornstein, *Matricellular proteins as modulators of wound healing and the foreign body response*. Thromb Haemost, 2003. **90**(6): p. 986-92.
7. Bornstein, P. and E.H. Sage, *Matricellular proteins: extracellular modulators of cell function*. Curr Opin Cell Biol, 2002. **14**(5): p. 608-16.
8. Wong, G.S. and A.K. Rustgi, *Matricellular proteins: priming the tumour microenvironment for cancer development and metastasis*. Br J Cancer, 2013. **108**(4): p. 755-61.
9. Wang, M., et al., *Fibulin-5 Blocks Microenvironmental ROS in Pancreatic Cancer*. Cancer Res, 2015. **75**(23): p. 5058-69.
10. Lomas, A.C., et al., *Fibulin-5 binds human smooth-muscle cells through alpha5beta1 and alpha4beta1 integrins, but does not support receptor activation*. Biochem J, 2007. **405**(3): p. 417-28.
11. Schluterman, M.K., et al., *Loss of fibulin-5 binding to $\alpha 1$ integrins inhibits tumor growth by increasing the level of ROS*, in *Disease Models & Mechanisms*. 2010. p. 333-342.
12. Chiarugi, P., et al., *Reactive oxygen species as essential mediators of cell adhesion: the oxidative inhibition of a FAK tyrosine phosphatase is required for cell adhesion*. J Cell Biol, 2003. **161**(5): p. 933-44.
13. Holmstrom, K.M. and T. Finkel, *Cellular mechanisms and physiological consequences of redox-dependent signalling*. Nat Rev Mol Cell Biol, 2014. **15**(6): p. 411-21.
14. Trachootham, D., J. Alexandre, and P. Huang, *Targeting cancer cells by ROS-mediated mechanisms: a radical therapeutic approach?* Nat Rev Drug Discov, 2009. **8**(7): p. 579-91.
15. Alexandre, J., et al., *Accumulation of hydrogen peroxide is an early and crucial step for paclitaxel-induced cancer cell death both in vitro and in vivo*. Int J Cancer, 2006. **119**(1): p. 41-8.
16. Ju, H.Q., et al., *Mechanisms of Overcoming Intrinsic Resistance to Gemcitabine in Pancreatic Ductal Adenocarcinoma through the Redox Modulation*. Mol Cancer Ther, 2015. **14**(3): p. 788-98.
17. Wang, J. and J. Yi, *Cancer cell killing via ROS: to increase or decrease, that is the question*. Cancer Biol Ther, 2008. **7**(12): p. 1875-84.

18. Nakamura, T., et al., *DANCE, a novel secreted RGD protein expressed in developing, atherosclerotic, and balloon-injured arteries*. J Biol Chem, 1999. **274**(32): p. 22476-83.
19. Kawaguchi, Y., et al., *The role of the transcriptional regulator Ptf1a in converting intestinal to pancreatic progenitors*. Nat Genet, 2002. **32**(1): p. 128-34.
20. Aguirre, A.J., et al., *Activated Kras and Ink4a/Arf deficiency cooperate to produce metastatic pancreatic ductal adenocarcinoma*. Genes Dev, 2003. **17**(24): p. 3112-26.
21. Hingorani, S.R., et al., *Trp53R172H and KrasG12D cooperate to promote chromosomal instability and widely metastatic pancreatic ductal adenocarcinoma in mice*. Cancer Cell, 2005. **7**(5): p. 469-83.
22. Budatha, M., et al., *Extracellular matrix proteases contribute to progression of pelvic organ prolapse in mice and humans*. J Clin Invest, 2011. **121**(5): p. 2048-59.
23. Schluterman, M.K., et al., *Loss of fibulin-5 binding to beta1 integrins inhibits tumor growth by increasing the level of ROS*. Dis Model Mech, 2010. **3**(5-6): p. 333-42.
24. Mah, L.J., A. El-Osta, and T.C. Karagiannis, *gammaH2AX: a sensitive molecular marker of DNA damage and repair*. Leukemia, 2010. **24**(4): p. 679-86.
25. Sullivan, K.M., et al., *Fibulin-5 functions as an endogenous angiogenesis inhibitor*. Lab Invest, 2007. **87**(8): p. 818-27.
26. Siegel, D., et al., *NAD(P)H:quinone oxidoreductase 1: role as a superoxide scavenger*. Mol Pharmacol, 2004. **65**(5): p. 1238-47.
27. Lee, J.M., et al., *Identification of the NF-E2-related factor-2-dependent genes conferring protection against oxidative stress in primary cortical astrocytes using oligonucleotide microarray analysis*. J Biol Chem, 2003. **278**(14): p. 12029-38.
28. Taddei, M.L., et al., *Integrin-mediated cell adhesion and spreading engage different sources of reactive oxygen species*. Antioxid Redox Signal, 2007. **9**(4): p. 469-81.
29. Lee, J.J., et al., *Stromal response to Hedgehog signaling restrains pancreatic cancer progression*. Proceedings of the National Academy of Sciences, 2014. **111**(30): p. E3091-E3100.
30. Rhim, Andrew D., et al., *Stromal Elements Act to Restrain, Rather Than Support, Pancreatic Ductal Adenocarcinoma*. Cancer Cell, 2014. **25**(6): p. 735-747.
31. Provenzano, Paolo P., et al., *Enzymatic Targeting of the Stroma Ablates Physical Barriers to Treatment of Pancreatic Ductal Adenocarcinoma*. Cancer Cell. **21**(3): p. 418-429.
32. Ostapoff, K.T., et al., *Neutralizing murine TGFβR2 promotes a differentiated tumor cell phenotype and inhibits pancreatic cancer metastasis*. Cancer Research, 2014.
33. Yue, W., et al., *Fibulin-5 suppresses lung cancer invasion by inhibiting matrix metalloproteinase-7 expression*. Cancer Res, 2009. **69**(15): p. 6339-46.
34. Lee, Y.H., et al., *Fibulin-5 initiates epithelial-mesenchymal transition (EMT) and enhances EMT induced by TGF-beta in mammary epithelial cells via a MMP-dependent mechanism*. Carcinogenesis, 2008. **29**(12): p. 2243-51.

35. Hu, Z., et al., *Fibulin-5 is down-regulated in urothelial carcinoma of bladder and inhibits growth and invasion of human bladder cancer cell line 5637*. Urol Oncol, 2011. **29**(4): p. 430-5.
36. Wang, Q., et al., *[Expression of EVEC in ovarian carcinoma and its biological significance]*. Zhonghua Zhong Liu Za Zhi, 2010. **32**(9): p. 676-80.
37. Olive, K.P., et al., *Inhibition of Hedgehog signaling enhances delivery of chemotherapy in a mouse model of pancreatic cancer*. Science, 2009. **324**(5933): p. 1457-61.
38. Singh, M. and N. Ferrara, *Modeling and predicting clinical efficacy for drugs targeting the tumor milieu*. Nat Biotechnol, 2012. **30**(7): p. 648-57.
39. Olive, K.P. and D.A. Tuveson, *The use of targeted mouse models for preclinical testing of novel cancer therapeutics*. Clin Cancer Res, 2006. **12**(18): p. 5277-87.
40. Ansari, D., et al., *The role of quantitative mass spectrometry in the discovery of pancreatic cancer biomarkers for translational science*. J Transl Med, 2014. **12**: p. 87.
41. Jagadeeshan, S., et al., *Transcriptional regulation of fibronectin by p21-activated kinase-1 modulates pancreatic tumorigenesis*. Oncogene, 2014.
42. Nakamura, T., et al., *Fibulin-5/DANCE is essential for elastogenesis in vivo*. Nature, 2002. **415**(6868): p. 171-5.
43. Yanagisawa, H., et al., *Fibulin-5 is an elastin-binding protein essential for elastic fibre development in vivo*. Nature, 2002. **415**(6868): p. 168-71.
44. Zheng, Q., et al., *Molecular analysis of fibulin-5 function during de novo synthesis of elastic fibers*. Mol Cell Biol, 2007. **27**(3): p. 1083-95.
45. Hirai, M., et al., *Fibulin-5/DANCE has an elastogenic organizer activity that is abrogated by proteolytic cleavage in vivo*. J Cell Biol, 2007. **176**(7): p. 1061-71.
46. Kardeh, S., S. Ashkani-Esfahani, and A.M. Alizadeh, *Paradoxical action of reactive oxygen species in creation and therapy of cancer*. Eur J Pharmacol, 2014. **735C**: p. 150-168.
47. Awadallah, N.S., et al., *NQO1 expression in pancreatic cancer and its potential use as a biomarker*. Appl Immunohistochem Mol Morphol, 2008. **16**(1): p. 24-31.
48. DeNicola, G.M., et al., *Oncogene-induced Nrf2 transcription promotes ROS detoxification and tumorigenesis*. Nature, 2011. **475**(7354): p. 106-9.
49. Edderkaoui, M., et al., *Extracellular matrix stimulates reactive oxygen species production and increases pancreatic cancer cell survival through 5-lipoxygenase and NADPH oxidase*. Am J Physiol Gastrointest Liver Physiol, 2005. **289**(6): p. G1137-47.
50. Kietadisorn, R., R.P. Juni, and A.L. Moens, *Tackling endothelial dysfunction by modulating NOS uncoupling: new insights into its pathogenesis and therapeutic possibilities*. Am J Physiol Endocrinol Metab, 2012. **302**(5): p. E481-95.
51. Aguilera, K.Y., et al., *Collagen signaling enhances tumor progression after anti-VEGF therapy in a murine model of pancreatic ductal adenocarcinoma*. Cancer Res, 2014. **74**(4): p. 1032-44.
52. Dineen, S.P., et al., *Smac mimetic increases chemotherapy response and improves survival in mice with pancreatic cancer*. Cancer Res, 2010. **70**(7): p. 2852-61.

53. Ostapoff, K.T., et al., *PG545, an angiogenesis and heparanase inhibitor, reduces primary tumor growth and metastasis in experimental pancreatic cancer*. Mol Cancer Ther, 2013. **12**(7): p. 1190-201.
54. Hallmann, R., et al., *Novel mouse endothelial cell surface marker is suppressed during differentiation of the blood brain barrier*. Dev Dyn, 1995. **202**(4): p. 325-32.
55. Ye, R., et al., *Grp78 heterozygosity promotes adaptive unfolded protein response and attenuates diet-induced obesity and insulin resistance*. Diabetes, 2010. **59**(1): p. 6-16.
56. Rivera, L.B. and R.A. Brekken, *SPARC promotes pericyte recruitment via inhibition of endoglin-dependent TGF-beta1 activity*. J Cell Biol, 2011. **193**(7): p. 1305-19.
57. Pink, J.J., et al., *NAD(P)H:Quinone oxidoreductase activity is the principal determinant of beta-lapachone cytotoxicity*. J Biol Chem, 2000. **275**(8): p. 5416-24.
58. Fitzsimmons, S.A., et al., *Reductase enzyme expression across the National Cancer Institute Tumor cell line panel: correlation with sensitivity to mitomycin C and EO9*. J Natl Cancer Inst, 1996. **88**(5): p. 259-69.

Chapter 3. Hypoxia and TGF- β cooperate to induce fibulin-5 expression in pancreatic cancer

Introduction:

As described in Chapter 2, the loss of Fbln5-integrin binding in GEMMs of PDA results in reduced tumor growth and angiogenesis and increased survival [1]. This phenotype is a consequence of elevated ROS production through increased FN-integrin signaling in Fbln5 mutant animals. Fbln5 suppresses integrin-induced ROS production by competing with FN for integrins and blocking downstream integrin signaling. The enhanced deposition of FN in PDA subjects these tumors to high levels of ROS production via integrins. Similarly, Fbln5 expression is upregulated in PDA compared to normal pancreas and thus protects tumors from cytotoxic levels of integrin-induced ROS production thereby contributing to tumor progression. IHC analysis of human and mouse PDA reveals a heterogeneous pattern of Fbln5 expression within the tumor stroma but virtually no expression in tumor cells. These results suggest that the expression of Fbln5 is controlled tightly. However, the molecular mechanism underlying Fbln5 expression in the microenvironment of PDA is unknown.

During tumor progression, cancer cells release factors that maintain a microenvironment conducive for growth. For example, TGF- β is a cytokine expressed in many cancers that enhances the expression of multiple ECM molecules including but not limited to FN, collagen, elastin, and fibulins [2-4]. Fbln5 is expressed during development, particularly in the vasculature but is significantly downregulated in most adult tissues [5]. Reactivation of Fbln5 occurs in injured vessels and other pathological

conditions, including cancer [5-7]. The function and expression of Fbln5 in cancer is largely context dependent. Others have reported that Fbln5 is downregulated in some cancers, however, these studies focused largely on mRNA expression in tumor lysates and cell lines and on tissue microarray (TMA) analysis [8, 9]. In our previous studies, we found that Fbln5 is produced mainly by stromal fibroblasts and endothelial cells while epithelial derived cells do not produce Fbln5 [1]. Furthermore, accurate evaluation of Fbln5 via TMA analysis is challenging due to variability in stromal content between samples and the heterogeneous staining pattern of Fbln5 within tumors [1]. In addition to PDA, Fbln5 is abundant in the stroma of human breast cancer and its presence is associated with a more invasive phenotype in 4T1 mouse tumors [10].

Previous studies examining the molecular pathways leading to Fbln5 expression have been performed strictly *in vitro*. For example, Fbln5 has been identified as a TGF- β inducible gene in fibroblasts [2], whereas another study revealed hypoxia enhances Fbln5 expression in endothelial and HeLa cells [11]. These studies have independently shown that Fbln5 induction is dependent on the PI3K/Akt pathway. However, it is unclear whether hypoxia induces Fbln5 in a TGF- β dependent manner and if these factors regulate Fbln5 expression in an *in vivo* context. Hypoxia and TGF- β expression and activity are elevated in a number of advanced solid tumors, including PDA [12, 13]. Therefore, through biochemical and IHC analyses, we sought to strengthen our understanding of the factors and elucidate a mechanism by which pancreatic tumors stimulate Fbln5 expression *in vivo*.

Results

Fbln5 expression is restricted to the stroma of PDA

Fbln5 is expressed aberrantly in a number of malignancies [8, 10, 14-16]. Expression analysis of various cell types has identified fibroblasts and endothelial cells as major producers of Fbln5 [1]. Moreover, histological analysis of Fbln5 reveals a stromal staining pattern in tumors ([1], Fig. 1). The *KIC* and *KPC* models of PDA show abundant Fbln5 staining (green) compared to normal pancreas (Fig. 1). We also counterstained this tissue with the fibroblast markers α SMA (Fig. 1A-C, red) and GFAP (Fig. 1D-F, red) [17]. Given that fibroblasts are a major source of Fbln5, it is tempting to speculate that the increased infiltration of these cells in PDA is contributing to the accumulation of Fbln5 in PDA. However, we found that not all stromal areas are positive for Fbln5, and while Fbln5 does colocalize with α SMA and GFAP (arrows), there are areas that show expression of Fbln5 in the absence of α SMA or GFAP (arrowheads). This suggests that expression of Fbln5 in PDA is tightly regulated and warrants investigation into the factors that control its expression.

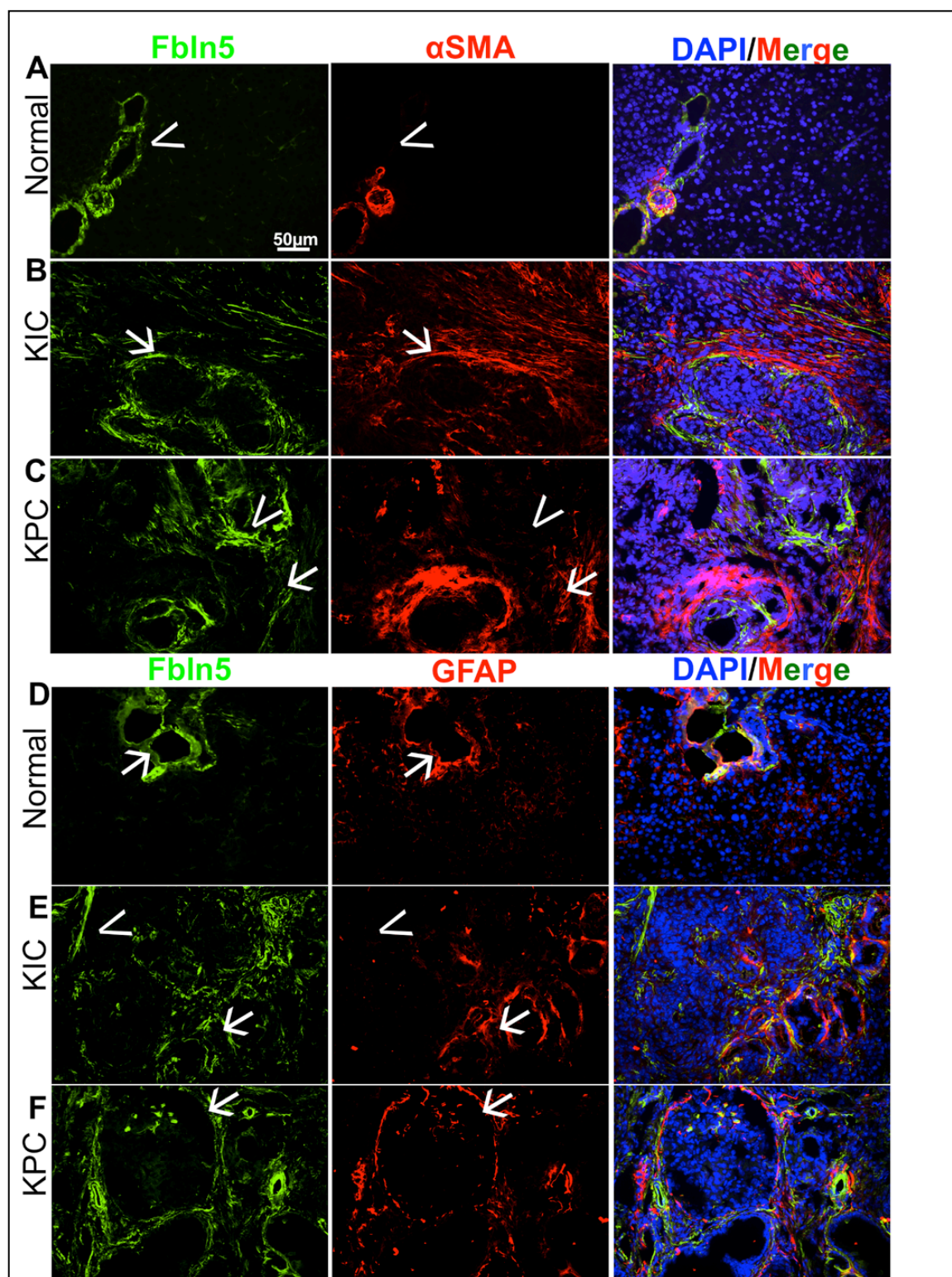


Figure 1 (legend on top of next page)

Figure 1. Fbln5 expression is restricted to the stroma of PDA

Normal (A,D) and tumor-bearing pancreata (B-C,E-F) were harvested from WT, 1.5 mon old KIC (B,D), and 3 mon old KPC (C,F) mice, snap frozen, and sectioned. Frozen tissue was stained for Fbln5 (green, A-F), alpha-smooth muscle actin (α SMA, red, A-C), and GFAP (red, D-F). Nuclei were counterstained with DAPI (merge). Total magnification: 200. Scale bars: 50 μ m for all images.

Hypoxia induces Fbln5 expression and requires TGF- β activity

Fbln5 regulates angiogenesis in a context dependent manner [18-22]. We reported that loss of functional Fbln5 leads to decreased microvessel density specifically in the TME of mouse PDA [19]. Furthermore, it has been shown that hypoxia upregulates Fbln5 in endothelial cells and protects these cells from hypoxia-induced apoptosis [11]. Given the hypoxic nature of PDA [23, 24], it is plausible that Fbln5 is induced by hypoxia to support angiogenesis and tumor growth. Since fibroblasts are a major source of Fbln5 in PDA, we tested whether fibroblasts express Fbln5 in response to hypoxia. 3T3 fibroblasts and MEFs were exposed to hypoxia (0.8% O₂) for 24 hrs. Western blot analysis revealed an induction of Fbln5 protein compared to cells plated under normoxic conditions (Fig. 2A). Hypoxia-inducible factor 1 α (Hif-1 α) and Glut1 were also analyzed by Western blot to confirm hypoxic conditions (Fig. 2A). To corroborate this data, 3T3 fibroblasts were treated with CoCl₂, a hypoxia-mimicking agent reported to stabilize Hif-1 α by inhibiting prolyl hydroxylation [25, 26]. CoCl₂ treatment enhanced Fbln5 expression in a time-dependent manner (Fig. 2B).

Fbln5 has been identified as a TGF- β inducible gene *in vitro* [2]. Our results also support this as 3T3 fibroblasts and MEFs treated with 10 ng/ml of TGF- β induced Fbln5

expression compared to untreated cells (Fig. 2C). Furthermore, blockade of TGF- β receptor 1 (TGF- β R1) by the small molecule inhibitor LY2157299 significantly reduced Fbln5 induction by TGF- β (Fig. 2D). However, it is unclear whether hypoxia-induced Fbln5 requires TGF- β signaling, therefore, we explored the relationship between TGF- β and hypoxia with regard to Fbln5 expression. We found that blocking TGF- β R1 using two distinct inhibitors (LY2157299 and SB-431542) while cells were under hypoxia (in the absence of exogenous TGF- β) resulted in decreased Fbln5 expression (Fig. 2E). This experiment demonstrates that hypoxia-driven Fbln5 expression requires TGF- β R1 activity. Moreover, we examined the effect of hypoxia on TGF- β activity in fibroblasts. We saw increased TGF- β activity as evidenced by phospho-Smad2 levels in MEFs under hypoxic conditions and 3T3 cells treated with CoCl₂ (Fig. 2F-G). These results suggest a linear mechanism by which hypoxia induces TGF- β activity leading to enhanced Fbln5 expression.

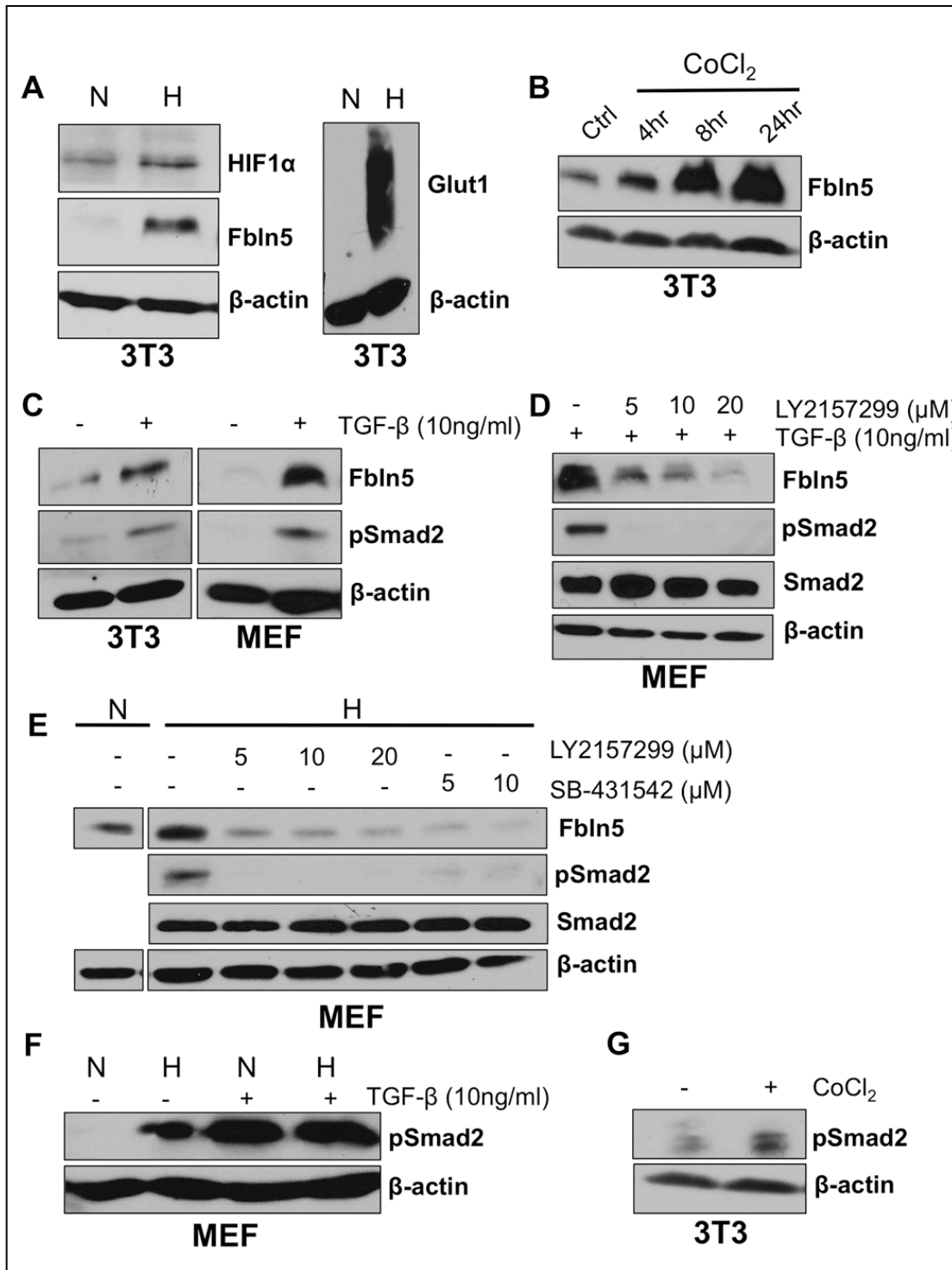


Figure 2 (legend on top of next page)

Figure 2. Hypoxia induces Fbln5 expression and requires TGF- β activity

(A) 3T3 fibroblasts were cultured under normoxic (N) or hypoxic (H) conditions for 24 hrs and probed for Fbln5, Hif-1 α , and Glut1 by Western blot. (B) 3T3 fibroblasts were treated with 100 μ M of CoCl₂ and harvested at 4, 8, and 24 hrs and probed for Fbln5 by Western blot. (C) 3T3 fibroblasts and MEFs were serum starved prior to no treatment (-) or treatment (+) with 10ng/ml of TGF- β . Cells were harvested 24 hrs post-treatment and probed for Fbln5 and phospho-Smad2 (pSmad2 S465/467) by Western blot. (D) MEFs were serum starved and pre-treated with LY2157299 for 1 hr prior to adding TGF- β . Cells were harvested 24 hrs post-treatment and probed for Fbln5, phospho-Smad2, and total Smad2. (E) MEFs were serum starved and treated with either LY2157299 or SB-431542 and were cultured under hypoxic (H) conditions for 24 hrs. Untreated normoxic (N) cells were used as a control. Cells were harvested and probed for Fbln5, phospho-Smad2, and total Smad2. (F) MEFs were cultured under hypoxic conditions or normoxic conditions with (+) or without (-) TGF- β treatment for 24 hrs and probed for phospho-Smad2. (G) 3T3 cells were treated with CoCl₂ for 4 hrs and probed for phospho-Smad2. B-actin was used as a loading control for all Western blots shown in the paper.

Fbln5 expression requires PI3K/Akt activity

TGF- β can induce phosphorylation of a number of downstream targets, including Akt [27]. Furthermore, the induction of Fbln5 by TGF- β and hypoxia individually require the PI3K/Akt pathway [2, 11]. Expanding on these findings, we have shown that the combination of TGF- β and hypoxia treatment requires Akt activity. Inhibition of PI3K using LY294002 blocked TGF- β -induced Fbln5 expression and phosphorylation of Akt under normoxic and hypoxic conditions in 3T3 cells (Fig. 3A). LY294002 also blocked basal Fbln5 expression (Fig. 3B). Moreover, we tested the effect on Fbln5 expression using two other inhibitors that target the PI3K/AKT pathway, BKM120 (PI3K inhibitor) and an Akt1/2 inhibitor (Akt1/2 KI). These alternative inhibitors also reduced Fbln5 expression in fibroblasts under normal conditions (Fig. 3C-D). We confirmed that each inhibitor successfully reduced its target by assessing phospho-Akt levels at both major

activation sites (Fig. 3A-E). The inhibitors did not affect the expression of total AKT. These results indicate that PI3K/Akt activity is required for Fbln5 expression in normoxic and hypoxic conditions with or without exogenously added TGF- β .

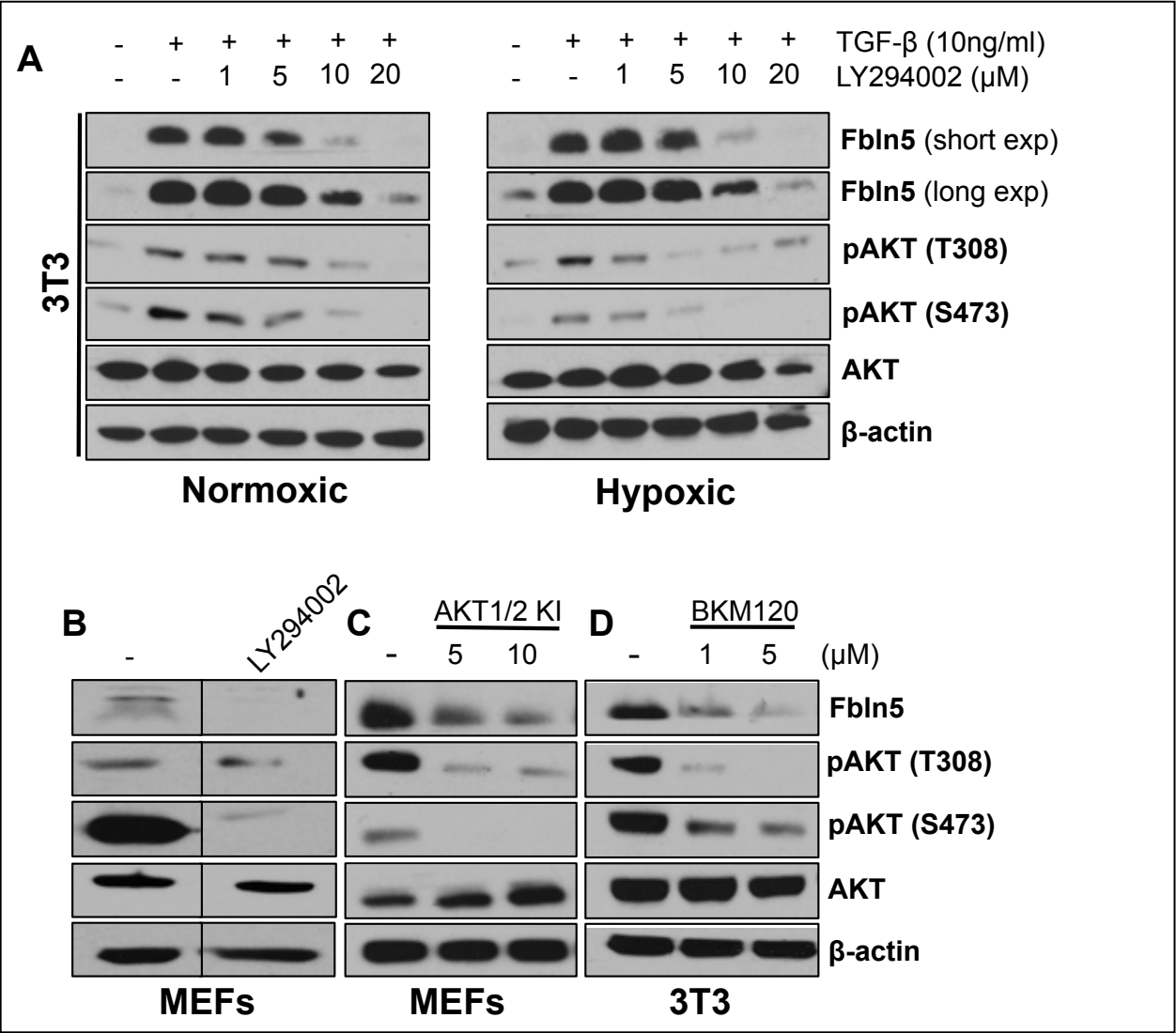


Figure 3 (legend on top of next page)

Figure 3. Fbln5 expression requires PI3K/Akt activity

(A) 3T3 cells were treated were cultured in a normoxic or hypoxic chamber and treated with the PI3K inhibitor LY294002 for 24 hrs in the presence of TGF- β . Cells were harvested for Western blot analysis and probed for Fbln5, phospho-AKT (T308 and S473), and total AKT. Long and short exposures are shown in (A) for Fbln5 to show the upregulation of Fbln5 under hypoxia seen by the longer exposure. (B) LY294002 treatment in MEFs for 24 hrs under normoxic conditions without TGF- β treatment. (C) MEFs under normoxic conditions treated with an AKT1/2 inhibitor for 24 hrs without TGF- β treatment. (D) 3T3 cells under normoxic conditions treated with another PI3K inhibitor (BKM-120) for 24 hrs without TGF- β treatment.

Fbln5 expression in tumor-associated fibroblasts also requires TGF- β and PI3K activity

To validate our findings in a more tumor relevant cell type we isolated tumor-associated fibroblasts (TAFs) from mouse PDA. We used PDGFR- α as a marker to specifically select for fibroblasts [28]. Bright field images of these TAFs revealed spindle-like morphology typical of fibroblasts (Fig. 4A). Furthermore, we characterized these TAFs by immunostaining for α SMA (Fig. 4B). TAFs were treated with TGF- β , which induced Fbln5, an effect that was sensitive to inhibition of TGF- β R1 by LY2157299 or SB-431542 (Fig. 4C). TGF- β -induced activation of Akt was also reduced by TGF- β R1 inhibition (Fig. 4C). Fbln5 expression by TAFs was also sensitive to PI3K inhibition (Fig. 4D).

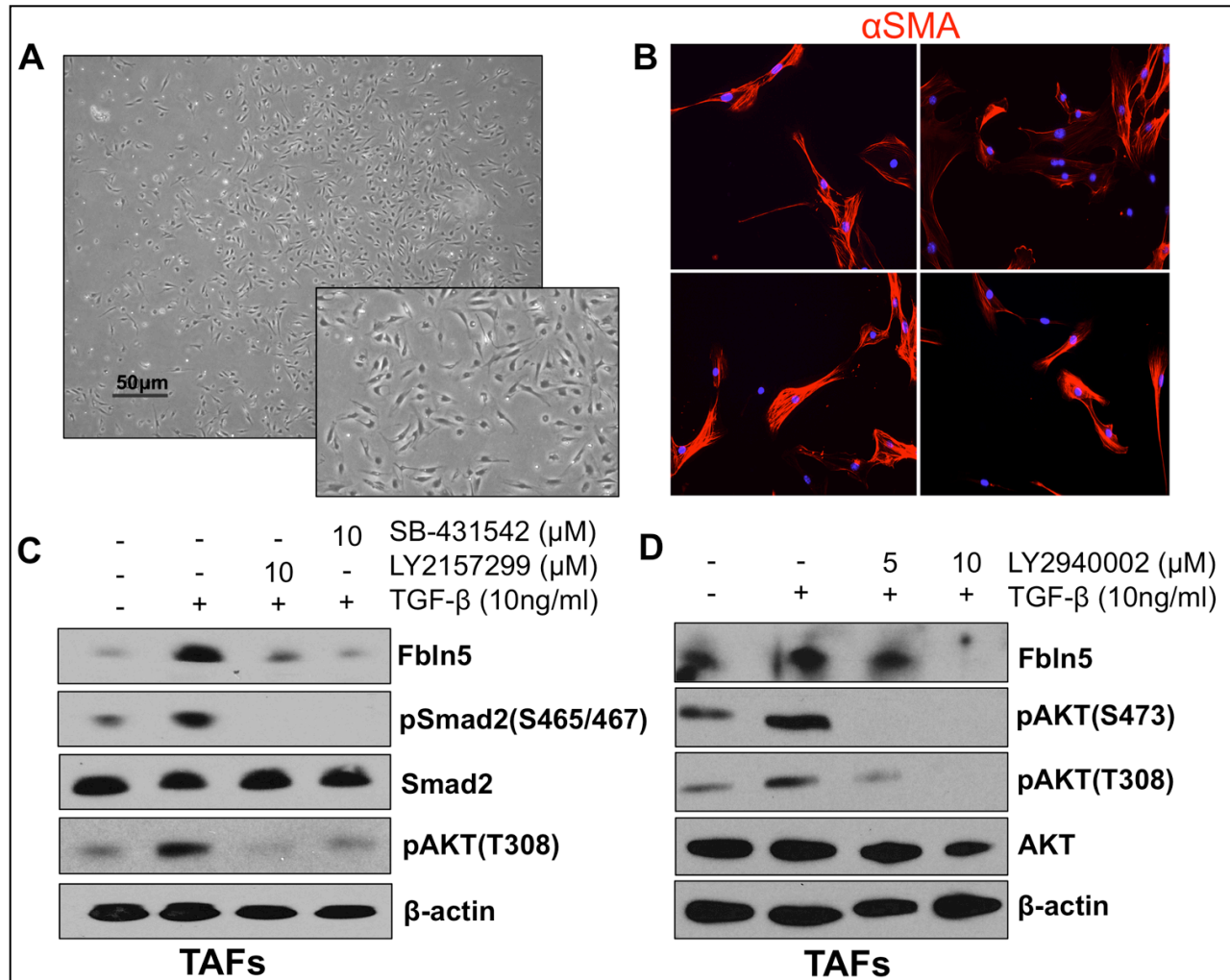


Figure 4. Fbln5 expression in tumor-associated fibroblasts is also driven by hypoxia and requires TGF-β and PI3K activity (A) Representative bright-field image of tumor-associated fibroblasts (TAFs) isolated from mouse PDA. Scale bars 50μm, 4x magnification, inlet is zoomed in 5x. (B) Representative images of TAFs stained for αSMA in red and counterstained with DAPI in blue. 20x magnification. (C) TAFs were serum-starved and pre-treated with either LY2157299 or SB-431542 for 1 hr prior to adding TGF-β. TAFs were harvested after 24 hrs and probed for Fbln5, phospho-Smad2, phospho-AKT (T308), and total Smad2. (D) TAFs were serum-starved and pre-treated with LY2940002 for 1 hr prior to adding TGF-β. TAFs were harvested after 24 hrs and probed for Fbln5, phospho-

Inhibition of TGF- β signaling reduces Fbln5 expression in mouse PDA

To confirm that TGF- β signaling is critical for Fbln5 expression in pancreatic tumors, we examined Fbln5 levels in tumor tissue from *KPC* mice that had been treated with TGF- β inhibitors. *KPC* mice were treated with LY2157299 as well as an inhibitor of TGF- β receptor 2 (2G8) [13]. Immunohistochemical analysis of frozen tumor sections revealed a significant decrease in Fbln5 expression in tumors of treated mice (Fig. 5A-B).

Hypoxia drives Fbln5 expression in mouse PDA

Next we examined the influence of hypoxia on Fbln5 expression *in vivo*. To achieve this, we analyzed tissue from *KIC* mice that had been treated with the VEGF inhibitor, mouse chimeric r84 (mcr84) [29]. The rationale behind this approach is that anti-angiogenic therapy increases intratumoral hypoxia [12, 30]. Using these mice, we have previously confirmed that treatment with mcr84 induces hypoxia in tumors compared to untreated tumors as seen by pimonidazole staining [12]. Consistent with our *in vitro* results hypoxia increased Fbln5 expression such that tumors from mice treated with mcr84 displayed a significant increase in Fbln5 expression compared to untreated tumors (Fig 5C). We also found that expression of Fbln5 is coincident with hypoxic areas in *KIC* tissue as shown by pimonidazole staining (Fig 5D). Together, these results demonstrate that Fbln5 expression is induced by a hypoxic TME.

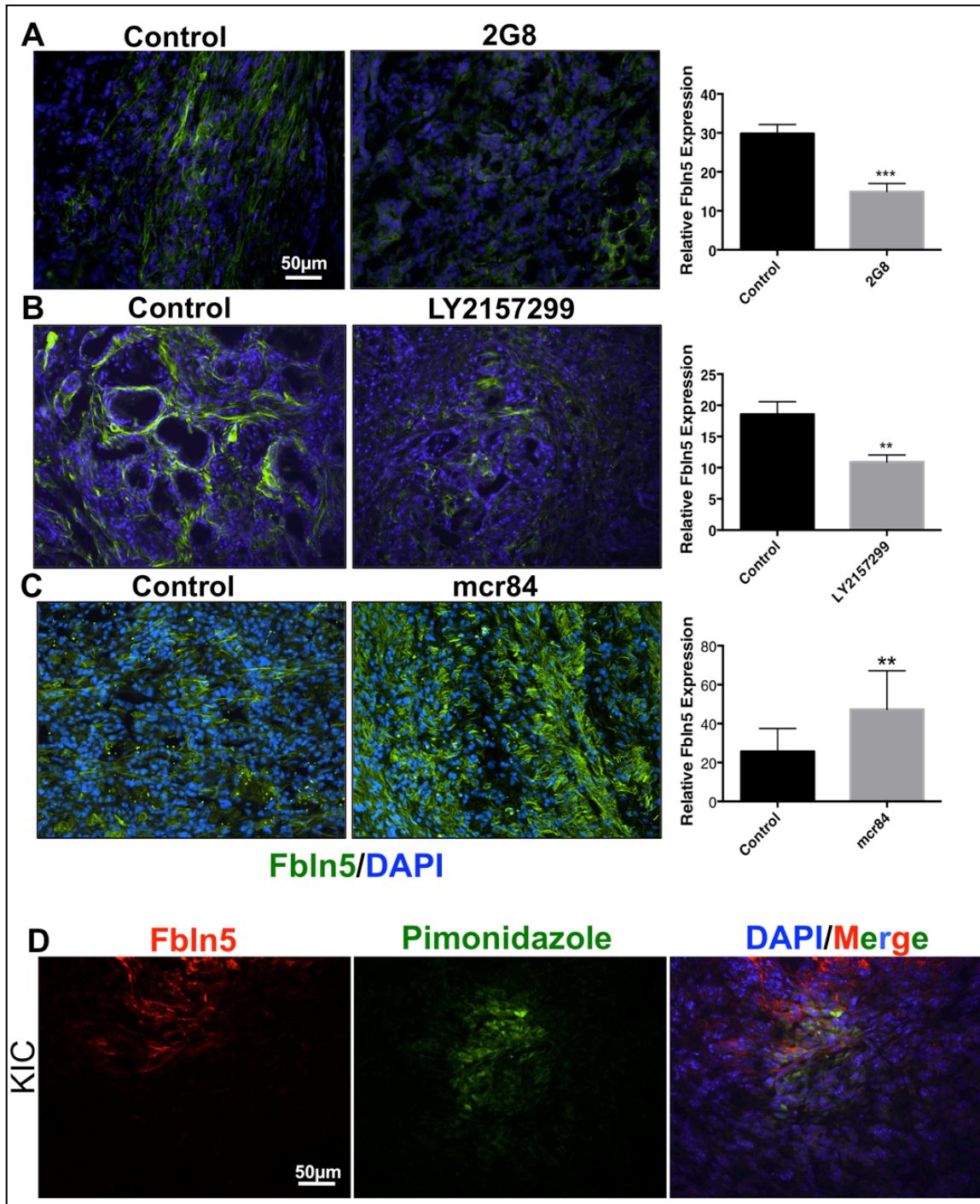


Figure 5 (legend on top of next page)

Figure 5. Inhibition of TGF- β receptors reduces Fbln5 expression while anti-VEGF therapy induces its expression in mouse PDA

(A) Frozen tumor sections from KPC mice treated with 2G8 30mg/kg/wk (n=4) or untreated (n=4). (B) Frozen tumor sections from KPC mice treated with 75mg/kg LY2152799 2x daily (n=4) or untreated (n=4). (C) Frozen tumor sections from KIC mice treated with 500ug/wk mcr84 (n=5) or untreated (n=4). (D) Mice were injected intravenously with 60 mg/kg of pimonidazole that was allowed to circulate for 90 minutes before sacrificing animals. Frozen tissue sections were interrogated with FITC-conjugated anti-pimonidazole primary antibody (green) and Fbln5 (red). (n=3). Images A-C were stained for Fbln5 (green) and counterstained with DAPI (blue). 8-12 pictures were taken from each tumor section (total magnification, 200) for analysis. Results shown are \pm s.e.m. Fluorescent intensity was quantified per 20X field image using the software NIS Elements. *P<0.01, **P<0.001. ***P<0.0001. Scale bars: 50 μ m for all images.

Discussion

In PDA, Fbln5 expression is limited to stromal cells, such that all tumors examined were Fbln5-positive but not all stromal cells expressed Fbln5, suggesting context-dependent regulation of intra-tumoral Fbln5 expression. *In vitro* examination of signaling cascades by use of pharmacological inhibitors demonstrated that Fbln5 induction is dependent on TGF- β -PI3K/Akt signaling, a pathway that can be induced by hypoxia (Fig 6). Our *in vitro* results were recapitulated by investigation of Fbln5 expression in PDA tumors from animals treated with pharmacologic agents that either block Tgf- β activity or induce hypoxia. As shown in Chapter 2, Fbln5 expression in the TME of mouse PDA leads to enhanced tumor burden and decreased survival.

Fbln5 is expressed by stromal cells but typically not by cells of epithelial origin [1, 10]. We have not seen evidence of Fbln5 expression by pancreatic tumor cells, in fact, treatment of PDA cells with TGF- β , hypoxia, or both failed to induce Fbln5 protein *in*

vitro (data not shown). It is unclear why tumor cells, which are responsive to TGF- β , fail to express Fbln5 after stimulation with TGF- β . It is plausible that tumor cells may be subject to epigenetic regulation that inhibits the Fbln5 promoter. Further studies are needed to validate this hypothesis. Interestingly, while Fbln5 is readily expressed by fibroblasts *in vitro* and co-localizes with the fibroblast marker α SMA *in vivo*, there are still areas within the tumor where Fbln5 and α SMA do not overlap. This supports the idea that Fbln5 expression is tightly regulated and signal-dependent, and to this extent, we see abundant Fbln5 expression coincident with select areas of hypoxia in mouse PDA. Furthermore, areas that are positive for Fbln5 but negative for α SMA and GFAP may represent a specific population of fibroblasts within the tumor. Additional characterization is needed to determine whether Fbln5 marks a distinct group of fibroblasts within the TME.

Aberrant deposition of ECM proteins is characteristic of PDA and contributes to overall tumor progression and chemoresistance. Thus, therapies that target the ECM or more specifically, target proteins known to stimulate ECM production are very attractive as potential therapeutic strategies. For example, TGF- β functions as a tumor suppressor under normal conditions and during early tumorigenesis; however, mutations are commonly acquired in this pathway, which switch TGF- β to a factor that promotes tumor progression. Blocking TGF- β in pre-clinical models of PDA has shown a robust effect in reducing metastatic occurrence [13]. Our studies reveal that a possible and underappreciated method by which blocking TGF- β may reduce tumor burden and metastasis is by inhibiting the synthesis of pro-tumorigenic ECM molecules, such as

Fbln5. In fact, *Fbln5*^{-/-} mice exhibited a reduction in metastatic incidence when pancreatic tumors were implanted [19]. Along these lines, our *in vitro* data encourages the analysis of tissues that have been treated with inhibitors of the PI3K/Akt pathway for Fbln5 expression. Altogether, these results indicate a TGF- β specific mechanism by which Fbln5 is upregulated in PDA mouse tumors in response to hypoxia, with the ability to block this induction by the use of pre-existing TGF- β R inhibitors.

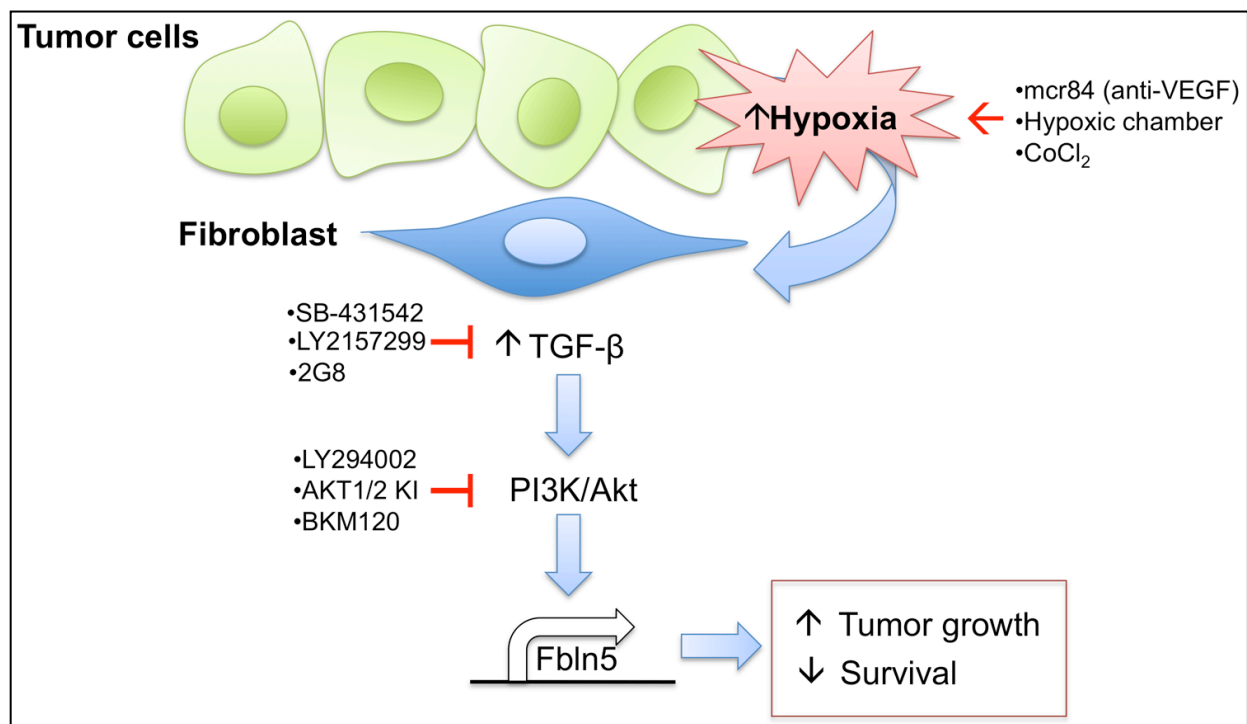


Figure 6. Hypoxia stimulates TGF- β activity and downstream Fbln5 expression in PDA

We propose a model where hypoxia stimulates TGF- β signaling and induces Fbln5 expression via a PI3K/Akt dependent mechanism in fibroblasts. We stimulated hypoxia *in vitro* by incubating cells in a hypoxic chamber or through chemically stabilizing Hif-1 α with CoCl₂, which enhanced Fbln5 expression. Anti-VEGF therapy by mcr84 augmented hypoxia in PDA tumors, which also increased Fbln5 levels. Blocking TGF- β signaling *in vitro* (LY2152799 and SB431542) and *in vivo* (LY2152799 and 2G8) reduced Fbln5 expression. Moreover, hypoxia-induced Fbln5 requires TGF- β activity as inhibition of TGF β -R1 under hypoxic conditions also mitigated Fbln5 expression. Finally, inhibition of the PI3K/Akt pathway (LY294002, AKT1/2 KI, and BKM120) blocked hypoxia- and TGF- β -induced Fbln5 expression.

Materials and Methods

Mouse models:

Kras^{LSL-G12D/+}; *Trp53*^{LSL-R172H/+}; *p48*^{Cre/+} (*KPC*) and *Kras*^{LSL-G12D/+}; *Cdkn2a*^{ff}; *p48*^{Cre/+} (*KIC*) mice were generated as previously described [5, 31-33]. All animals were housed in pathogen-free facility with access to food and water ad libitum. Experiments were performed under protocols approved by the Institutional Animal Care and Use Committee at the University of Texas Southwestern Medical Center at Dallas.

Animal Studies:

Survival studies were performed in *KIC* mice treated with the anti-VEGF mAb mcr84 and *KPC* mice treated with the Tgfβ inhibitors, 2G8 or LY2157299. Mice were monitored and sacrificed when they appeared moribund. Dosing regimens were as follows: *KIC* mice were treated with 500 μg/wk of mcr84 as described [5], and *KPC* mice were treated 2G8 30 mg/kg/wk or 75 mg/kg LY2152799 2x daily. The efficacy of anti-VEGF in the *KIC* model has been reported previously [5]. Studies on the therapeutic efficacy of Tgfβ blockade in *KPC* animals will be reported in more detail elsewhere.

Cell culture (inhibitors/reagents):

Mouse NIH/3T3 cells and mouse brain endothelial cells (bEnd.3) were obtained from ATCC. Mouse embryonic fibroblasts (MEFs) were isolated at embryonic day E12.5-

E14.5. All cells were maintained in DMEM supplemented with 10% FBS (Mediatech, Inc.) and were grown in 37°C humidified incubator with 20% O₂ and 5% CO₂. Confluent cultures were synchronized using reduced serum Opti-MEM (Life Technologies) for MEFs and TAFs or 1% FBS in DMEM for 3T3 cells for at least 6 hrs before experimentation. MEFs were used between passages 2-5 for all experiments. Synchronized cells were treated with 10 ng/ml TGF- β (Peprotech, 100-21C) for 24 hrs. The following inhibitors were used in culture: LY2157299 (Cayman Chemical, 15312), SB431542 (Tocris, 1614), LY2940002 (Cell Signaling, 9901). Inhibitors (at various concentrations, see figure legends) were added 1 hour prior to TGF- β stimulation and/or hypoxic stimulus, and cells were harvested at 24 hrs for Western blot analysis. For hypoxia studies, cells were kept in a humidified atmosphere containing 5% CO₂ and 0.8% O₂ in a modular incubator chamber (Billups-Rothenberger). CoCl₂ (232696, Sigma) was used as a chemical inducer of hypoxia. Synchronized cells were treated with 100 μ M of CoCl₂ and cells were harvested at 4, 8, and 24 hrs.

Immunofluorescence analysis of cells and tissue:

Tissues were either frozen in liquid nitrogen and embedded in OCT (Tissue-Tek) for frozen sections or fixed with 10% neutral buffered formalin solution of 4% paraformaldehyde (PFA) overnight and embedded in paraffin for sectioning. Frozen sections were subject to mild fixation in ice-cold acetone for 5 min and air-dried for 10 min. Frozen sections were then incubated with PBS for 10 min at room temperature. Paraffin sections were deparaffinized and rehydrated with xylene and decreasing serial dilutions of ethanol followed by heat-mediated antigen retrieval with 0.01 M citric acid

buffer (pH 6.0). Tissue sections were outlined with a pap pen and blocked with 20% aquablock for 1 hour. In the case of mouse on mouse staining, unconjugated Fab fragment donkey anti-mouse IgG (Jackson ImmunoResearch Labs) was diluted in PBS and added to tissues for 1 hour. Primary antibodies were diluted in blocking solution (5% BSA in TBST) and incubated at 4°C overnight. Primary antibodies and dilutions used for tissue staining were: anti- α -smooth muscle actin – Cy3 (1:500; C6198, Sigma), mouse anti-GFAP (1:500; MAB360, Millipore), rabbit anti-Fbln5 (1:100; purified polyclonal IgG by our lab, 1.6 mg/ml). FITC or Cy3-conjugated anti-rabbit secondary antibodies were used (1:1000, Jackson ImmunoResearch) for immunofluorescent staining of tissues. For immunocytochemistry, cells were plated onto 4-well chamber slides and allowed to attach and grow for at least 24 hr. Media was removed and cells were washed 3 times in PBS. Cells were fixed in ice-cold acetone for 10 min followed by 3 washes in PBS. Cells were blocked in 20% Aquablock for 1 hr and stained with mouse anti- α -smooth muscle actin – Cy3 (1:500; C6198, Sigma) diluted in 5% BSA in TBST at 4°C overnight.

Western blot:

Western blots were performed as previously described [25]. Cells were lysed in ice-cold RIPA buffer (50 mM Tris-Cl, 150 mM NaCl, 1% NP-40, 0.5% sodium deoxycholate, 0.1% SDS) containing cocktails of protease (Thermo Scientific) and phosphatase inhibitors (Sigma-Aldrich) inhibitors. Lysates were centrifuged for 10 min at 13000g at 4°C. Proteins were separated by SDS-PAGE and transferred to a methanol activated polyvinylidene difluoride (PVDF) membrane (VWR). Primary antibodies were diluted in

5% milk in TBST except phospho-specific antibodies, which were diluted in 5% BSA in TBST. Primary antibodies used for Western blot were: rabbit anti-Fbln5 (1:1000), mouse anti-Hif-1 α (1:500, MAB5382, Millipore), rabbit anti-Glut (1:1000, AM32430PU-M, Acris), mouse anti-Smad2 (1:1000; 3103, Cell Signaling), rabbit anti-phospho-Smad2 (1:1000; 3104S, Cell Signaling), rabbit anti-AKT (1:1000; 9272S, Cell Signaling), rabbit anti-phospho-AKT (Ser473) (1:1000; 4060, Cell Signaling), rabbit anti-phospho-AKT (Thr308) (1:1000; 2965, Cell Signaling), rabbit anti-actin (1:5000; A2066, Sigma). Rabbit anti-actin was used as a loading control for all Western blots shown. HRP-conjugated donkey anti-rabbit or anti-mouse IgGs (1:10000, Jackson ImmunoResearch) secondary antibodies were used for Western blots.

FACs isolation of tumor-associated fibroblasts (TAFs):

Isolation of TAFs from fresh mouse PDA was done as previously described [34]. Briefly, sizeable tumors were dissected from KIC mice and minced manually using a sterile razorblade. Minced tumors were subjected to enzymatic digestion using collagenase for 45 minutes at 37°C with constant agitation. Digestion was stopped by adding 10% FBS in DMEM. Tissue digest was centrifuged and resuspended in fresh 10% FBS DMEM. The tissue/media mixture was strained through a 70 μ m cell strainer placed on top of a 50 ml conical tube. Cells were counted using a hemocytometer to obtain a concentration of 10 million cells in 2 ml of FACs Buffer I (Dulbecco's Phosphate Buffered Saline CMF (Calcium Magnesium Free) + 0.5% BSA). To block endogenous Fc receptor, anti-mouse CD16/CD32 (BD Pharmingen, 553142) was added at 10 μ g/ml to cell suspension for 20 min on ice. After blocking, 10 μ g/ml of anti-mouse CD140 α -PE

(PDGFR- α , e-Bioscience, 12-1401-81) was added directly to cell suspension for 1 hr on ice in order to select for fibroblasts. After 1 hr, cells were spun down and supernatant was aspirated. Cells were resuspended in FACS Buffer II (Dulbecco's Phosphate Buffered Saline CMF + 1% FBS) and subjected to FACS sorting at the UT Southwestern FACS core facility. After isolating PDGFR- α -positive fibroblasts, cells were immediately spun down and media was replaced with 20% FBS in DMEM and plated for further experimentation. TAFs were used between passages 1-3 for all experiments.

References:

1. Wang, M., et al., *Fibulin-5 Blocks Microenvironmental ROS in Pancreatic Cancer*. Cancer Res, 2015.
2. Kuang, P.P., et al., *Fibulin-5 gene expression in human lung fibroblasts is regulated by TGF-beta and phosphatidylinositol 3-kinase activity*, in *AJP: Cell Physiology*. 2006. p. C1412-C1421.
3. Kuang, P.P., et al., *Activation of elastin transcription by transforming growth factor-beta in human lung fibroblasts*. Am J Physiol Lung Cell Mol Physiol, 2007. **292**(4): p. L944-52.
4. Massagué, R.A.I.a.J., *Transforming Growth Factor- β Stimulates the Expression of Fibronectin and Collagen and Their Incorporation into the Extracellular Matrix*. Journal of Biological Chemistry, 1986. **261**(9): p. 4337-4345.
5. Kowal, R.C., et al., *EVEC, a Novel Epidermal Growth Factor Like Repeat-Containing Protein Upregulated in Embryonic and Diseased Adult Vasculature*, in *Circulation Research*. 1999. p. 1166-1176.
6. Tomoyuki Nakamura, P.R.-L., Volkhard Lindner, fDaisuke Yabe, and Y.F. Masafumi Taniwaki, Kazuhiro Kobuke, Kei Tashiro, Zhijian Lu, Nancy L. Andon, Robert Schaub, Akira Matsumori, Shigetake Sasayama, Kenneth R. Chien, and Tasuku Honjo, *DANCE, a Novel Secreted RGD Protein Expressed in Developing, Atherosclerotic, and Balloon-injured Arteries*. The Journal of Biological Chemistry, 1999. **274**(32): p. 22467-22483.
7. Ping-Ping Kuang, R.H.G., Yue Liu, David C. Rishikof, Jyh-Chang Jean, and Martin Joyce-Brady, *Coordinate expression of fibulin-5/DANCE and elastin*

- during lung injury repair. *Am J Physiol Lung Cell Mol Physiol*, 2003. **285**: p. L1147-L1152.
8. Yue, W., et al., *Fibulin-5 Suppresses Lung Cancer Invasion by Inhibiting Matrix Metalloproteinase-7 Expression*, in *Cancer Research*. 2009. p. 6339-6346.
 9. Schiemann, A.R.A.W.P., *Fibulin-5 function during tumorigenesis*. *Future Oncology*, 2005. **1**(1): p. 23-35.
 10. Lee, Y.H., et al., *Fibulin-5 initiates epithelial-mesenchymal transition (EMT) and enhances EMT induced by TGF- β in mammary epithelial cells via a MMP-dependent mechanism*, in *Carcinogenesis*. 2008. p. 2243-2251.
 11. Guadall, A., et al., *Fibulin-5 Is Up-regulated by Hypoxia in Endothelial Cells through a Hypoxia-inducible Factor-1 (HIF-1 α)-dependent Mechanism*, in *Journal of Biological Chemistry*. 2011. p. 7093-7103.
 12. Aguilera, K.Y., et al., *Collagen signaling enhances tumor progression after anti-VEGF therapy in a murine model of pancreatic ductal adenocarcinoma*. *Cancer Res*, 2014. **74**(4): p. 1032-44.
 13. Ostapoff, K.T., et al., *Neutralizing murine TGF β 2 promotes a differentiated tumor cell phenotype and inhibits pancreatic cancer metastasis*. *Cancer Res*, 2014. **74**(18): p. 4996-5007.
 14. Schiemann, W.P., *Context-specific Effects of Fibulin-5 (DANCE/EVEC) on Cell Proliferation, Motility, and Invasion. FIBULIN-5 IS INDUCED BY TRANSFORMING GROWTH FACTOR- β AND AFFECTS PROTEIN KINASE CASCADES*, in *Journal of Biological Chemistry*. 2002. p. 27367-27377.
 15. Shi, X.Y., et al., *Effect of Fibulin-5 on cell proliferation and invasion in human gastric cancer patients*. *Asian Pac J Trop Med*, 2014. **7**(10): p. 787-91.
 16. Hwang, C.F., et al., *Oncogenic fibulin-5 promotes nasopharyngeal carcinoma cell metastasis through the FLJ10540/AKT pathway and correlates with poor prognosis*. *PLoS One*, 2013. **8**(12): p. e84218.
 17. Phillips, P., *Pancreatic stellate cells and fibrosis*, in *Pancreatic Cancer and Tumor Microenvironment*, P.J. Grippo and H.G. Munshi, Editors. 2012: Trivandrum (India).
 18. Chapman, S.L., et al., *Fibulin-2 and Fibulin-5 Cooperatively Function to Form the Internal Elastic Lamina and Protect From Vascular Injury*, in *Arteriosclerosis, Thrombosis, and Vascular Biology*. 2009. p. 68-74.
 19. Schluterman, M.K., et al., *Loss of fibulin-5 binding to α 1 integrins inhibits tumor growth by increasing the level of ROS*, in *Disease Models & Mechanisms*. 2010. p. 333-342.
 20. Sullivan, K.M., et al., *Fibulin-5 functions as an endogenous angiogenesis inhibitor*, in *Lab Invest*. 2007. p. 818-827.

21. Xie, L., et al., *Basement Membrane Derived Fibulin-1 and Fibulin-5 Function as Angiogenesis Inhibitors and Suppress Tumor Growth*, in *Experimental Biology and Medicine*. 2008. p. 155-162.
22. Albig, A.R. and W.P. Schiemann, *Fibulin-5 antagonizes vascular endothelial growth factor (VEGF) signaling and angiogenic sprouting by endothelial cells*. *DNA Cell Biol*, 2004. **23**(6): p. 367-79.
23. Shibaji, T., et al., *Prognostic significance of HIF-1 alpha overexpression in human pancreatic cancer*. *Anticancer Res*, 2003. **23**(6C): p. 4721-7.
24. Buchler, P., et al., *Tumor hypoxia correlates with metastatic tumor growth of pancreatic cancer in an orthotopic murine model*. *J Surg Res*, 2004. **120**(2): p. 295-303.
25. Chan, D.A., et al., *Role of prolyl hydroxylation in oncogenically stabilized hypoxia-inducible factor-1alpha*. *J Biol Chem*, 2002. **277**(42): p. 40112-7.
26. Piret, J.P., et al., *CoCl₂, a chemical inducer of hypoxia-inducible factor-1, and hypoxia reduce apoptotic cell death in hepatoma cell line HepG2*. *Ann N Y Acad Sci*, 2002. **973**: p. 443-7.
27. Horowitz, J.C., et al., *Activation of the pro-survival phosphatidylinositol 3-kinase/AKT pathway by transforming growth factor-beta1 in mesenchymal cells is mediated by p38 MAPK-dependent induction of an autocrine growth factor*. *J Biol Chem*, 2004. **279**(2): p. 1359-67.
28. Sharon Y, A.L., Glanz S, Servais C, Erez N., *Isolation of normal and cancer-associated fibroblasts from fresh tissues by Fluorescence Activated Cell Sorting (FACS)*. *J Vis Exp*, 2013. **71**: p. 4425.
29. Sullivan, L.A., et al., *r84, a novel therapeutic antibody against mouse and human VEGF with potent anti-tumor activity and limited toxicity induction*. *PLoS One*, 2010. **5**(8): p. e12031.
30. Miyazaki, S., et al., *Anti-VEGF antibody therapy induces tumor hypoxia and stanniocalcin 2 expression and potentiates growth of human colon cancer xenografts*. *Int J Cancer*, 2014. **135**(2): p. 295-307.

Chapter 4. Discussion

ECM production in solid tumors, particularly PDA, is associated with a more aggressive phenotype and a worse overall prognosis [1, 2]. My thesis work has challenged this paradigm and provided a more nuanced view showing that the effect of ECM signaling on tumor outcome depends on the presence and activity of matricellular proteins. While integrin signaling by FN promotes cancer cell proliferation and survival [3-5], it also produces ROS, which can be toxic if integrin activation by FN is not controlled [6, 7]. FN signaling is regulated by matricellular proteins such as Fbln5, tenascin-C, and endothelial monocyte activating polypeptide II (EMAP II), which block the activation of integrins by FN [2].

Integrins convey signals to the small GTPase Rac, which activates ROS producing enzymes including 5-lipoxygenase, NADPH oxidase, and the mitochondrial electron transport chain [6-9]. Integrin signaling is also tightly joined to growth factor receptor signaling [10]. Growth factor-induced ROS production is necessary for propagation of downstream signals [11, 12]. Simultaneous stimulation of integrins and growth factor receptors results in synergistic ROS production; however, this appears to be an anchorage-dependent phenomenon [6]. Thus, in adherent cells, integrins are likely the major contributors to ROS production in response to mitogenic stimuli.

Using GEMMs of PDA, our lab has shown that expression of Fbln5 is elevated in the stroma of PDA compared to normal pancreas [13]. Fbln5 binds to integrins via a

conserved RGD motif and inhibits receptor activation through passive ligation of FN-binding integrins [14]. Introducing a point mutation in the integrin-binding RGD sequence of Fbln5 (RGD→RGE) blocks integrin binding while maintaining other functions of Fbln5 [15, 16]. PDA GEMMs harboring this point mutation curbed tumor growth and extended survival. Further investigation revealed that tumors in *Fbln5*^{RGE/RGE} mice had elevated levels of oxidative stress as a result of increased FN-integrin signaling. Increased ROS production had a negative effect on tumor angiogenesis in *Fbln5*^{RGE/RGE} tumors as evidenced by a decrease in microvessel density. Treatment with the antioxidant NAC restored tumor growth and MVD in *Fbln5*^{RGE/RGE} tumors, confirming that the initial decrease in tumor growth and MVD seen was a direct consequence of elevated ROS levels. Moreover, NAC treatment decreased survival in *Fbln5*^{RGE/RGE} bearing mice compared to untreated *Fbln5*^{RGE/RGE} mice [13].

In an effort to identify the source of integrin-induced ROS production in the context of mutant Fbln5, we screened a small panel of inhibitors that target the major producers of ROS in the cell – NADPH oxidase, 5-lipoxygenase, and the electron transport chain. We have demonstrated that inhibition of 5-lipoxygenase specifically blocked ROS signaling in Fbln5 mutants *in vitro*. However, the ability of 5-lipoxygenase to promote intratumoral ROS production in PDA mice mutant for Fbln5 is unknown. It would be interesting to see if treating *Fbln5*^{RGE/RGE} PDA mice with a 5-lipoxygenase inhibitor is akin to using NAC with regard to restoring tumor growth due to a reduction in overall oxidative stress. Future studies should also focus on the upstream factors that lead to enhanced 5-lipoxygenase activity and subsequent ROS production in the context of mutant Fbln5.

One appealing target to examine is Rac, as it has been reported to be downstream of integrin-induced ROS [6, 7] and involved in the activation of 5-lipoxygenase [17]. To determine if this is a Rac-mediated event, one can knockdown, knockout, or chemically inhibit Rac in Fbln5 mutants and evaluate ROS production. Furthermore, it is believed that translocation of 5-lipoxygenase to the nucleus is necessary for its activation [17]. To this end, nuclear accumulation of 5-lipoxygenase should be assessed in Fbln5 mutants by subcellular fractionation or immunostaining of cells or tissue.

Given the strong pro-tumorigenic effect of FN signaling in PDA, it seems counterintuitive that elevated FN signaling would result in smaller tumors. However, in the context of dysfunctional Fbln5 in PDA, tumors were subjected to chronic high levels of ROS resulting in decreased microvessel density and increased tumor cell apoptosis. Our studies highlight that an important function of Fbln5 is to control integrin-induced ROS production by FN, particularly in tissues where FN expression is high. These results demonstrate that the effect of FN on tumorigenesis is context-dependent. Moreover, our data support the idea that increasing ROS levels in tumors is a potentially viable therapeutic strategy. Pro-oxidant therapy is a burgeoning area of research that encompasses the biochemical exploitation of the increased oxidative state of tumors, which makes these tumors hypersensitive to further ROS insults while sparing normal tissue [18]. This approach relies on the “ROS threshold concept”, which proposes that when normal and tumor cells are exposed to equal levels of ROS, tumor cells will more quickly reach a threshold of cell death triggered by overwhelming ROS levels given the enhanced basal ROS production of tumor cells [19]. In this case, normal cells may be

better equipped to manage such increases in ROS because they have a lower basal ROS output and have not exhausted their antioxidant systems. Thus, Fbln5 is an attractive therapeutic target to enhance ROS production in the TME as we have shown that genetic manipulation of Fbln5 results in decreased tumor burden due to augmented ROS levels. Furthermore, the elevated expression of Fbln5 in PDA compared to normal adult pancreas provides a therapeutic window to target tumor-specific Fbln5.

Expression of Fbln5 is seen mainly during early development and wound repair [20]. Interestingly, Fbln5 expression is significantly increased in PDA, and given its pro-tumorigenic effects, we sought to understand the factors that contribute to its expression in the TME. We performed IHC for Fbln5 on human PDA samples using full sections as well as TMAs. We found that the expression pattern of Fbln5 in PDA is heterogeneous. While Fbln5 is restricted to the stromal compartment, we found a number of stromal areas that were either negative or weakly positive for Fbln5 [21]. This finding suggests that the expression of Fbln5 in the TME is tightly controlled and likely signal-dependent. Furthermore, when examining Fbln5 in full sections from PDA patients (n=25) we found 100% of the samples had positive Fbln5 areas. Conversely, out of about 150 samples provided by the TMA, only roughly 50% of these sections were positive for Fbln5. The heterogeneous staining pattern that we observe may help explain the discrepancy in Fbln5 expression between cancer models, where some have reported an upregulation of Fbln5 in patients with breast cancer [22] or a downregulation in lung cancer patients [23]. It is important to note that the analysis of Fbln5 expression in lung cancer has been limited to tissue microarray (TMA) analysis, which in our experience is not an accurate

representation of Fbln5 expression given the heterogeneous staining pattern of Fbln5 and the relatively small tissue sections provided in a TMA. The reported upregulation of Fbln5 in human breast cancer samples was accomplished by IHC of full tissue sections as opposed to a TMA [22].

Previous studies have provided *in vitro* evidence that demonstrates TGF- β and hypoxia are factors that stimulate Fbln5 expression [24, 25]. We harnessed this information and investigated these factors in controlling Fbln5 expression in PDA. Consistent with the *in vitro* data, we found that TGF- β and hypoxia increase Fbln5 expression *in vivo*. Inhibition of TGF- β receptors 1 & 2 resulted in a significant decrease of Fbln5 expression in *KPC* tumors, whereas therapy-induced hypoxia through inhibition of angiogenesis enhanced Fbln5 expression in *KIC* tumors. Furthermore, we discovered that hypoxia-induced Fbln5 requires TGF- β and PI3K activity *in vitro*, thus proposing a mechanism by which hypoxia stimulates TGF- β signaling which activates PI3K/Akt leading to transcription of Fbln5. Currently, it is unclear which transcription factors drive Fbln5 expression in PDA. The Fbln5 promoter has not been characterized extensively; however, studies have revealed the presence of two Smad response elements and a hypoxia regulatory element near the promoter [24, 25]. Chromatin-immunoprecipitation (ChIP) of PDA tumors could help determine if Smad and/or HIF is binding to the Fbln5 promoter in this context.

The upregulation of Fbln5 in PDA may be an adaptive response of the tumor to survive conditions of hypoxia and oxidative stress. We showed that Fbln5 protects tumors from

high levels of integrin-induced ROS; however, it is unclear whether induction of Fbln5 protects tumors from hypoxia. One study has shown that knockdown of Fbln5 in endothelial cells potentiates hypoxia-induced apoptosis *in vitro*, but the underlying mechanism of this pro-survival response by Fbln5 remains elusive. It is plausible that Fbln5 may activate certain integrins while inhibiting other types or that Fbln5 binds to other membrane receptors involved in cell survival. To this end, hypoxia may be eliciting differential expression of integrins or other ECM receptors that may come into contact with Fbln5. Further experiments in various cell types are required to understand the mechanism of this pro-survival effect by Fbln5 under hypoxic conditions. Additionally, comparing the efficacy of anti-angiogenic therapy in *WT* vs. *Fbln5*^{-/-} mice in the background of the PDA model (genetic or implant) would help us understand if Fbln5 is protecting endothelial cells from tumor hypoxia. For example, if Fbln5 does promote endothelial cell survival in response to hypoxia in this context, then we would anticipate increased sensitivity to anti-angiogenic therapy in tumors derived from *Fbln5*^{-/-} mice. However, because there is a reduction in tumor angiogenesis in Fbln5 mutant animals due to elevated ROS production [21, 26], it may be challenging to distinguish if enhanced sensitivity to anti-angiogenic therapy is due to elevated intratumoral ROS or a loss of the pro-survival effect that Fbln5 may provide in response to hypoxia. Thus, understanding the mechanism behind the pro-survival effect of Fbln5 on hypoxic endothelial cells becomes critical. Moreover, one should explore the relationship between ROS production and hypoxia in PDA. Current evidence suggests that when oxygen levels are low, mitochondria begin to produce ROS to assist in the activation of hypoxia response pathways [27]. Therefore, one hypothesis may be that in a hypoxic

TME, such as in PDA, the induction of Fbln5 by hypoxia protects the tumor from excessive ROS production, which is partly contributed to by hypoxia. To this extent, the ability of ROS to induce Fbln5 expression should also be thoroughly examined. Ultimately, combination therapies targeting Fbln5 and blood vessels may help overcome resistance to anti-angiogenic therapy in PDA [28].

Together, this work sheds light on the function of Fbln5 in cancer and how its expression is regulated in the context of the TME. Solid tumors such as PDA are enriched with stromal components that contribute to overall tumor progression and response to chemotherapy. The poor prognosis associated with PDA has remained unchanged over several decades; therefore, identifying novel strategies to combat this deadly disease is of poignant interest. Our studies were focused on the matricellular protein Fbln5 and its effect on FN signaling. The overall goal of my project was to further understand the complex interactions between the tumor and its surrounding matrix and uncover a potential therapeutic strategy for treating PDA. Herein, we provide genetic evidence that Fbln5 is a pro-tumorigenic factor that protects tumors from toxic ROS production and is specifically upregulated in PDA, thus revealing its potential as a drug target. In addition, we have discovered novel and indirect methods to block production of Fbln5 by inhibition of TGF- β and/or PI3K/Akt signaling. This work has laid a strong foundation that warrants further investigation and efforts into the development of a Fbln5 inhibitor to be tested in pre-clinical models of PDA.

References:

1. Neesse, A., et al., *Stromal biology and therapy in pancreatic cancer*, in *Gut*. 2011. p. 861-868.
2. Topalovski, M. and R.A. Brekken, *Matrix control of pancreatic cancer: New insights into fibronectin signaling*. *Cancer Lett*, 2015.
3. Kaspar, M., L. Zardi, and D. Neri, *Fibronectin as target for tumor therapy*, in *Int. J. Cancer*. 2005. p. 1331-1339.
4. Pankov, R., *Fibronectin at a glance*, in *Journal of Cell Science*. 2002. p. 3861-3863.
5. Stenman, S. and A. Vaheri, *Fibronectin in human solid tumors*. *Int J Cancer*, 1981. **27**(4): p. 427-35.
6. Chiarugi, P., et al., *Reactive oxygen species as essential mediators of cell adhesion: the oxidative inhibition of a FAK tyrosine phosphatase is required for cell adhesion*. *J Cell Biol*, 2003. **161**(5): p. 933-44.
7. Werner, E., *Integrins engage mitochondrial function for signal transduction by a mechanism dependent on Rho GTPases*, in *The Journal of Cell Biology*. 2002. p. 357-368.
8. Svineng, G., et al., *The Role of Reactive Oxygen Species in Integrin and Matrix Metalloproteinase Expression and Function*, in *Connect Tissue Res*. 2008. p. 197-202.
9. Aguilera, K.Y., et al., *Collagen signaling enhances tumor progression after anti-VEGF therapy in a murine model of pancreatic ductal adenocarcinoma*. *Cancer Res*, 2014. **74**(4): p. 1032-44.
10. Eliceiri, B.P., *Integrin and growth factor receptor crosstalk*. *Circ Res*, 2001. **89**(12): p. 1104-10.
11. Finkel, T., *Reactive oxygen species and signal transduction*. *IUBMB Life*, 2001. **52**(1-2): p. 3-6.
12. Gulati, P., et al., *Redox regulation in mammalian signal transduction*. *IUBMB Life*, 2001. **52**(1-2): p. 25-8.
13. Wang, M., Topalovski¹, M.*, Toombs, J.E., Wright, C.M., Moore, Z.R., Boothman, D.A., Yanagisawa, H., Wang, H., Witkiewicz, A., Castrillon, D.H., Brekken, R.A., *Fibulin-5 blocks microenvironmental ROS in pancreatic cancer*. *Cancer Research*, 2015. **In Press**.
14. Lomas, A.C., et al., *Fibulin-5 binds human smooth-muscle cells through alpha5beta1 and alpha4beta1 integrins, but does not support receptor activation*. *Biochem J*, 2007. **405**(3): p. 417-28.
15. Nakamura, T., et al., *DANCE, a novel secreted RGD protein expressed in developing, atherosclerotic, and balloon-injured arteries*. *J Biol Chem*, 1999. **274**(32): p. 22476-83.

16. Budatha, M., et al., *Extracellular matrix proteases contribute to progression of pelvic organ prolapse in mice and humans*. J Clin Invest, 2011. **121**(5): p. 2048-59.
17. Eom, Y.W., et al., *Rac and p38 kinase mediate 5-lipoxygenase translocation and cell death*. Biochem Biophys Res Commun, 2001. **284**(1): p. 126-32.
18. Wang, J. and J. Yi, *Cancer cell killing via ROS: to increase or decrease, that is the question*. Cancer Biol Ther, 2008. **7**(12): p. 1875-84.
19. Kong, Q., J.A. Beel, and K.O. Lillehei, *A threshold concept for cancer therapy*. Med Hypotheses, 2000. **55**(1): p. 29-35.
20. Yanagisawa, H., M.K. Schluterman, and R.A. Brekken, *Fibulin-5, an integrin-binding matricellular protein: its function in development and disease*, in *J. Cell Commun. Signal*. 2009. p. 337-347.
21. Wang, M., et al., *Fibulin-5 Blocks Microenvironmental ROS in Pancreatic Cancer*. Cancer Res, 2015. **75**(23): p. 5058-69.
22. Lee, Y.H., et al., *Fibulin-5 initiates epithelial-mesenchymal transition (EMT) and enhances EMT induced by TGF- β in mammary epithelial cells via a MMP-dependent mechanism*, in *Carcinogenesis*. 2008. p. 2243-2251.
23. Yue, W., et al., *Fibulin-5 Suppresses Lung Cancer Invasion by Inhibiting Matrix Metalloproteinase-7 Expression*, in *Cancer Research*. 2009. p. 6339-6346.
24. Kuang, P.P., et al., *Fibulin-5 gene expression in human lung fibroblasts is regulated by TGF- β and phosphatidylinositol 3-kinase activity*, in *AJP: Cell Physiology*. 2006. p. C1412-C1421.
25. Guadall, A., et al., *Fibulin-5 Is Up-regulated by Hypoxia in Endothelial Cells through a Hypoxia-inducible Factor-1 (HIF-1 α)-dependent Mechanism*, in *Journal of Biological Chemistry*. 2011. p. 7093-7103.
26. Schluterman, M.K., et al., *Loss of fibulin-5 binding to α 1 integrins inhibits tumor growth by increasing the level of ROS*, in *Disease Models & Mechanisms*. 2010. p. 333-342.
27. Bell, E.L., et al., *The Qo site of the mitochondrial complex III is required for the transduction of hypoxic signaling via reactive oxygen species production*. J Cell Biol, 2007. **177**(6): p. 1029-36.
28. Tamburrino, A., et al., *Mechanisms of resistance to chemotherapeutic and anti-angiogenic drugs as novel targets for pancreatic cancer therapy*. Front Pharmacol, 2013. **4**: p. 56.

ACKNOWLEDGEMENTS

I would like to first thank my wonderful thesis mentor, Dr. Rolf Brekken. I am so grateful for the past 4 years that I have spent in your lab as a graduate student. You have fostered a fun and positive environment of learning, sharing, and independence. Thank you for always making me feel like a valuable asset to the lab, even when my experiments were failing. I am now able to graduate from your lab with the most confidence that I have ever felt in my life, as a scientist and overall human being. Thank you for your unwavering encouragement and for being my “cheerleader”, your support means a great deal to me.

Thank you to the members of the Brekken laboratory for all the advice, laughs, and encouragement. I have learned so much from you all, and I deeply appreciate everyone who has offered their help to me over the years. It has been a pleasure working alongside such a unique and positive group. I would like to extend a special thanks to Dr. Miao Wang who trained me when I initially joined the lab and who has been a great collaborator and friend. Also, thank you Dr. Kristina Aguilera and Victoria Burton for your friendship and all of our WISMAC talks. And finally, thank you Dr. Michael Dellinger for your genuine interest in my research and individual success. You are a diligent and admirable scientist whose standards I will surely aim for in this next stage of my career.

Thank you to my committee members, Drs. Lance Terada, Melanie Cobb, and John Abrams, for your insight and motivation. Our meetings challenged me to think about my

data in different ways, which has immensely fueled my research and helped me grow as a scientist. Thank you for your help with manuscripts, recommendation letters, and ultimately for helping me reach the next stage of my career.

I would also like to thank the Mechanisms of Disease Translational Science Program and the Cellular and Molecular Biology Training Grant at UT Southwestern for providing funding and invaluable experience for the majority of my graduate school career.

Thank you to my parents, it is with your constant love and support that I am where I am today. Thank you for encouraging me during the tough times of graduate school. You always remind me to look forward, keep moving, and most importantly, to find happiness - in Macedonian terms, “samo napred”. And thank you to my older sister Terri, my first role model in life. Thank you for always providing insight and wisdom without judgment. You truly understand me, and I am so grateful for our bond.

Graduate school would be a long and painful journey without all of the bright and loving friends that I have made along the way. I will look back on this period of my life with such fondness because of you all. You guys are all-stars. And finally, to my best friend Eddie, thank you for making me laugh when I wanted to cry and for making me laugh until I cried. The happiness that you have brought me thus far in my life is unmatched. I am a stronger scientist, and more importantly, a stronger person because of you.